Integration of ES cell-derived neurons into pre-existing neuronal circuits

Von der Fakultät für Lebenswissenschaften

der Technischen Universität Carolo-Wilhelmina

zu Braunschweig

zur Erlangung des Grades einer

Doktorin der Naturwissenschaften

(Dr. rer. nat.)

genehmigte

D i s s e r t a t i o n

von Stephani Franziska Neuser

aus Essen

1. Referent:	Professor Dr. Martin Korte
2. Referent:	Professor Dr. Hans-Henning Arnold
eingereicht am:	12.05.2010
mündliche Prüfung (Disputation) am:	16.07.2010

Druckjahr 2010

Vorveröffentlichungen der Dissertation

Teilergebnisse aus dieser Arbeit wurden mit Genehmigung der Fakultät für Lebenswissenschaften, vertreten durch den Mentor der Arbeit, in folgenden Beiträgen vorab veröffentlicht:

Tagungsbeiträge

Neuser, F. & Korte, M. *Integration of ES cell-derived neurons into pre-existing neuronal circuits*. The 8th Göttingen Meeting of the German Neuroscience Society; March 25-29, 2009 (Göttingen, DE).

Neuser, F., Gonschior, C., Korte, M. *Establishing a model system to examine the role of neurotrophins during maturation of embryonic stem cell-derived neuronal precursors and their integration into a pre-existing neuronal circuit*. Society for Neuroscience 39th Annual Meeting; October 17-21, 2009 (Chicago, USA).

Neuser, F., Janßen, S., Gonschior, C., Korte, M. *Analyzing the integration of wild type versus $p75^{NTR}$ knock out embryonic stem cell-derived neuronal precursors into a pre-existing neuronal circuit.* 7th Forum of European Neuroscience; July 3-7, 2010 (Amsterdam, NL).

TABLE OF CONTENTS

1 Abstract 6

2 Introduction 8

2.1 Neurogenesis and neuronal maturation 8

2.1.1 Neurogenesis during development 8

2.1.2 Adult neurogenesis 11

2.1.3 Transplantation studies 13

2.2 The hippocampus 14

2.2.1 The hippocampal circuitry 14

2.2.2 Principal hippocampal neurons 15

2.3 Synaptic plasticity 18

2.3.1 Structural and functional synaptic plasticity 18

2.3.2 The role of neurotrophins and their receptors 20

2.4 Aim of this study 23

3 Material and Methods 24

3.1 Equipment 24

3.2 Disposables 24

3.3 Reagents 25

3.4 Solutions and media 26

3.4.1 ES cell culture and differentiation 26

3.4.2 Neuronal cell culture 29

3.4.3 Immunohistochemistry 31

3.5 Antibodies 32

3.6 Cell culture techniques 32

3.6.1 Cultivation and differentiation of mouse embryonic stem cells 32

3.6.2 Preparation and cultivation of organotypic hippocampal slice cultures 36

3.6.3 Preparation of primary hippocampal cultures 37

3.7 Transplantation of ESNPs into hippocampal slice cultures 37

3.8 Immunohistochemistry 38

3.8.1 Organotypic cultures 38

3.8.2 Dissociated cultures 39

3.8.3 Cryosections 39

3.9 Imaging and analysis 40

3.9.1 Live imaging of ESNs in hippocampal slice cultures ... 40
3.9.2 Tracing the entire dendritic tree ... 40
3.9.3 Detection of synapses ... 41
3.9.4 Imaging dissociated cultures ... 41
3.10 Cell lines ... 42

4 Results ... 43
4.1 Transplantation of ESNPs into hippocampal slice cultures ... 43
4.1.1 Survival of transplanted precursors ... 43
4.1.2 Growing up in a stimulating neighborhood ... 45
4.2 Characterization of ESNs ... 46
4.2.1 Morphology ... 46
4.2.2 Connectivity of type A ESNs ... 56
4.2.3 Associated type A ESNs ... 58
4.2.4 Characteristics of type B ESNs ... 61
4.2.5 Identity ... 63
4.3 The role of $p75^{NTR}$ during maturation and integration ... 67

5 Discussion ... 73
5.1 Survival and distribution of ESNs ... 74
5.2 Type A *versus* type B ESNs - two distinct ESN populations? ... 76
5.3 Maturation of ESNs ... 83
5.4 ESNP fate ... 85
5.5 Significance of associated cells ... 88
5.6 The role of $p75^{NTR}$ during maturation of ESNs ... 91
5.7 Conclusions and outlook ... 94

6 References ... 96

7 Appendices ... 108
7.1 Supplementary Figures ... 108
7.2 Table of Figures ... 111
7.3 Frequently used abbreviations ... 112

1 ABSTRACT

During neuronal development undifferentiated precursor cells mature into highly complex neurons serving extremely specific functions. In the dentate gyrus (DG) of the hippocampus this process continues during adult life, implying that newly generated neurons integrate into a pre-existing circuit.

In the present study, I asked whether neuronal precursors derived from murine embryonic stem cells (ESNPs) are capable of integrating into the hippocampal circuitry. Embryonic stem (ES) cells carrying a *tau*EGFP transgene were pre-differentiated into radial glial cells, precursors of cortical neurons, and transplanted into the subfields of organotypic hippocampal slice cultures. While a high percentage of ES cell-derived neurons (ESNs) showed immature morphology, some ESNs acquired the structure and orientation typical of intrinsic hippocampal neurons. Although their dendritic arborization was less complex, hippocampal-like ESNs specifically adopted the shape of CA1 and CA3 pyramidal subtypes and DG granule neurons, respectively, showing a region-specific morphological integration into the host circuitry. A fraction of ESNs carried postsynaptic spines co-localizing with presynaptic markers, indicating that they receive excitatory synaptic input from host projections.

Neurotrophins and their receptors have been suggested to be involved in neurogenesis, neuronal survival and activity-dependent plasticity. To find out whether the p75 neurotrophin receptor ($p75^{NTR}$) plays a cell-autonomous role during maturation and integration of an ESNP into the hippocampal network, homozygous $p75^{NTR}$ knockout ESNPs were transplanted. Comparable to wild type ESNs, a fraction of $p75^{NTR-/-}$ ESNs developed a structure and orientation typical of intrinsic neurons. However, a significantly higher dendritic complexity was observed in the CA3 region and the DG, where a principle ligand of $p75^{NTR}$ is known to be expressed. This finding is in line with previous reports showing that $p75^{NTR}$ negatively modulates dendritic complexity in mature pyramidal neurons, and proves the validity of my approach. Interestingly, the morphologically immature fraction of $p75^{NTR-/-}$ ESNs showed the opposite phenotype: In a time-lapse imaging approach dendritic length and complexity were significantly lower than in wild type ESNs. $P75^{NTR}$ might therefore have a stabilizing effect on the dendrites of developing neurons, which could depend on neurotrophin signaling.

In summary, ESNPs transplanted into hippocampal slice cultures showed a region-specific maturation into hippocampal-like neurons. $P75^{NTR}$ plays a cell-autonomous role in ESN morphology, most likely through stabilization of the dendritic tree. The presented method can be used as a model system to examine other ES cell lines carrying mutations relevant in the context of neuronal maturation and plasticity.

ZUSAMMENFASSUNG

Im Zuge der neuronalen Entwicklung reifen undifferenzierte Vorläufer-Zellen zu komplexen Neuronen heran, die extrem spezifische Funktionen ausüben. Im Gyrus Dentatus (DG) des Hippokampus bleibt dieser Prozess auch im adulten Organismus aktiv, was bedeutet, dass sich neu gebildete Neurone in bereits existierende Netzwerke integrieren.

Die vorliegende Arbeit beschäftigt sich mit der Frage, ob aus embryonalen Maus-Stammzellen (ES-Zellen) generierte neuronale Vorläufer (ESNPs) in der Lage sind, sich in das hippokampale Netzwerk zu integrieren. *Tau*EGFP-transgene ES-Zellen wurden in radiale Gliazellen – Vorläufer von kortikalen Neuronen – differenziert und in hippokampale Schnittkulturen transplantiert. Während ein hoher Prozentsatz der aus ES-Zellen gebildeten Neurone (ESNs) eine unreife Morphologie aufwies, bildeten einige ESNs die für intrinsische hippokampale Neurone typische Struktur und Ausrichtung aus. Obwohl ihr Dendritenbaum eine geringere Komplexität zeigte, nahmen Hippokampus-ähnliche ESNs spezifisch die Form von CA1- und CA3-Pyramidenneuronen sowie DG-Körnerzellen an. Dieser Befund deutet auf eine Regions-spezifische morphologische Integration in das Wirts-Netzwerk hin. Ein Teil der ESNs trug postsynaptische *spines*, die mit prä-synaptischen Markern ko-lokalisierten. Dies zeigt, dass sie exzitatorischen synaptischen Input von Wirtsprojektionen empfangen.

Es ist bekannt, dass Neurotrophine und ihre Rezeptoren an Neurogenese, neuronalem Überleben und aktivitätsabhängiger Plastizität beteiligt sind. Um herauszufinden, ob der p75 Neurotrophin-Rezeptor ($p75^{NTR}$) eine zellautonome Rolle während der Reifung und Integration eines ESNPs in das hippokampale Netzwerk spielt, wurden homozygote $p75^{NTR}$-Knockout-ESNPs transplantiert. Wie beim Wildtyp nahm ein Teil der $p75^{NTR-/-}$-ESNs die typische Struktur und Ausrichtung von intrinsischen Neuronen an. In der CA3-Region und im DG, wo der Haupt-Ligand von $p75^{NTR}$ exprimiert wird, wurde allerdings eine signifikant höhere dendritische Komplexität festgestellt. Dieses Ergebnis stimmt mit vorherigen Studien überein, die zeigten, dass $p75^{NTR}$ die dendritische Komplexität reifer Neurone negativ moduliert, und belegt die Aussagekraft meines Versuchsansatzes. Der morphologisch unreife Teil der $p75^{NTR-/-}$-ESNs zeigte allerdings den entgegengesetzen Phänotyp: In einer *time-lapse*-Studie waren die dendritische Länge und Komplexität signifikant geringer als die des Wildtyps. $P75^{NTR}$ könnte daher einen stabilisierenden, möglicherweise Neurotrophin-abhängigen Effekt auf die Dendriten heranreifender Neurone ausüben.

Zusammengefasst reiften transplantierte ESNPs regionsspezifisch in Hippokampus-ähnliche Neurone. $P75^{NTR}$ spielt eine zellautonome Rolle in der Morphologie von ESNs, höchstwahrscheinlich durch eine Stabilisierung des Dendritenbaums. Die vorgestellte Methode kann als Modellsystem zur Untersuchung anderer ES-Zelllinien verwendet werden, die mit neuronaler Reifung und Plastizität in Zusammenhang stehende Mutationen tragen.

2 INTRODUCTION

One of the fundamental processes of life is the transformation of a newly generated unspecified cell into a fully differentiated cell occupying a unique niche within the organism. During maturation, the developing shape of each cell is directly linked to its specific function. To unravel this fascinating interplay is particularly challenging in neurons, which comprise hundreds of highly specialized and plastic cell types. By now, it is an accepted fact that in specific regions of the mature central nervous system (CNS), newborn neurons are integrated into an existing network. The mechanisms underlying this complex integration process, however, are largely unknown.

2.1 Neurogenesis and neuronal maturation

2.1.1 Neurogenesis during development

The human brain consists of approximately 10^{11} neurons (Kandel et al., 2000). An individual has to be able to perceive sensory signals and to integrate the incoming input in interconnected neuronal circuits. In order to respond with an appropriate input/output characteristic, each neuron has to find its final destination and be functionally active. To this aim, a sequence of defined steps has to be accomplished: First, a mitotically active neuronal precursor (multipotent or lineage-restricted mitotic cell) is generated. Second, it produces an immature neuron that exits the cell cycle. Third, the immature neuron migrates to its destination. Fourth, the neuron is signaled to survive. And fifth, it starts to communicate pre- and postsynaptically with other neurons.

In mammals, by far the major part of CNS neurons is generated prior to birth. Following gastrulation, the neuroectoderm appears at the dorsal part of the embryo as a layer of early neuronal precursor cells, the neuroepithelial cells, oriented radially between the neural tube and the pial surface. These progenitors undergo asymmetrical division accounting for the initial wave of neurogenesis and for the genesis of radial glial cells (RG), the most abundant precursor type in the developing brain (for a review see Pinto and Gotz, 2007; Gotz and Huttner, 2005). Originally, RG were thought to only serve as a scaffold for newly generated neurons while the latter migrate from the ventricular zone toward the pial surface. There, the new neurons settle at their destined location, contributing to the development of the six neocortical layers. It could be shown, however, that RG also represent a major source for newborn neurons in the entire brain, but most prominently in the dorsal telencephalon, origin of the neocortex as well as the hippocampus (Malatesta et al., 2000). In the mature telencephalon, different transmitter phenotypes are found. Glutamatergic neurons, which use

glutamate as excitatory neurotransmitter, represent a major fraction. They derive from RG in the subventricular zone (SVZ). Inhibitory interneurons on the other hand, using γ-aminobutyric acid (GABA) as transmitter, derive from the ganglionic eminence in the ventral telencephalon, and migrate dorsally.

Some general principles account for the developmental changes of neuronal precursors. First of all, neuronal development and migration depend on external factors. An example for a molecule involved in determining the neuronal fate of a precursor cell is the bone morphogenetic protein (BMP) (Cleaver and Melton, 2003). Conversely, other secreted factors (e.g. ciliary neurotrophic factor and platelet-derived growth factor) mediate the generation of oligodendrocytes and astrocytes, respectively. Generally, the binding of fate-determining signaling molecules to cell surface receptors activates intracellular signaling cascades, and results in the activation or inhibition of transcription factors (TF). One of the TF required for a neuronal fate of cortical RG is the paired box gene 6 (Pax6). In the Pax6 mutant mouse, the neuron number is reduced by 50% (Heins et al., 2002). Secondly, during embryonic development, more neurons are generated than will be needed later on. In the 1950s, R. Levi-Montalcini and S. Cohen discovered the nerve growth factor (NGF) (Cohen et al., 1954). NGF is secreted by a target tissue and this signal turned out to be crucial for neuronal cells to survive. Newborn neurons are programmed to undergo cell death which can only be prevented by the presence of neurotrophic factors. Besides neurotrophins, which belong to the transforming growth factor β (TGFβ) family, other neurotrophic factors such as the fibroblast growth factor (FGF) (Gospodarowicz et al., 1974; Carlone et al., 1981), sonic hedgehog (SHH) (Riddle et al., 1993; Ericson et al., 1995), and interleukin 6-related cytokines were identified (Hirota et al., 1996). Apparently, survival is directly linked to activity, since neuronal activity can regulate production of neurotrophic factors as well as responsiveness to the latter (e.g. the expression of receptors).

Neurons show a highly polarized organization: After the initial neurite outgrowth, one of the immature cell processes develops into an axon, specialized to neurotransmitter release, whereas all other processes become dendrites (Fig. 1). The time course of maturation has been extensively investigated in primary hippocampal rat neurons and can be summarized in five major stages *in vitro* (Dotti et al., 1988). Directly after plating, the neurons form small protrusions (stage 1) developing into immature neurites within half a day (stage 2). The most important transition takes place around 1.5 days after plating, when one of the emanating processes develops a growth cone and transforms into an axon (stage 3). Two and a half days later, the other immature processes acquire dendritic morphology (stage 4), but the establishment of synaptic connections, concomitant with the generation of dendritic spines, does only happen after one week *in vitro* (Arimura and Kaibuchi, 2007). The establishment of

neuronal polarity was found to depend on external signals. While a negative feedback loop prevents the elongation of future dendrites, a positive feedback-loop induces the elongation of the single axon (reviewed in Andersen and Bi, 2000). Order and time scale of these processes differ between cell types and *in vitro versus in vivo*. Hippocampal and cortical pyramidal cells *in vivo*, for example, are known to grow a single axon toward the pial surface serving as leading process when the neuron migrates toward its destination. No immature neurites are formed in advance (Arimura and Kaibuchi, 2007). Conclusively, axonal path finding represents a crucial mechanism, since it determines the migration route of the immature neuron, and the selection of specific synaptic targets. Axonal path finding depends on four different processes: contact attraction, chemo-attraction, contact repulsion, and chemo-repulsion (for a review see Tessier-Lavigne and Goodman, 1996).

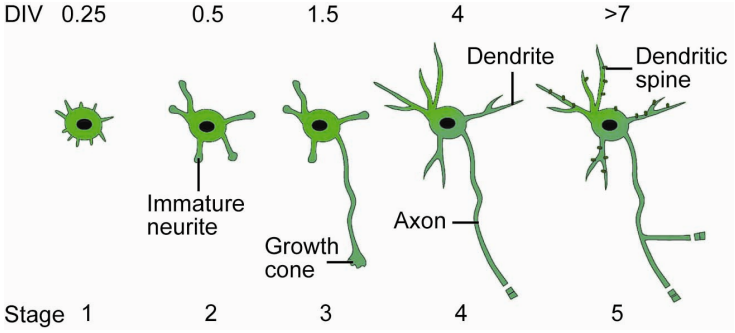

Figure 1 | A maturing neuron traverses 5 characteristic stages. Stage 1 lamellipodia; stage 2 minor processes; stage 3 axonal outgrowth; stage 4 dendritic outgrowth; stage 5 maturation. DIV = days *in vitro.* Modified after Dotti (1988); Arimura (2007)

Dendritic structures develop later, during the first postnatal weeks. Several studies indicate that the dendritic tree develops in direct relation to afferent inputs (reviewed by Wong and Ghosh, 2002). In the visual system, it has been shown that dendritic branching and stabilization in response to sensory stimulation were mediated by released glutamate which was bound to N-methyl-D-aspartic acid (NMDA) receptors (Sin et al., 2002). Others reported that Ca^{2+}/calmodulin-dependent kinase IV (CaMKIV) and the cyclic AMP response element binding protein (CREB) mediate Ca^{2+}-induced dendritic growth in cortical neurons (Redmond et al., 2002). Similar mechanisms are likely to be involved in most brain regions. Neuronal maturation is completed by the formation of synapses. Also in this case, intercellular interactions are critical, leading to a selective connection between the axon and its target. Subsequently, the axonal growth cone converts into a nerve terminal, and the target cell forms a postsynaptic specification. The following synaptic fine tuning is maintained throughout life (synaptic plasticity, see below).

Different strategies have been chosen to identify proteins playing a role during developmental processes. The most common approach is the generation of a knockout

system which is homo- or heterozygous for the gene encoding the protein of interest. This strategy can be refined by the use of conditional knockouts – animals in which the excision of the respective gene is achieved selectively, either in a specific tissue or at a time point of interest. This is particularly useful when the protein of interest exerts different tissue-specific functions, or is essential during early development. Nevertheless, the use of knockout mutants generally includes surrounding cells and tissue which can equally be affected. Interactions of the analyzed cell with these affected cell populations can mask the phenotype and complicate the interpretation of the result. In the present study, a model system is presented which allows the analysis of a single genetically modified ES cell-derived neuron (ESN) within a wild type environment. In this way, the cell-autonomous effect of a protein of interest can be examined during maturation and integration.

2.1.2 Adult neurogenesis

In most brain regions, the generation of new neurons largely ceases at E18, shortly before birth. However, gliogenic RG generate glial precursors that mature into astrocytes and oligodendrocytes after the first postnatal days (Pinto and Gotz, 2007; Qian et al., 2000). The adult brain and spinal cord were assumed to be devoid of any regenerative capacity for a long time. As early as 1911, Ramón y Cajal suggested that no new neurons are generated after birth, which became a central dogma during the following decades (Ramón y Cajal, 1911). However, the last 45 years have revealed more and more signs for ongoing neurogenesis in the telencephalon of adult rodents (Altman and Das, 1965; Cameron et al., 1993), monkeys (Kornack and Rakic, 1999) and humans (Eriksson et al., 1998). Neural stem cells reside in adult nervous tissue, in the subventricular zone (SVZ) at the lateral ventricle as well as in the dentate gyrus (DG) of the hippocampus. The process of neurogenesis, its contribution to brain function and potential meaning for regenerative medicine are subject of extensive investigation (reviewed by Gage, 2000; Gage, 2002; Ming and Song, 2005; Zhao et al., 2008). Since the hippocampus is involved in learning and memory processes (see below), many studies on adult neurogenesis focus on this interesting system. Initially, generation of new DG granule neurons was described in rats by using the radioactive labeled nucleotide [H^3]-thymidine (Altman and Das, 1965). Currently, a series of new methods permits the co-detection of DNA synthesis and neuron-specific markers (Kuhn et al., 1996), as well as the structural and functional analysis of newly generated cells (van Praag et al., 2002).

It has been observed that neurogenesis can be influenced by several factors. Keeping mice in an enriched environment led to a higher number of newly generated neurons, and increased the volume of the granule cell layer (Kempermann et al., 1997). In a comparable experiment, an improved recognition memory was found (Bruel-Jungerman et al., 2005).

Similarly, voluntary wheel running selectively led to a stimulation of cell proliferation and neurogenesis in the mouse hippocampus (van Praag et al., 1999; Tashiro et al., 2007). In rats, training in hippocampus-dependent learning tasks doubled the number of adult-generated neurons (Gould et al., 1999). In turn, it has been reported that newly formed granule neurons were preferentially incorporated into spacial memory networks in mice (Kee et al., 2007). On the other hand, pathologic conditions such as epileptic seizures or ischemic stroke equally caused an increase in neurogenesis (Parent et al., 1997), whereas stress has been linked to a reduction of newly formed neurons (Lemaire et al., 2000). Just recently, major differences in adult neurogenesis and neuronal survival and maturation have been found for mice and rats, respectively. Mice were reported to display considerably lower neurogenesis rates and a slower progress ofmaturation (Snyder et al., 2009).

It is now an acknowledged fact that astrocyte-like stem cells in the subgranular zone (SGZ) of the mammalian DG are the source of adult-born neurons (Seri et al., 2001). Furthermore, glial stem cells create a neurogenic niche in some areas of the dental blade (see orange dots in Fig. 2), where they self-renew and produce intermediate progenitors (reviewed in Alvarez-Buylla and Lim, 2004). Others suggested a regulatory role for astrocytes in inducing neurogenesis from neural stem cells (Song et al., 2002). Progenitors subsequently migrate into the granule cell layer, and mature into dentate granule cells as reviewed by Ming and Song (2005). Proliferation and fate specification are followed by migration, axon/dendrite targeting and synaptic integration. The mechanisms that regulate the integration of newly generated neurons are unknown. It has been shown, however, that during earlier stages ambient γ-aminobutyric acid (GABA) and GABAergic input from hilar interneurons regulate their synaptic integration, initially exerting excitatory function (Ge et al., 2006). Later on, perforant path (PP) afferents are crucial for synaptic integration *in vivo* (reviewed by Zhao et al., 2008), which is achieved after two to four weeks (Zhao et al., 2006). NMDA receptor-mediated transmission thereby plays a cell-specific role in regulating the survival of newly generated neurons (Tashiro et al., 2006).

The use of a retrovirus labeling dividing cells allows the *in vivo* analysis of neuronal morphology down to the level of postsynaptic spines. Thereby, adult-born granule neurons were found to carry synapses at dendritic spines (Toni et al., 2007), and to show electrophysiological properties similar to neonatal granule neurons (van Praag et al., 2002). Newborn granule neurons also have axons projecting on CA3 pyramidal neurons and using glutamate as neurotransmitter (Toni et al., 2008). They develop more slowly than neonatal granule cells in terms of both dendritic morphology and electrophysiological properties, such as excitability and spontaneous synaptic activity (Overstreet-Wadiche et al., 2006). A similar observation was made by Schmidt-Hieber et al. (2004), who found that new granule neurons

displayed substantially different membrane properties, leading to a more easily induced associative long-term potentiation (LTP, see below). The authors therefore suggested that the enhanced synaptic plasticity could be involved in the formation of new memories.

Altogether, it has been suggested that adult neurogenesis is critically involved in hippocampus-dependent behavior, although its precise function still remains elusive (Kempermann, 2002). New neurons are more likely to be part of a long-term adaptation process, rather than to cause acute benefits for the animal (Kempermann et al., 2004). According to a current theory, adult-born neurons could be involved in pattern integration, a process thought to underlie the separation of different overlapping memories during memory consolidation (Deng et al., 2010). Although most studies on adult neurogenesis have been performed on mice or rats *in vivo*, it has also been reported to take place in organotypic slice cultures of the hippocampus (Raineteau et al., 2004; Kamada et al., 2004).

2.1.3 Transplantation studies

With the discovery of neurogenesis in the adult brain, the integration of extrinsic neurons into pre-existing circuits suddenly seemed possible. Stem cells and neuronal precursors were transplanted into different brain regions, aiming at the reconstitution of damaged brain structures. Transplanting undifferentiated ES cells into an animal model of Parkinson's disease resulted in fully differentiated dopaminergic neurons and behavioral restoration (Bjorklund et al., 2002). In a different therapeutical approach, damaged adult motor pathways were reestablished by grafted embryonic cortical neurons in mice (Gaillard et al., 2007). On the other hand, the integration process of precursors *per se* was examined in the embryonic brain (Brustle et al., 1995), in the adult hippocampus (Carpentino et al., 2008) and neocortex (Ideguchi et al., 2010). Generally, it was found that under defined conditions the transplanted precursors acquired some characteristics of local neurons, such as the expression of regional markers and axonal projections. In order to avoid tumor formation, ES cells were pre-differentiated toward a neuronal fate. After transplantation of ES cell-derived neuronal precursors (ESNPs) into the telencephalic vesicles of embryonic rats, a functional integration of ESNs was reported (Wernig et al., 2004). Functional integration was equally found when ESNPs were transplanted into the DG of rat hippocampal slice cultures (Benninger et al., 2003). In the present study, I used ES cells that were pre-differentiated into Pax6-positive RG. After transplantation into different regions of the hippocampus, their differentiation into neurons and their integration into the hippocampal circuit could be observed.

2.2 The hippocampus

Long before adult neurogenesis was found in the DG, it was already known that the hippocampus is involved in learning and memory processes. Patients bilaterally devoid of the hippocampus suffer from severe anterograde amnesia (Scoville and Milner, 1957). The hippocampus was more precisely shown to mediate the transition from short to long-term memory (Alvarez et al., 1994). Deep within the temporal lobe, underneath the neocortex, the hippocampus resides as a bilateral and phylogenetically ancient structure. Its laminar organization has been extensively described by different neuroanatomists such as Camillo Golgi (1886), Santiago Ramón y Cajal (1911) and Lorente de Nó (1934).

2.2.1 The hippocampal circuitry

Although the principal hippocampal neurons resemble those found in other brain regions (see below), their wiring and projection pattern is unique to the hippocampal formation. In rodents, excitatory fibers run perpendicular to the septotemporal axis, therefore transverse slices of the hippocampal formation contain functionally connected populations of neurons. In 1971, this kind of preparation was used to successfully activate intrinsic pathways *in vitro* for the first time (Skrede and Westgaard, 1971). This technique has been refined and extensively applied to examine the hippocampal circuitry (Fig. 2). Coming in from the entorhinal cortex (EC), nerve fibers enter the hippocampus as the perforant path (PP) at the dentate gyrus (DG). These axons project on the DG granule neurons in the molecular layer (*ml*), as well as, in the *stratum lacunosum-moleculare* (*sl-m*), on the apical dendrites of CA3 neurons. In turn, granule neurons also extend their axons, the mossy fibers (MF), through the polymorphic layer (*pl*, also called the hilus) toward the proximal parts of CA3 neuronal dendrites in the *stratum lucidum* (*sl*). The axonal projections from CA3 to CA1 are the Schaffer collaterals (SC). Communication with the contra lateral hippocampus is also mediated via CA3 by associational commissural fibers (AC). Both inputs reach CA1 in the *stratum radiatum* (*sr*) as well as the *stratum oriens* (*so*). In addition to input from CA3, CA1 neurons are also projected on by the PP (in *sl-m*). CA1 axons extend toward the EC, either directly or via the subiculum (SB). The capability of hippocampal wiring to respond to electrophysiological stimuli in strengthening or weakening its synaptic connections, referred to as synaptic plasticity, is considered to represent the basis of hippocampal memory function (see 2.3).

In addition to the aforementioned hippocampal pathway that uses glutamate as neurotransmitter, the hippocampus is the target of other excitatory projections from different brain regions. Its CA1 region is innervated by axons from amygdala and thalamus, and receives neuromodulatory input from various brain regions, using acetylcholine, noradrenalin,

serotonin and dopamine as transmitters. CA3 is only innervated by cholinergic fibers, whereas the DG receives cholinergic, noradrenergic, dopaminergic, and serotonergic inputs. Furthermore, all primary hippocampal neurons are subject to the input of inhibitory interneurons present in all subfields whose function is mediated by GABA (Andersen et al., 2007).

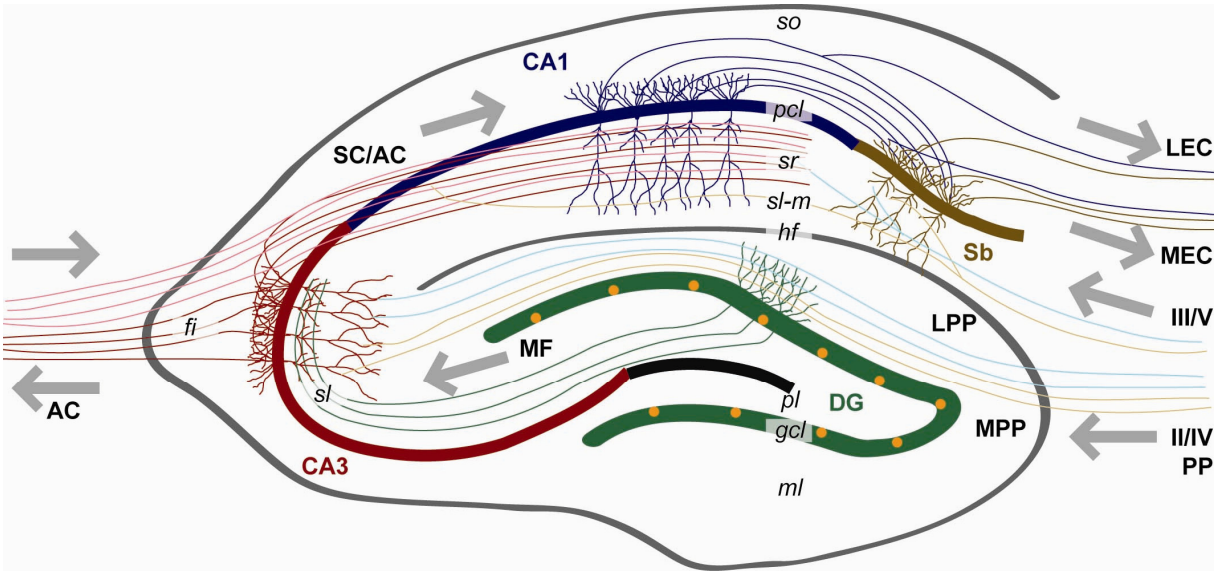

Figure 2 | Overview of the hippocampal pathway. The main input arrives from the entorhinal cortex (EC) via the perforant path (PP) which is divided into the lateral and the medial perforant path (LPP/MPP). Axons project onto neurons in the dentate gyrus (DG) as well as the CA3 region. CA3 also receives input from the DG via the mossy fibers (MF). From CA3, axons project to CA1 via the Schaffer collaterals (SC) as well as to the CA1 region of the contra-lateral hippocampus via the associational comissural pathway (AC). CA1 neurons also receive input directly from the PP, and they project on neurons in the subiculum (Sb). These, in turn, send axons back to the EC. Orange regions in the DG represent neurogenic areas in the subgranular zone (SGZ). *fi* – fimbria; *gcl* – granule cell layer; *hf* – hippocampal fissure; *ml* – molecular layer; *pcl* – pyramidal cell layer; *pl* – polymorphic layer; *sl* – *stratum lucidum*; *sl-m* – *stratum lacunosum-moleculare*; *so* – *stratum oriens*; *sr* – *stratum radiatum*. Adjusted after Deng (2010).

Another feature qualifies the hippocampus as an attractive model system: Its cells – neurons and glia – can easily be held in culture. Monolayer cultures can be obtained by dissociating the embryonic hippocampus. Organotypic cultures from transverse hippocampal slices have additional advantages (Gahwiler, 1981). They survive up to several weeks, leaving the characteristic cytoarchitecture almost unaltered, since the trisynaptic pathway of hippocampal projections (DG, CA1, CA3) remains intact.

2.2.2 Principal hippocampal neurons

The described function of the hippocampus is closely linked to the neurons found in the respective subdivisions. The two major neuron types are referred to as principal hippocampal neurons. On the one hand, there are pyramidal neurons which reside in the CA regions, and on the other hand, there are granule neurons in the DG (Fig. 3A). Both cell types, pyramidal

cells and granule neurons, release glutamate and receive excitatory as well as inhibitory synaptic input.

Pyramidal neurons also occur in the neocortex and the amygdala, structures that are associated with advanced cognitive functions (for a review see Spruston, 2008). They have a pyramidal-shaped cell body and a characteristic dendritic arbor, composed of a basal and an apical compartment, the basal pole of the soma being defined by the emanating axon (Fig. 3B). Throughout the hippocampal formation, pyramidal neurons show the same orientation. The soma is organized within the pyramidal cell layer (pc; Fig. 2; Fig. 3A), surrounded by other pyramidal cell bodies. Basal dendrites reach into the *stratum oriens* (*so*), the outer hippocampal layer. The longer apical dendritic tree can reach a considerable length of 700 µm (in mice) and extends toward the centre, through the *stratum radiatum* (*sr*) into the *stratum lacunosum-moleculare* (*sl-m*). Although CA1 and CA3 neurons share many similarities, they can easily be distinguished by morphological characteristics. The main apical shaft of CA3 neurons bifurcates closer to the soma (Amaral et al., 1990). On the other hand, CA1 apical shafts give rise to short secondary dendrites in the proximal apical compartment. Additionally, the group of CA3 neurons is remarkably heterogeneous in terms of its dendritic complexity (Fitch et al., 1989). Both apical and basal dendrites are specialized to the reception of a defined input according to their position within the CA formation. CA1 neurons are innervated by the SC in their basal and proximal apical part and by the PP and the thalamus in the most apical region, the apical tuft (Fig. 2; 3). CA3 neurons, on the other hand, receive MF input in the most proximal 100 µm of the apical shaft; basal and apical dendrites are innervated by CA3 collaterals of the ipsy- and contra-lateral hippocampus. Similar to CA1 neurons, the most distal CA3 dendrites receive input from the PP. Hippocampal pyramidal neurons are generated between E10 and E18 in the mouse, resulting in an already complete CA region at the date of birth (Angevine, Jr., 1965). They derive from the ventricular germinative layer next to the future CA1 region, and migrate toward CA1 and CA3, respectively (Altman and Bayer, 1990).

Most of the excitatory synapses on pyramidal neurons are located on dendritic protrusions, so-called dendritic spines, emanating from the dendritic shaft (Fig. 3C, red rectangle). Spines generate micro-compartments that isolate the postsynaptic milieu from that of the main dendritic shaft. Additionally, spines are known to be highly plastic structures, leading to the hypothesis that they provide the morphological basis for synaptic plasticity (reviewed in Hering and Sheng, 2001; Segal, 2005). Spine density and shape vary across the different dendritic compartments and cell types, and are related to the amount of excitatory synaptic input (Woolley et al., 1997; Matsuzaki et al., 2001). CA3 pyramidal neurons carry exceptionally complex and highly branched spines, also referred to as thorny excrescences,

in their proximal apical compartment (Fig. 3C, green rectangle). These represent the postsynaptic sites of mossy fiber projections from the DG (see Fig. 2).

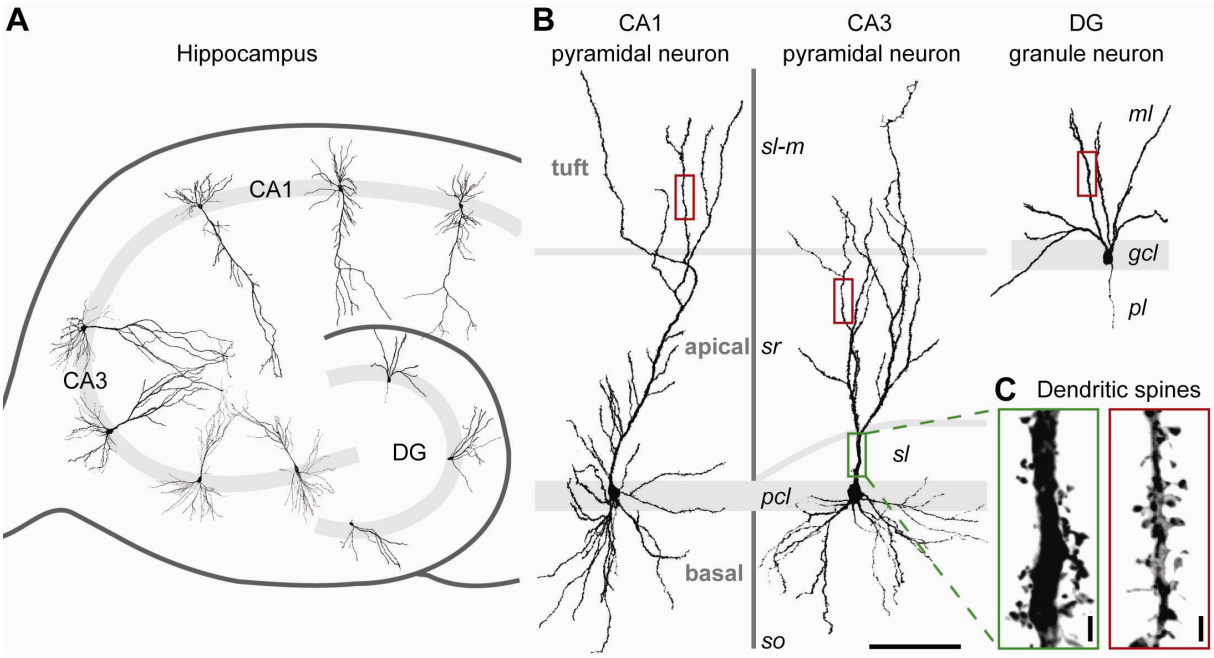

Figure 3 | The hippocampus displays a unique cytoarchitecture. A | Schematic transverse section of the murine hippocampus with its subfields CA1, CA3 and DG. **B** | Principle neuron types from the respective subfields, pyramidal neurons in CA1 and CA3, granule neuron in the DG. **C** | Hippocampal neurons carry postsynaptic protrusions. While spines are found in the apical and basal compartments of all principal neurons (red rectangle), CA3 pyramidal cells show so-called thorny excrescences in their proximal apical compartment (green rectangle). Legend see Fig. 2. Scale bars 100 µm in **B**; 2 µm in **C**. Thorny excrescences taken from Hatanaka et al. (2009).

The rather small cell bodies of granule neurons have an ovoid shape, which accounts for their given name. Granule cells are not only found in the hippocampus, but also in the cerebellum, and in the olfactory bulb. In contrast to the granule cells in the olfactory bulb, however, hippocampal granule neurons are glutamatergic. The somas of hippocampal granule neurons are located in the granule layer (*gl*) of the DG. Similar to the pyramidal neurons, they show a characteristic orientation. However, granule cells solely carry apical dendrites, and basal dendrites only occur during development (Jones et al., 2003). Their conical dendritic arbor is much shorter than that of pyramidal cells (around 200 µm long), and extends into the molecular layer (*ml*), where it is innervated by the PP. It has been shown that granule cells in the infra-pyramidal blade are less complex than those in the supra-pyramidal blade (Claiborne et al., 1990). Their dendrites are heavily covered with dendritic spines. During embryonic and early postnatal development, precursors of granule neurons invade the hippocampus from the ventricular germinative layer and migrate through CA1 and CA3 to the hilar region. In this region, a secondary germinative layer is generated, giving rise to the granule neurons of the supra-pyramidal and subsequently the infra-pyramidal blade. Hippocampal granule neurons represent one of the two neuron types that are newly

generated in the adult brain, and are thought to functionally integrate into the pre-existing hippocampal circuitry as discussed above.

The second largest group of neuronal cells in the hippocampus is represented by GABAergic interneurons. They differ from pyramidal as well as granule neurons in their morphology, by missing a clear dendritic polarization. GABAergic interneurons are often highly complex and devoid of dendritic spines. Many of the interneuron types found in the hippocampus do not reside within the cell layers of the pyramidal neurons in the CA, or the granule neurons in the DG, and can accordingly be identified by their position and orientation.

2.3 Synaptic plasticity

As already described above, the central nervous system is an extremely plastic organ. With the discovery of adult neurogenesis, a potential mechanism underlying hippocampus-dependent learning and memory was found. Apart from the addition of new neurons in two distinct regions of the adult brain, other, more general mechanisms allowing neurons and entire neuronal circuits to respond to environmental stimulation have been described.

2.3.1 Structural and functional synaptic plasticity

The most prominent form of functional synaptic plasticity is the so-called long-term potentiation (LTP), which was first described in 1973 by Bliss and Lømo in granule neurons of the rabbit hippocampus *in vivo* (Bliss and Lomo, 1973). Much research went into the elucidation of the mechanisms of LTP, although similar mechanisms most likely also underlie functional plasticity during development. Here it is instrumental to know that glutamatergic synapses have different receptor types. A-amino-3-hydroxy-5-methyl-4-isoxazole propionic acid (AMPA) receptors (AMPARs) represent ligand-dependent ion channels which upon glutamate binding open their pore to Na^+ influx. The resulting depolarization of the postsynaptic membrane leads to an excitatory postsynaptic potential (EPSP) which might – or might not – be sufficient for the generation of an action potential. A second receptor type, the NMDA receptor (NMDAR), is also activated by the binding of glutamate. Its pore, however, is blocked by one Mg^{2+} ion, as long as the depolarization does not reach a specific threshold. In case of strong depolarization, e.g. a high frequency electrophysiological stimulus, the Mg^{2+} ion is expelled, giving way to the influx of Ca^{2+} ions. These, in turn, act as second messengers and activate protein kinases. Several events contribute to LTP, the enhancement of an existing synaptic connection. First, AMPARs are phosphorylated, leading to a higher efficiency of ionic conductance. Second, new AMPARs from intracellular sources are recruited to the membrane (Fig. 4; Bliss and Collingridge, 1993; reviewed by Malenka

and Bear, 2004; Citri and Malenka, 2008). And third, gene expression and subsequent *de novo* protein synthesis can lead to processes of long-term memory storage (consolidation).

In addition to functional synaptic plasticity, it has also been reported that neurons can change their structure due to changed neuronal input. This type of plasticity is called structural synaptic plasticity. It was reported in hippocampal CA1 neurons in organotypic slice cultures that structural changes can be induced by mechanisms of LTP as well (Engert and Bonhoeffer, 1999; Maletic-Savatic et al., 1999; Toni et al., 1999). The structural rearrangements that have been observed in correlation with LTP range from broadening of the spine head and shortening of the neck to branching of a spine, and to the generation of new spines between the same pre- and postsynaptic structures. Yet, the function of these changes is not completely clear. On the one hand, they could contribute to the maintenance of the observed enhanced activity. On the other hand, however, they could prepare the neuron for future plasticity events (reviewed in Yuste and Bonhoeffer, 2001). In turn, changes are also seen in the pre-synapse (Fig. 4). Most likely, the increased number of released glutamate-containing vesicles is accounted for by a retrograde messenger, secreted by the post-synapse in response to the increased Ca^{2+} concentration (Bon and Garthwaite, 2003). Activity-dependent structural changes were also observed *in vivo*. It was shown that in the murine barrel cortex, dendritic spines are newly generated and eliminated in response to sensory experience (Lendvai et al., 2000; Trachtenberg et al., 2002).

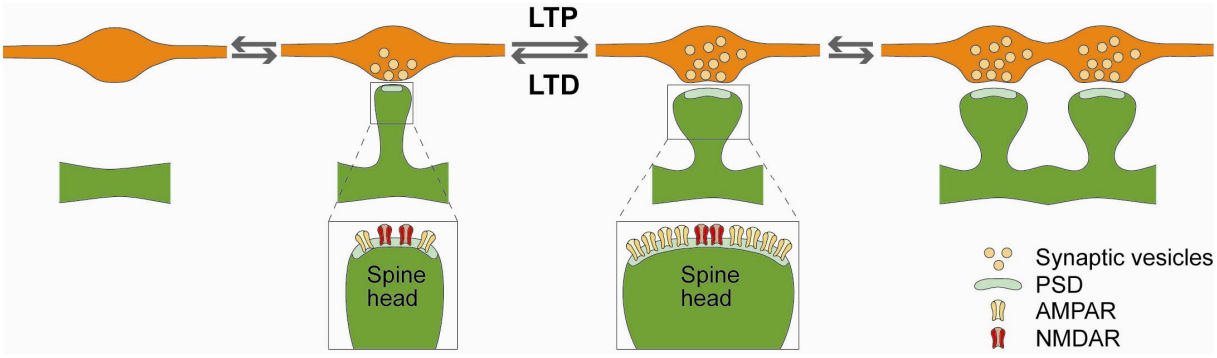

Figure 4 | Functional and structural plasticity are linked to one another. Upon long-term potentiation (LTP) synaptic strength is increased, concomitant with the insertion of new AMPA (α-amino-3-hydroxy-5-methyl-4-isoxazole propionic acid) receptors (AMPARs) into the postsynaptic membrane. The spine head grows, and new synapses, potentially on new spines, are generated. Upon long-term depression (LTD), synaptic strength is decreased, AMPARs leave the postsynaptic density (PSD), and the spine head shrinks. LTD might also lead to an elimination of synapses and a pruning of spines. NMDAR – N-methyl-D-aspartic acid receptor. Modified after Holtmaat and Svoboda (2009).

Since plasticity can ultimately only be guaranteed if strengthening and weakening, growth and retraction occur to the same extent, it was postulated that besides a mechanism enhancing synaptic transmission, there must also be one which mediates attenuation. The existence of long-term depression (LTD) was proven by Stanton and Sejnowski (1989).

Accordingly, it was found that while LTP induction leads to spine growth, the induction of LTD by a low frequency stimulus resulted in spine retraction in hippocampal neurons (Nagerl et al., 2004; Zhou et al., 2004). Interestingly, both mechanisms rely on the activation of NMDARs (Dudek and Bear, 1992), resulting in elevated Ca^{2+} levels in the post-synapse.

A special role in the induction of LTP and LTD at excitatory neurons is carried out by spines. Spines form micro-compartments (Yuste et al., 2000) and are able to regulate the connection to their parent dendrite by head enlargement or narrowing of their neck. Most likely, this has an effect on Ca^{2+} diffusion as well as the transport of receptors and other proteins into the spine (for a review see Segal, 2005). With the establishment of long-term time-lapse imaging, it is now possible to follow single spines and axonal boutons as they appear and retract in the cerebral cortex *in vivo*. In this context it is important to note that spines are highly motile structures that also show structural changes under baseline conditions. Some spine populations display a continuous turn-over, whereas others remain stable for months, most likely due to the wiring of different cell populations (reviewed in Holtmaat and Svoboda, 2009). The intracellular structure involved in structural plasticity, especially subsequent to LTP induction during the process of memory consolidation, is the actin cytoskeleton. As a consequence of Ca^{2+} influx, Rho GTPases, which control stabilization of actin filaments, are inactivated. Actin filaments, in turn, are required for the persistence of dendritic spines (for a review see Lamprecht and LeDoux, 2004; Cingolani and Goda, 2008).

LTP and LTD combine functional and structural changes at the synapse level. Similar processes are likely to take place during the interplay of morphological maturation and functional integration during neuronal development, and it has been reported that new neurons in the DG of the adult hippocampus are especially plastic (Schmidt-Hieber et al., 2004; Bischofberger, 2007).

2.3.2 The role of neurotrophins and their receptors

Neurotrophins have been shown to be related to synaptic plasticity (Thoenen, 1995). Furthermore, they not only support neuronal survival and differentiation during development, but are also known to be involved in adult hippocampal neurogenesis. This was especially shown for the brain-derived neurotrophic factor (BDNF) (Lee et al., 2002; Rossi et al., 2006; Bergami et al., 2008). Along with the nerve growth factor (NGF), BDNF and neurotrophins 3, 4/5, 6 and 7 (NT3, NT4/5, NT6, NT7), belong to the neurotrophin family, which are small signaling peptides of about 13-16 kDa. Whereas each neurotrophin specifically binds one tropomyosin-related kinase receptor (Trk), all have an equimolar affinity to the p75 neurotrophin receptor ($p75^{NTR}$), a member of the tumor necrosis factor (TNF) superfamily (reviewed in Bothwell, 1995; Dechant and Barde, 2002). In the neocortex as well as in the

hippocampus, BDNF plays an important role. Initially described in 1982 (Barde et al., 1982; Leibrock et al., 1989), binding of BDNF to TrkB was reported to mediate survival and proliferation in cultured fibroblasts lacking $p75^{NTR}$ (Glass et al., 1991). The roles of $p75^{NTR}$ have been described as enhancing the specificity of Trk receptors and, on the other hand, promoting cell death (Lee et al., 2001a; Huang and Reichardt, 2001). Since it was known that neurotrophins are secreted in an activity-dependent manner from dendrites, and that they are equally able to enhance synaptic transmission, a role of neurotrophins in promoting neuronal plasticity has been suggested (Thoenen, 1995). In 1995, it was found that in the absence of BDNF, LTP was significantly impaired (Korte et al., 1995). By re-introducing BDNF into the system, LTP could be restored (Korte et al., 1996; Patterson et al., 1996). The effect of BDNF on LTP was later shown to be dependent on the phospholipase Cγ (PLCγ) signaling pathway via its specific neurotrophin receptor TrkB (Minichiello et al., 2002). Neurotrophins are generated as a pro-form, a precursor which is proteolytically cleaved to produce the mature protein (Seidah et al., 1996). In addition to the mature neurotrophins, also their pro-forms were suggested to be secreted and act as signaling molecules. In contrast to mature BDNF, proBDNF binds $p75^{NTR}$ with high affinity, thereby inducing apoptosis (Lee et al., 2001b). Whether – and to what extent – proBDNF is secreted *in vivo* is still a matter of debate (Matsumoto et al., 2008; Yang et al., 2009).

Neurotrophin functions range from neuronal survival, axonal and dendritic growth and guidance to neurotransmitter release and synaptic plasticity (McAllister et al., 1999; Poo, 2001). They form stable dimers that bind to the extracellular domains of Trk receptors and $p75^{NTR}$, found pre- and postsynaptically on neurons, and in the membranes of some non-neuronal cells (Yan et al., 1997; Dougherty and Milner, 1999). Some signaling cascades leading to neurotrophin actions are well-characterized (see Fig. 5; reviewed by Chao, 2003; Reichardt, 2006). Upon ligand binding, Trk receptors dimerize, and their intracellular kinase domains become transphosphorylated. This leads to the activation of the Src homologous and collagen-like adaptor protein (Shc) which links Trk activation to two separate signaling pathways. On the one hand, Shc phosphorylation increases the activity of Ras and the extracellular signal-regulated kinase (ERK), promoting cell differentiation and survival. On the other hand, survival is also increased by Shc, activating the phosphatidylinositol 3-kinase (PI3K) and Akt. These processes are linked to the transcription factor CREB, which mediates protein expression that is needed for long-term synaptic changes. In addition, PLCγ is phosphorylated, a process which is responsible for the activation of Ca^{2+}- and protein kinase C-dependent pathways involved in synaptic plasticity. Binding of (pro-)neurotrophin dimers to $p75^{NTR}$, in turn, can lead to neuronal cell death by activation of the Jun N-terminal kinase (JNK) pathway. RhoA also binds to the intracellular domain of $p75^{NTR}$, and has been

linked to the inhibition of neurite outgrowth and growth cone collapse (Gehler et al., 2004; reviewed by Blochl and Blochl, 2007).

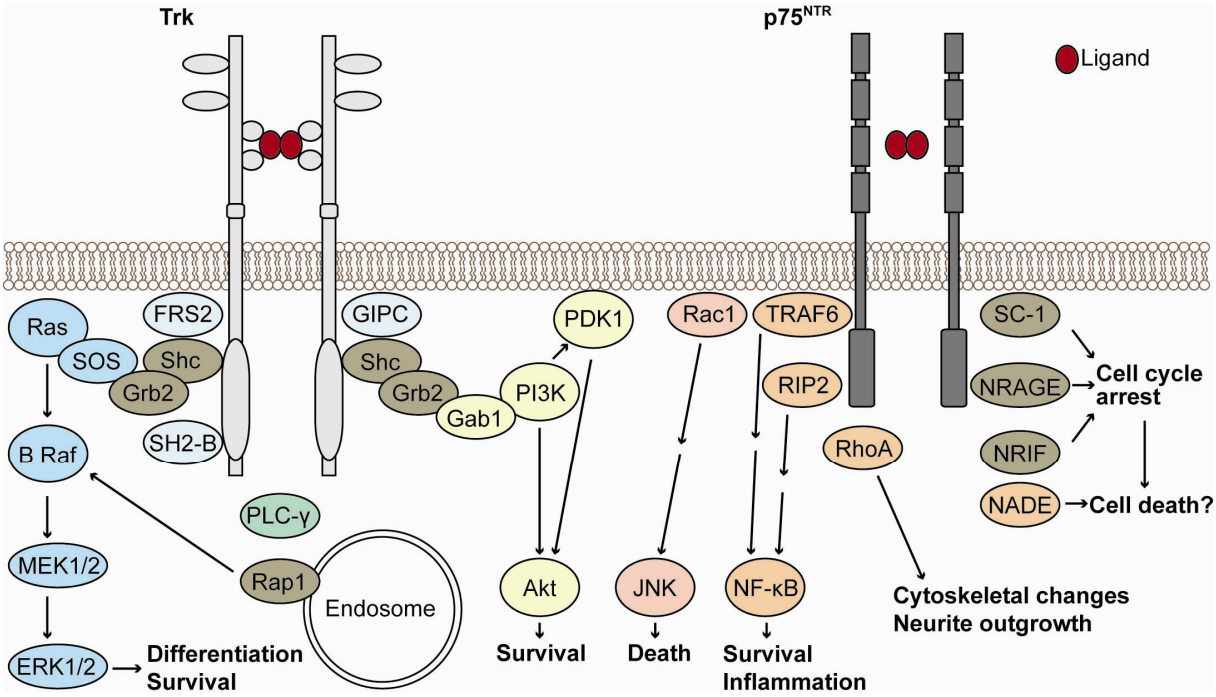

Figure 5 | Depending on the receptor system, neurotrophins trigger partly antagonizing cellular answers. Neurotrophin binding to Trk receptors leads to differentiation and survival through extracellular signal-regulated kinase (ERK), phosphatidylinositol 3-kinase (PI3K) and phospholipase Cγ (PLC-γ) pathways. PLC-γ and Src homologous and collagen-like adaptor protein (Shc) are phosphorylated leading to the activation of PI3K and ERK, while Rap1 acts from its location at the endosome. In contrast, $p75^{NTR}$ mainly activates NF-κB, Jun N-terminal kinase (JNK) and RhoA, mediated by the adaptor proteins neurotrophin receptor-interacting factor (NRIF), neurotrophin-associated cell death executor (NADE), neurotrophin receptor-interacting MAGE homologue (NRAGE), Schwann cell 1 (SC1) and receptor-interacting protein 2 (RIP2), binding to its intracellular domain. The resulting effects are apoptosis, survival, neurite outgrowth, and growth arrest. Akt – protein kinase B; FRS2 – fibroblast growth factor receptor substrate 2; Gab1 – Grb2-associated binder-1; Grb2 – growth factor receptor-bound protein 2; GIPC – GAIP interacting protein, C terminus; MEK – mitogen-activated protein kinase (MAPK)/ERK kinase; PDK1 – phosphoinositide-dependent kinase 1; SH2B – Src homology 2-B; SOS – Son of Sevenless; TRAF6 – tumor necrosis factor receptor-associated factor 6. Modified after Chao (2003).

Similar to TrkB, which upon binding of BDNF facilitates LTP, $p75^{NTR}$ could be shown to be specifically involved in LTD (Rosch et al., 2005; Woo et al., 2005). Furthermore, $p75^{NTR}$ plays a role in negatively modulating dendritic complexity and spine density. In homozygous organotypic hippocampal cultures lacking $p75^{NTR}$, neurons showed an increased complexity in their apical dendritic compartment, concomitant with an increase in spine density (Zagrebelsky et al., 2005). Thus, neurotrophins are able to positively and negatively influence neuronal function and structure. They therefore represent candidates for mediating the transition between functional and structural synaptic changes, which is required for memory consolidation (Bonhoeffer, 1996; McAllister et al., 1999).

Conclusively, the complex interactions between neurotrophins and their receptors profoundly influence neuronal structure and function during development and in the adult. In my work I

addressed the specific role of $p75^{NTR}$ during the morphological maturation of a single developing ESN over time.

2.4 Aim of this study

Since their first isolation in 1981 (Evans and Kaufman), embryonic stem (ES) cells have been used for a broad range of experimental approaches. ES cells are highly proliferative and genetically modifiable, allowing the generation of stable transgenic cell lines that derive from a single cell clone. Furthermore, ES cells can be differentiated into different cell types, amongst others defined populations of neurons. Therefore, ES cells represent the most plastic cell type available, and it is of special interest which factors influence their differentiation into neurons.

In the present study two separate aims were pursued. First, I was interested in whether ES cell-derived neuronal precursors (ESNPs) are able to integrate into a pre-existing neuronal circuit as complex as the hippocampus. Up to this point, this has only been shown for the hilar region of the DG (Benninger et al., 2003). To address this question, ES cells expressing the enhanced green fluorescent protein (EGFP) under the control of the *tau* promoter were differentiated into neuronal precursors (Bibel et al., 2004; 2007). Moreover, the transplantation of ESNPs into the different regions of the organotypic hippocampal cultures (DG, CA1 and CA3) was established. To find out whether ES cell-derived neurons (ESNs) are able to adopt hippocampal cell-like morphologies, the phenotypes of generated ESNs were described and categorized according to the regions where they were found. ESNs were compared to intrinsic hippocampal neurons in terms of dendritic length and complexity. Morphological maturation of ESNs was followed using time-lapse microscopy. It was of special interest to examine ESN dendrites for the occurrence of dendritic spines and synapses. Besides structural maturation, I investigated whether ESNs expressed hippocampal subtype-specific antigenic markers.

The second and major goal of my work was to establish a model system to examine the roles of neurotrophins and other plasticity-related proteins during maturation and integration of ESNPs into an existing circuit. The transplantation method I developed has the unique advantage that genetically modified neurons are growing surrounded by a wild type environment. Thereby, cell-autonomous effects could be analyzed. To this aim, a homozygous ES cell line – lacking exonIV of the $p75^{NTR}$ gene – was used for differentiation and subsequent transplantation, in parallel to the wild type line. The resulting $p75^{NTR}$-deficient ESNs were categorized and compared to wild type ESNs. Morphological analysis and time-lapse imaging were performed to determine the role of $p75^{NTR}$ during maturation and integration.

3 MATERIAL AND METHODS

3.1 Equipment

Camera	Nikon – Digital sight
Centrifuge	Sigma – 3K 15
Electrode holder	Biomedical instruments
Freezing microtome	Jung – Frigomobil
Gene gun	Biorad – Helios
Incubator	Heraeus – HeraCell 150
Inverse microscope	Nikon – Eclipse TS 100
Laminar flow hood	BDK-S 1200
Micromanipulator	Leitz
Water bath	Medingen – W12
Cell count chamber	Marienfeld – Neubauer improved
Pico spritzer	Toohey Company
Pipettus	Hirschmann
Tissue Chopper	Mc Illwain
Tubing prep station	Biorad
Vertical puller	Narishige – PC-10

3.2 Disposables

Bacteriological dishes 100 mm	Greiner Bio One (633102)
Cannulas 0.60 x 60 mm Sterican®	Braun (4665600)
Cell culture dishes 100 mm, 60 mm	Corning (3073078/3073080)
Cell culture plates 6-well, 12-well	Nunc (140675/150628)
Cell culture plates 6-well, 24-well	TPP (92406/92424)
Cell Strainer 40 µm	BD Falcon (352340)
Coverslips 13 mm	Marienfeld (No.1; 111530)
Cryotubes	Nunc (377267)
Filter for shooting	BD Falcon (353092)
Fluoro-Gel	Electron Microscopy Sciences (17985-10)
Glass capillaries 1.5 mm O.D. x 0.86 mm I.D.	Harward Apparatus (GC150F-10)
Millicell cell culture inserts	Millipore (PICMORG50)
Mycoalert® Mycoplasma detection kit	Lonza (LT-07-108)

Parafilm	Roth (H666.1)
Serological pipettes 2 ml, 5 ml, 10 ml, 25 ml	Sarstedt (86.125-2/3/4/5.001)
Stericup filter unit 250 ml, 500 ml	Millipore (SCGP U02 RE)
Suspension culture dishes 35 mm	Sarstedt (83.1800.002)
Syringes Inject®-F 1 ml	Braun (9166017V)
Tefzel tube	Biorad (165-2441)
Tissue tag	Hartenstein (4583)
*Trans*IT®-LT1 Reagent	Mirus Bio (MIR 2300)

3.3 Reagents

Aqua ad iniectabilia	Braun (3703452)
β-Mercaptoethanol	Sigma (M-7522)
B27-Supplement	Invitrogen (17504-044)
BME Medium	Invitrogen (41010-026)
BSA (Bovine serum albumin) - Immuno	Roth (8076.2)
BSA – ES cell culture	Sigma (A-9418)
BrdU (Bromodeoxyuridine)	Roche Diagnostics (10280879001)
Borax Decahydrat	Sigma (B-9876)
Boric acid	Merck (1.00165.0500)
Cytosin-β-D-Arabinofuranosid Hydrochlorid	Sigma (C-6645)
DAPI (4',6-diamidino-2-phenylindole)	Applichem (A4099)
D-Glucose	Applichem (A3666)
DMEM (Dulbeccos modified eagle medium) ES	Invitrogen (21969-035)
DMEM – Müller culture medium	Invitrogen (61965-026)
DMSO (Dimethyl sulfoxid)	Sigma (D-4540)
DTT (Di-thiothreitol)	Applichem (A2948)
EDTA (Ethylen-diamine-tetraactate)	Sigma (E-6511)
F12 Ham's nutrient mixture	Invitrogen (21765-029)
FCS (fetal calf serum) – differentiation-tested	Invitrogen (10270106)
5-Fluorodeoxyuridine	Sigma (856657)
Fungizone	Invitrogen (15290-018)
Gelatin	Sigma (G-1890)
GlutaMAX (200 mM)	Invitrogen (35050-038)
GS (goat serum)	PAA (B15-035)
HBSS (Hanks balanced salt solution)	Invitrogen (24020-091)

HBSS (10x)	Invitrogen (14065-049)
HS (horse serum), Hyclone	Perbio (SH30074.03)
Human apo-Transferrin	Sigma (T-1147)
Insulin	Sigma (I-6634)
Kynurenic acid	Sigma Fluka (61260)
Laminin	Roche Diagnostics (1243217)
L-Glutamine (200 mM)	Invitrogen (25030-024)
Microcarrier gold	Biorad (165-2262)
Mitomycin C	Sigma (M-0503)
Na-Selenite	Sigma (S-5261)
NB (Neurobasal) medium	Invitrogen (12348-017)
NEAA (nonessential amino acids)	Invitrogen (11140-035)
PBS (Phosphate buffered saline)	Invitrogen (14190-094)
Penicillin/Streptomycin	PAA (P11-010)
PFA (Paraformaldehyde)	Applichem (A3831)
Poly-L-Lysin Hydrobromid	Sigma (P-2636/53K5114)
Poly-Ornithine	Sigma (P-8638)
Progesterone	Sigma (P-8783)
Putrescine	Sigma (P-5780)
PVP (Polyvinylpyrrolidone)	Sigma (P-5288)
Retinoic acid	Sigma (R-2625)
Spermidine	Sigma (S-4139)
TritonX-100	Applichem (A1388)
Trypsin-EDTA solution	Sigma (T-3924)
Trypsin-EDTA ES cells	Invitrogen (25300-054)
Trypsin-Powder	Sigma (T-8802)
Uridine	Sigma (U-3750)

3.4 Solutions and media

3.4.1 ES cell culture and differentiation

EB medium (250 ml)

220 ml DMEM with Na-Pyruvat w/o L-Glutamine

25 ml FCS

2.5 ml non-essential amino acids

2.5 ml L-Glutamine

2.5 µl β-Mercaptoethanol

→ Filter sterile using a Stericup filter unit and store in 50 ml aliquots

ES medium (170 ml)

140 ml DMEM with Na-Pyruvat w/o L-Glutamine

25 ml FCS

1.7 ml non-essential amino acids

1.7 ml L-Glutamine

1.7 µl β-Mercaptoethanol

17 µl DTT stock solution (X)

→ Filter sterile using a Stericup filter unit and store in 50 ml aliquots, add LIF directly prior to medium change

2x Cryo medium (80 ml)

39 ml DMEM with Na-Pyruvat w/o L-Glutamine

25 ml FCS

16 ml DMSO (20%)

→ Filter sterile using a Stericup filter unit and store in appropriate aliquots at -20°C; thaw directly before use

N2 medium (50 ml)

25 ml DMEM with Na-Pyruvat w/o L-Glutamine

25 ml F12 (Ham's nutrient mixture)

1.25 ml Human apo-Transferrin stock (50 µg/ml)

250 µl Insulin stock (25 µg/ml)

250 µl BSA stock (50 µg/ml)

50 µl Progesterone stock (20 nM)

50 µl Putrescine stock (100 nM)

500 µl 200mM Glutamine (2 mM)

500 µl Penicillin/Steptomycin 100x

5 µl Sodium Selenite stock (30 nM)

→ Prepare quickly, filter and store in 10 ml aliquots at 4°C

→ Discard when pink

0.2% Gelatin (500 ml)

Add 1 g gelatin to 500 ml aqua ad iniectabilia and autoclave

→ Stir or shake in a warm state to dissolve gelatin and store at 4°C

Poly-Ornithine (0.5 mg/ml)

Dissolve 25 mg in 50 ml 150 mM Na-Borate ("Borax") solution pH 8.3 (adjust with HCl)

→ Filter and store at 4°C for 3 months

→ Dilute 1:5 in aqua ad iniectabilia to obtain a 0.1 mg/ml solution for coating the plate

Laminin (0.5 mg/ml)

→ Dilute 1:250 in PBS using glass pipettes and flask to obtain a working solution of 2 µg/ml Laminin

Mitomycin C (1 mg/ml)

Resuspend 10 mg in 10 ml of 5% DMSO in PBS

→ Filter and store in 1 ml aliquots at 4°C in the dark

→ Dilute 1:100 in dish (10 µg/ml)

Retinoic acid (5 mM)

Dissolve 15 mg in 10 ml DMSO

→ Prepare 100 µl aliquots in a dark bench and store at -20°C

→ Dilute 1:1000 in tube (5 µM) in the dark

4% EDTA in PBS (w/v)

Dissolve 400 mg EDTA in 10 ml PBS as 4% stock solution, filter and store at 4°C

→ Before use dilute 1:100 in PBS to obtain work solution with 0.04% EDTA

0.05% Trypsin in EDTA solution

Aliquot frozen trypsin powder into Eppendorf tubes containing 1-2 mg each

→ Directly before use dissolve 1 mg trypsin in 2 ml 0.04% EDTA in PBS

FCS (inactivated)

Thaw 500 ml bottle over night at 4°C

Heat-inactivate at 55°C for 30 min and store 25 ml aliquots at -20°C

→ Thaw directly before use at room temperature

→ FCS batch has to be tested for a successful completion of the differentiation procedure

Human apo-Transferrin stock solution (2 mg/ml)

Dissolve in H_2O, aliquot and store at -20°C

Insulin stock solution (5 mg/ml)

Dissolve in H_2O acidified with one drop of 25% HCl/10 ml

→ Aliquot and store at -20°C

BSA stock solution (10 mg/ml)

Dissolve in H_2O, aliquot and store at -20°C

Progesterone stock solution (20 µM)

Dilute 1:100 in H_2O to obtain 20 µM solution

→ Aliquot and store at -20°C

Putrescine stock solution (100 µM)

Prepare 100 µM solution in H_2O and store at -20°C

Sodium selenite stock solution (300 µM)

Prepare 300 µM solution in H_2O and store at -20°C

3.4.2 Neuronal cell culture

Müller culture medium (MKM)

100 ml BME-Medium (Invitrogen)

50 ml HBSS (Invitrogen)

50 ml Equine serum

1 ml Glutamax

2 ml Glucose (50%)

Preparation solution

98 ml GBSS

1 ml Kynurenic acid

1 ml Glucose (50 %)

→ Adjust pH to 7.2 using 1 M HCl and filter sterile

GBSS (g/l)

0.22 g $CaCl_2 * 2 H_2O$

0.37 g KCl

0.03 g KH_2PO_4

0.21 g $MgCl_2 * 6 H_2O$

0.07 g $MgSO_4 * 7 H_2O$

8.00 g NaCl

0.227 g Na_2HCO_3

0.12 g Na_2HPO_4

1.00 g D-Glucose

→ Filter sterile and keep at 4°C

Kynurenic acid (5 mM)

Dissolve 946 mg Kynurenic acid in 5 ml 1 M NaOH; add 45 ml MilliQ; filter sterile; prepare 1 ml fractions and store at -20°C

50% Glucose

Dissolve glucose in dH_2O 1:1 while heating, filter sterile in warm state and store 1 ml fractions at -20°C.

Antimitotics

2.422 mg Uridine in 10 ml dH_2O (1 M)

2.797 mg Cytosin-β-D-Arabinofuranosid Hydrochlorid in 10 ml dH_2O (1 M)

2.462 mg 5-Fluoro-2´-Deoxyuridin in 10 ml H_2O (1 M)

→ Mix stock solutions 1:1; filter sterile and freeze in 500 µl fractions

Borate buffer pH 8.5

1.24 g Boric acid

1.90 g Borax

→ Fill to 400 ml using sterile H_2O and adjust pH to 8.5

Poly-L-Lysin stock solution

Dissolve 10 mg/ml in H_2O, store at -20°C

GBSS/Glucose

50 ml GBSS

0.5 ml 50 % Glucose

→ Adjust pH to 7.2 using 1 M HCl and filter sterile

NB++ medium

50 ml NB

125 µl GlutaMAX

1 ml B27 supplement

Serum medium

200 µl inactivated FCS in 10 ml NB

1x HBSS for live imaging

50 ml HBSS 10x

175 mg $NaHCO_3$ (4.17 mM)

147 mg $CaCl_2$*$2H_2O$ (2 mM)

→ Fill to 500 ml with MilliQ

→ Stir to dissolve and filter sterile, store at 4°C

Spermidine

Dissolve 1 g Spermidine in 136 ml sterile MilliQ

→ Store at 4°C for one month

3.4.3 Immunohistochemistry

0.2 M Phosphate buffer pH 7.4

6.24 g NaH_2PO_4 * $2H_2O$

24.48 g Na_2HPO_4 * $2H_2O$

→ Fill to 1 l with MilliQ H_2O

4% PFA in 0.1 M phosphate buffer

Heat 500 ml H_2O to70°C (microwave)

Add 40 g PFA under the hood

→ Stir until PFA is completely dissolved (add a few drops of 1 M NaOH)

→ Allow to cool to room temperature

→ Filter through fluted filter

→ Add 500 ml 0.2 M phosphate buffer and mix

→ Store in 50 ml aliquots at -20°C

10x PBS (1 l)

80 g NaCl

2 g KCl

14.4 g Na_2HPO_4

2.4 g KH_2PO_4

→ Adjust pH to 7.4 using 10 N NaOH, fill to 1 l with MilliQ H_2O and filter

50 mM NH_4Cl

2.67 g NH_4Cl

100 ml 10x PBS

→ Fill to 1 l with MilliQ H_2O

Blocking solution

1% BSA (w/v)

10% GS (v/v)

0.2% Triton-X-100 (stock solution 2%)

30% Sucrose solution

9 g sucrose

15 ml 0.2 M phosphate buffer

→ Fill to 30 ml with MilliQ H_2O

3.5 Antibodies

Antigen	Organism	Work dilution	Source
αCaMKII (Ca^{2+}/calmodulin dep. kinase II)	mouse	1:500	Zymed (13-7300)
Ctip2	rat	1:1000	Abcam (ab18465)
GFAP (glial fibrillary acidic protein)	mouse	1:1000	Sigma (G-3893)
GFP (Green fluorescent Protein)	mouse	1:500	Millipore (MAB3580)
GFP	rabbit	1:500	Millipore (AB3080)
IB4 (Isolectin B4)–Alexa 568 (0.5 mg/ml)	--	1:100	Invitrogen (I21412)
MAP2 (microtubule associated protein)	mouse	1:1000	Sigma (M-4403)
NeuN (neuronal antigen N)	mouse	1:500	Millipore (MAB377)
Prox1	rabbit	1:1000	Covance (PRB-238C)
Synapsin1	rabbit	1:500	Millipore (AB1543)
Tau	rabbit	1:400	Dako (A0024)
vGAT (vesicular GABA transporter)	rabbit	1:1000	SYSY (131011)
vGLUT1 (vesicular glutamate transp.1)	rabbit	1:5000	SYSY (135311)
Mouse/rabbit/rat Cy2/Cy3/Cy5	goat	1:500	Jackson Immuno Res.

3.6 Cell culture techniques

3.6.1 Cultivation and differentiation of mouse embryonic stem cells

Basic ES cell culture

To keep mouse ES cells in an undifferentiated and proliferative state they were held under defined conditions. Two requirements had to be complied with: A layer of inactivated mouse embryonic fibroblasts (MEF) as well as the addition of leukemia inhibitory factor (LIF) to the ES cell medium. $1x10^6$ MEFs were sowed onto a gelatin-coated cell culture dish and cultured in EB medium until confluence was reached after 48 h (Fig. 6C). At this point MEFs were mitotically inactivated by incubating with 10 µg/ml Mitomycin for 4 h at 37°C. To stop the inactivation MEFs were washed with pre-warmed PBS three times and henceforth cultured in ES medium. Inactivated MEFs were used 4 h to 4 days later for ES cell culture.

Frozen mouse ES cells were quickly warmed at 37°C (water bath) until the cell suspension was almost completely thawed. The cells were then carefully transferred into 15 ml pre-warmed ES medium and centrifuged (5 min and 1000 rpm). The cell pellet was adsorbed in ES cell medium containing LIF (concentration depended on the batch used, production see below), and the cells were plated onto an inactivated MEF layer for cultivation at 7% CO_2 and 36.5°C. The first goal was to generate a homogenous and highly proliferative population of

pluripotent ES cells. To this end, medium was changed every day, and LIF was freshly added. Cells grew in oval-shaped multilayered colonies showing clearly reflecting borders in phase contrast (Fig. 6D). When this stage was reached (after 48-72 h) cells were passaged onto a new layer of inactivated MEFs and thereby diluted, according to colony density and quality 1:6 to 1:20. For this purpose cells were washed with PBS and incubated with 1 ml Trypsin/EDTA per 6 cm dish for 3 min at 37°C. Trypsin treatment was stopped by adding 10 ml ES medium and pipetting until the cell suspension was homogenous. After centrifugation the pellet was taken up in 10 ml ES medium, the corresponding volume of cell suspension (according to the splitting ratio) was diluted and plated. To reach optimal proliferation and homogeneity, passaging was repeated twice. For detection of a possible mycoplasma infection every thawed vial of ES cells was routinely tested using the Mycoalert® mycoplasma detection kit. During the first splitting step a few ml of the cell suspension were plated onto a gelatin-coated dish and incubated for four to eight days without medium change. During this time period the supernatant was tested repeatedly. In case of infection the cells were discarded and everything was cleaned, before restarting with completely fresh solutions and media.

Differentiation of ES cells into neuronal precursors

Differentiation of mouse ES cells was performed according to the protocol developed by Bibel et al. (Fig. 6A; Bibel et al., 2004; 2007). In a highly proliferative state ES cells were passaged on gelatin-coated cell culture dishes to deprive them of MEFs. The cells were sowed in parallel at different dilutions (1:6, 1:8, 1:10) to assure optimal cell density and proliferation. ES medium (LIF-enriched) was changed every day. After 36-72 h in culture, 80% confluence had to be reached on one of the dishes, showing that cells were ready to be passaged again. On gelatin, ES cells grew in a monolayer covering the surface of the dish not taken by residual MEFs (Fig. 6E). It took four passages on gelatin before MEFs were sufficiently diluted to proceed. At this stage it was very important that the cells were small and dark with clearly defined borders, as this indicates that they are still proliferative. Cells in the process of differentiation became bigger and less rich in contrast and were not able to produce neurons anymore. The ES cells were trypsinized, and the cell number was determined. $3.5x10^6$ cells were sowed onto a bacteriological dish in 15 ml EB medium without LIF. At this stage the cells grew in suspension and formed cellular aggregates, so-called EBs (embryoid bodies; Figure 6F). The medium was changed after 2 d, 4 d and 6 d, respectively, while at day four and six 5 µM retinoic acid was accurately mixed with the medium before getting in contact with the cells. To change the medium, the cells were carefully taken up in a 25 ml pipette and transferred into a falcon tube. Residual medium was slowly added by letting it flow from the side of the tube. Five minutes later, when the EBs had settled down, the old medium could be aspirated. New medium had to be added with care as

well. After eight days in culture, EBs were washed three times in PBS and subsequently dissociated using freshly thawed trypsin in a 0.05% solution in 0.04% EDTA in PBS. 0.5 ml per EB dish were added directly to the EB pellet in the bottom of the tube, followed by a shaking incubation at 37°C for exactly 3 min. The reaction was stopped by adding 10 ml of EB-Medium and careful but vigorous pipetting until a single-cell suspension was reached. After centrifugation, the pellet was adsorbed in 10 ml EB again. Re-suspension had to be performed extremely carefully, and cells were filtered through a cell strainer to remove residual cell clumps. After counting, 2x cryomedium was added to the cell suspension, and aliquots of $5x10^6$ neuronal precursors were frozen. Freezing was done in an isopropanol-filled container at -80°C, leading to a slow and gentle cooling process. Once precursor quality had been tested, the vials were transferred to liquid nitrogen.

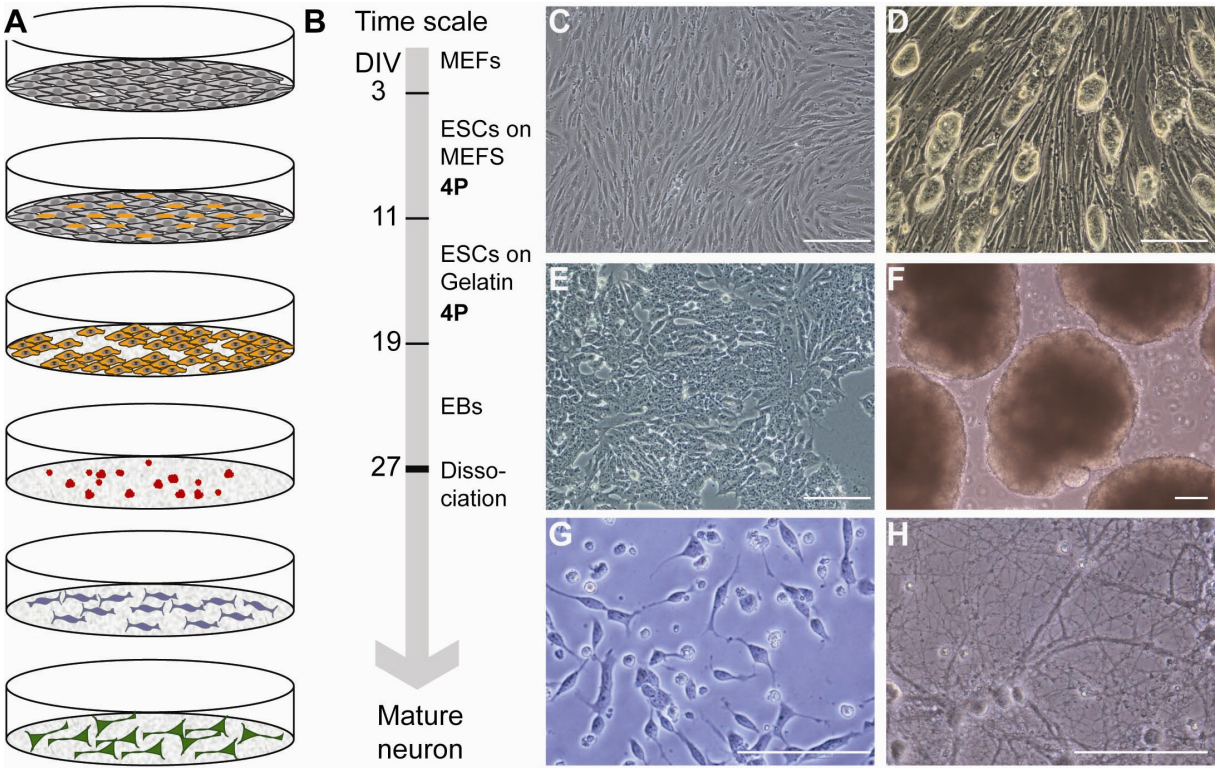

Figure 6 | ES cell culture and differentiation into neuronal precursors. A | Schematic view of the differentiation procedure developed by M. Bibel, different steps from plating MEFs until growing mature neurons on a cell culture dish (according to Bibel et al., 2004). **B** | Time scale of differentiation procedure. DIV – days *in vitro;* MEFs – mouse embryonic fibroblasts; ESCs – embryonic stem cells; 4P – 4 passages; EBs – embryoid bodies. **C-H** | Photographs of MEFs, ESCs and neurons in the respective stages corresponding to **A**. Scale bars 100 µm.

Culture of neuronal precursors

ES cell-derived neuronal precursors (ESNPs) were grown on Poly-ornithine and Laminin-coated surfaces. Cover slips needed to be pre-treated with NaOH (see below 3.5.4). The surface – plate, dish or cover slip – was washed once with clinically pure water (*aqua ad iniectabilia*, Braun). 0.1 mg/ml Poly-Ornithine was added and incubated over night at 37°C.

As a next step the surface had to be washed three times with *aqua ad iniectabilia* before adding 2 µg/ml Laminin in PBS. Washing had to be fast, as the surface should not dry. After 2 h to 72 h of Laminin-coating, the surface was washed with PBS, and precursors were plated.

Frozen precursors were quickly warmed at 37°C (water bath) until the cell suspension was almost completely thawed. Then it was carefully transferred into 20 ml of pre-warmed EB medium and centrifuged. The pellet was adsorbed in an adequate volume of N2 medium; re-suspension was performed extremely carefully. The cells were plated onto the coated cell culture plate and allowed to adhere at 37°C. As a quality test after EB dissociation, different cell numbers were plated on a 12-well plate (e.g. 0.7/ 1/ 1.3/ $2x10^6$). After 2 h of incubation, radially shaped neuronal precursors had attached to the surface (Fig. 6G). The Medium was changed to fresh N2 after 2 h and after 24 h again. The last medium change was done 48 h after plating. From this point on the neurons were grown in NB medium. They matured and formed elaborate processes (Fig. 6H).

Production of LIF using COS-7 cells

COS-7 cells were cultured in EB medium and expanded on 10 cm culture dishes. One day before transfection they were split 1:6. Transfection with the LIF plasmid ("pCAGGS-LIF" from Y.-A. Barde, Basel) was done using the *Trans*IT®-LT1 Reagent (Mirus). To this end 18 µl reagent were diluted in 1.5 ml serum-free DMEM per 10 cm plate and incubated 5 to 20 min at room temperature. 6 µl DNA (1 µg/µl) were added followed by an incubation of 15 to 30 min. Subsequently, the mix was carefully dropped on the cells. 24 h after transfection, the medium was changed. At this point the cells started to secrete the expressed LIF into the medium. The cells were cultured for five more days until the medium started to become yellow. Then the medium of all plates was harvested, pooled and centrifuged. The supernatant was filtered and frozen in 10 ml aliquots which were stored at -80°C. A small volume of supernatant was kept and tested for mycoplasma infection using the Mycoalert® Mycoplasma detection kit.

Frozen LIF aliquots were taken off the freezer, and immediately 1.4 µl DTT stock solution and 0.1 µl β-Mercaptoethanol were added. The solution was warmed by hand, gently inverting the tube, and subsequently stored at 4°C for one month. Every week, 1.4 µl DTT stock solution and 0.1 µl β-Mercaptoethanol were added to prevent the LIF from oxidizing. The concentration of LIF to be used for ES cell culture had to be tested. For this purpose different dilutions of newly produced LIF were used in parallel to a well-established LIF batch. ES cells were tested for differentiation on gelatin (they should not differentiate for at least six passages) as well as for a successful course of the differentiation procedure described above, resulting in an appropriate yield of neurons.

3.6.2 Preparation and cultivation of organotypic hippocampal slice cultures

Cultures were prepared and cultivated as previously described (Stoppini et al., 1991). Postnatal day 5 mice (p5; C57/Bl6) were decapitated, and the skin was removed from the upside of the head. Using scissors and forceps the skull was opened to expose the brain. The brain was horizontally cut with a sharpened spatula starting caudally between cerebellum and *inferior colliculus*. The removed section was transferred upside down into cooled preparation solution. Cerebellum and *colliculi* were removed using a spatula. Hemispheres were separated, and the exposed hippocampi were flapped out of the brain. After detaching from the cortex, the hippocampi were moved onto the teflon disc of the tissue chopper, and 400 µm slices were cut. The slices were rinsed into a dish containing cooled preparation solution, carefully separated and incubated for 30 min at 4°C. Subsequently, Millicell® cell culture inserts were placed in pre-warmed 6-well plates containing 1.1 ml MKM medium per well. Four slices were transferred onto one insert. After 72 h of cultivation at 36.5°C and 5% CO_2, 15.4 µl antimitotics were added to the wells. 24 h later, the inserts were transferred into a new plate containing pre-warmed MKM medium. Slices were cultured for up to six weeks, the medium being changed twice a week. For this purpose 500 µl of the old medium were replaced by new MKM to which 1.25 µg/ml Fungizone as well as 100 U Penicillin and 100 µg/ml Streptomycin had been added.

Biolistic gene transfer to transfect hippocampal control neurons

Intrinsic hippocampal neurons were transfected with a plasmid containing farnesylated EGFP, using biolistic particle transfer via the Helios Gene Gun. First, 600 nm gold micro particles were loaded with the respective plasmid. This was done by $CaCl_2$ precipitation as follows: 12.5 mg gold particles were mixed with 100 µl of 50 mM spermidine solution; formation of aggregates was prevented by sonicating for 10 s. 12.5 µg DNA were added to the gold solution. While vortexing carefully, 100 µl of 1 M $CaCl_2$ were added drop-wise, followed by 10 min incubation at room temperature. Residual spermidine was removed by four consecutive washing steps in 96% ethanol using a micro centrifuge at 100g, before the micro particles were dissolved in 3 ml 0.05 mg/ml PVP in 96% ethanol. The Tefzel tube was inserted into the tubing preparation station and blown with nitrogen for 10 min before the gold suspension was loaded. After letting the gold sink for 3-5 min, the ethanol was removed. For a homogenous distribution of the gold particles, the tube was rotated for 30 s, followed by a drying period of 5 min. Shooting was done using helium pressure (100 psi) and a 3 µm filter in front of the barrel aligner to prevent damage of the culture by gold clusters.

3.6.3 Preparation of primary hippocampal cultures

Treatment of cover slips

Cover slips were kept in steel racks and incubated in 10 M NaOH for three to five hours at 100°C. Afterwards they were washed with MilliQ water, five times for 20 min. As soon as they had dried, the cover slips were transferred into a glass Petri dish and sterilized for six hours at 225°C. When they had cooled down, 10 ml Poly-L-Lysin solution (0.5 mg/ml in Borate buffer) was added for coating which took place either at 37°C for two to three hours or at 4°C over night. Subsequently, the cover slips were washed with sterile water four to five times and dried.

Preparation and culture

A pregnant mouse at E18 was etherized until heart beat stopped. The abdomen was sterilized using ethanol, and the abdominal wall was opened with scissors. The uterus was detached at the left and right side and transferred into a cooled Petri dish. The uterus was opened to remove the embryos which in turn were decapitated, and their heads were conveyed into a dish containing chilled GBSS/Glucose. The hippocampi were dissected and collected in a new dish with GBSS/Glucose. Residual cortex was removed, and the hippocampi (max. 12) were transferred into an Eppendorf tube containing 1 ml Trypsin/EDTA solution. After incubation for 30 min at 37°C, the solution was carefully removed, and the reaction was stopped by adding 1 ml of serum medium. The tissue was washed four times with new serum medium followed by dissociation using a fire-polished glass pipette. After centrifugation (1.500 rpm; 5 min), the supernatant was discarded, and the pellet was re-suspended in 1 - 1.5 ml NB^{++} medium. The cell number was determined, and the respective volume was added to the wells (24-well plate) into which 500 µl NB^{++} had been given previously.

3.7 Transplantation of ESNPs into hippocampal slice cultures

Glass micropipettes were produced using a Narishige vertical puller. The puller was set “step2 heater”, heaters were adjusted to 62.7 and 49, respectively, and the capillary was stretched between the two heating steps for 8 mm. The needle opening size had to be between 25 and 35 µm, and was controlled under the microscope (Fig. 7A). This was especially important since precursors (Fig. 7B) had to pass the pipette, but on the other hand the lesion to the culture was to be kept as little as possible. After the frozen precursors were centrifuged for 5 min in 20 ml EB (see 3.6.1), the pellet was carefully re-suspended in 100 µl N2 medium, and the cell suspension was transferred to a suspension culture dish to be stored inside the incubator for up to 30 min. Precursors were transferred into the pipette as fast as possible (Fig. 7C). The micro injection device was set to 10 psi and 0.1 ms (Fig. 7D),

allowing a clearly visible volume of cell suspension to be pressed out the pipette. Slice cultures had been prepared from p5 mice as described above and were used five days after preparation. Upon transplantation, small drops of fluid were initially placed on top of the tissue in the main regions of the hippocampus, CA1, CA3 as well as the dentate gyrus (DG; Fig. 7G). After establishing the procedure, precursors were injected into the tissue. During the process of transplantation the properties of the pipette could change, e.g. the pipette could clog. Therefore, the volume leaving the pipette as well as the presence of cells within the fluid was visually controlled, and the injection time was adjusted if necessary. In case of clogging, pressure application was repeated until ejection could be seen.

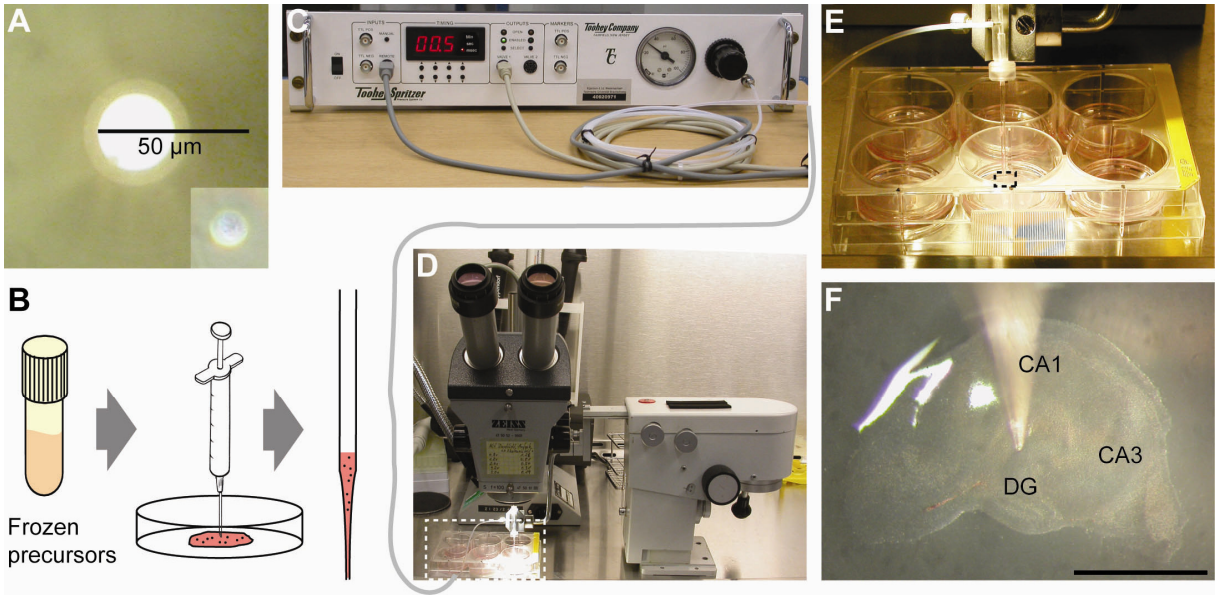

Figure 7 | Transplantation setup and procedure. A | Glass micropipette with a needle opening size of 25 µm; bottom right corner shows neuronal precursor cell. **B** | The pipette is loaded with precursors using a syringe. **C** | Picospritzer controls compressed air to apply pressure on the pipette. **D,E** | Controlled by a micromanipulator, the pipette is moved into the wells of the cell culture plate, observed through a binocular. **E** | Higher magnification view of boxed region in **D**. **F** | ESNPs are transplanted into the different regions of the hippocampal slice culture CA1, CA3 and DG; higher magnification view of boxed region in **E**. Scale bar 1 mm.

3.8 Immunohistochemistry

3.8.1 Organotypic cultures

After transplantation of ESNPs, immunohistochemistry using a αGFP antibody was performed on a routine basis in order to increase the EGFP signal. Organotypic cultures were fixed over night in freshly thawed 4% PFA solution at 4°C. After warming to room temperature, they were washed eight times with PBS for 15 min on the shaker. Quenching was done in 50 mM NH_4Cl for one hour at room temperature, followed by a short wash in PBS. Subsequently, the membranes were excised, and the slice cultures were transferred into a 24-well plate filled with PBS. The PBS was exchanged for blocking solution (300 µl per

well) with which the cultures were incubated over night at 4°C. The binding of the first antibody was done in blocking solution without BSA for six days at 4°C as well (see 3.5 for antibodies and dilutions, respectively). Afterwards the slices were washed again eight times for 15 min in PBS and then incubated with the secondary antibody in PBS for two days. Finally, the cultures were again washed, stained with DAPI (1:1000 in PBS) for five minutes, washed and mounted with Fluoro-Gel®.

3.8.2 Dissociated cultures

Cells growing on cover slips were fixed using 4% PFA at 4°C for 15 min. This was followed by washing with PBS – three times for 20 min – and incubation in blocking solution for one hour at room temperature (300 µl per well). All washing and incubation steps were done on the shaker. Incubation with the first antibody took place in blocking solution without BSA over night at 4°C. Afterwards cells were allowed to warm to room temperature and washed again three times for 20 min with PBS. The secondary antibody was diluted in PBS and incubated with the cultures for two hours. After washing with PBS, DAPI staining (1:1000 in PBS, 5 min) and repeated washing, cover slips were mounted upside-down in a small drop of Fluoro-Gel® onto a slide.

3.8.3 Cryosections

Organotypic cultures were fixed for one hour in 4% PFA solution. They were washed in PBS (three times 15 min) before they could be detached from the membrane using a small paint-brush under the binocular. By transferring the cultures in a 24-well plate containing 30% sucrose solution, they were dehydrated over night at 4°C. To horizontally freeze the slices they were brought upon a piece of parafilm in a drop of sucrose solution. Importantly, their correct orientation had to be controlled under the binocular, before the parafilm was placed upside down on top of a freezing drop of Tissue Tek. The parafilm was removed quickly, and a second drop of Tissue Tek was added before the bottom part was completely frozen. Cryosections (30 µm) were prepared using a freezing microtome, and the slices were transferred into fresh PBS. For immunohistochemical staining sections were kept free-floating in miniature sieves that were moved from well to well in a 12-well plate. Blocking was performed in blocking solution for one hour at room temperature (2 ml per well). The primary antibody was added to blocking solution without BSA and incubated with the sections at 4°C over night. On the following day, sections were allowed to reach room temperature for 15 min, followed by three washing steps with PBS, 30 min each. The secondary antibody was diluted in PBS and incubated with the sections for two hours. Again, two 30 min washing steps in PBS followed. Staining was completed by adding DAPI (1:1000 in PBS) for 5 min and repeated washing afterwards. Sections were mounted in Fluoro-Gel®.

3.9 Imaging and analysis

3.9.1 Live imaging of ESNs in hippocampal slice cultures

During the culture period ESNs growing in the slice culture were pictured repeatedly. The goal was either to localize interesting neurons that would be matter of investigation later on, or to follow the maturation of a single neuron over a period of time (time-lapse imaging). In some cases live microscopy was used to image dendritic spines, as well. The live-imaging setup consists of an Olympus BX61WI microscope combined with the Cell^M software designed for gentle and fast exposure and computation of three-dimensional image stacks. It is equipped with a 10x, a 20x as well as a 40x objective. Culture inserts were transferred into a 35 mm dish containing a drop of pre-warmed HBSS and covered by 2 ml additional HBSS. Beyond that, live imaging was performed as previously described (Gogolla et al., 2006a; Gogolla et al., 2006b). Times outside the incubator were kept short (max. 20 min). When screening the slices, single plane records were taken to recognize a specific ESN later on. While screening after 28 to 32 DIV, ESNs were counted and attributed to the different ESN types A and B (see below). Quantification was done based on the screening because after fixation, fewer cells were found in some cases. Since the fluorescence signal was often very low and not all classification criteria could be controlled via live imaging, some false-positive type A ESNs might have been included. For analysis of the three-dimensional structure, image stacks were recorded, the step width being dependent on the chosen objective. Since it was found that repeated imaging impaired quality and survival of ESNs after four to five days, time-lapse analysis was restricted to a sequence of four days.

3.9.2 Tracing the entire dendritic tree

Following a culture period of 32 days after transplantation (in most cases), slice cultures were fixed and immunohistochemically stained for EGFP. Within the mounted slices, neurons were imaged at the Axioplan2 microscope combined with an ApoTome module (Zeiss), using a 20x objective and 1 µm step width to capture their entire dendritic tree. Image stacks were either flattened to generate a maximum intensity projection (Fig. 8A) or transferred into the Neurolucida® software and traced (Fig. 8B). The program calculates crossing points of concentrical globes around the soma with the apical and basal dendritic tree, respectively (Sholl analysis), leading to a characteristic complexity curve providing detailed information about length and complexity of a neuron (Fig. 8C). Mean values were determined for the neuron population, and the standard deviation of the mean was divided by the square root of the analyzed neuron number, to calculate the error. For statistical analysis, a two-tailed student's t-test (type 3) was conducted, $p < 0.05$ showing a statistical significant difference between two groups of neurons.

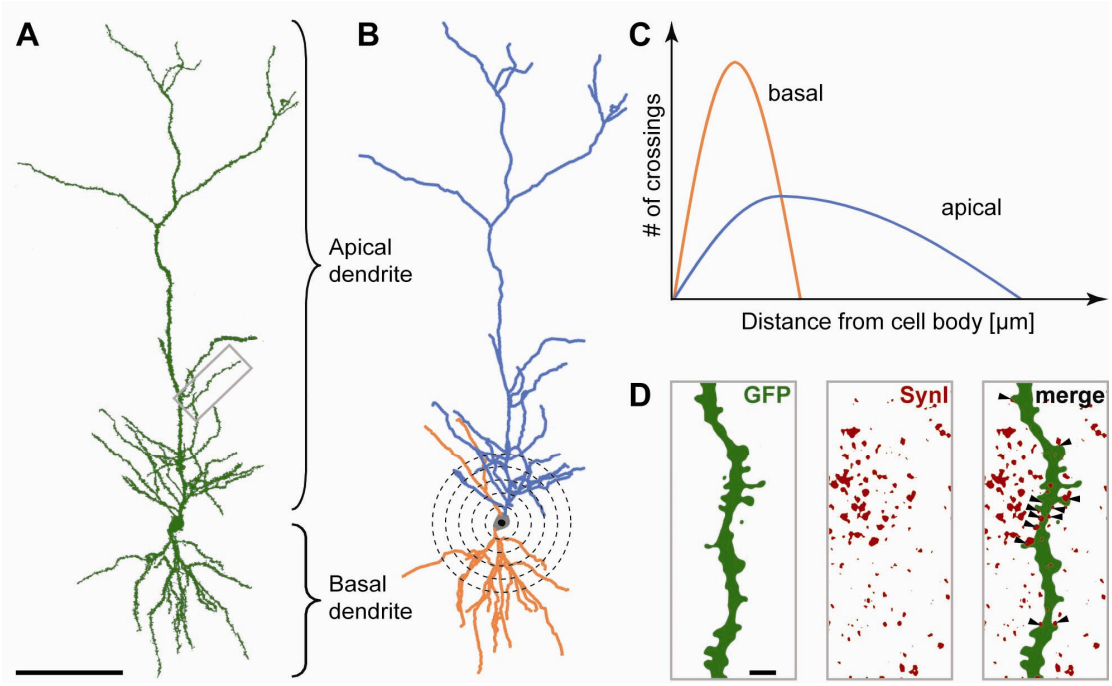

Figure 8 | Analysis of neuronal morphology. A | Maximum intensity projection of three dimensional image stack recorded at the Zeiss Axioplan2 using the Apotome. Scale bar 100 µm. **B** | Tracing of the complete dendritic arbor using the Neurolucida® software; distinction between apical and basal dendrites. Crossings with concentrical globes around soma are determined. **C** | Sholl analysis for apical as well as basal dendrites from **B**, calculated by the software. **D** | High resolution confocal image of an EGFP-positive dendrite co-stained for a presynaptic marker. Arrowheads point to synapses detected by co-localization of both markers. Scale bar 2 µm.

3.9.3 Detection of synapses

Synapses were detected by co-staining fixed slice cultures with antibodies against GFP and a presynaptic marker. Image stacks were taken at the LSM5-Meta confocal laser scanning microscope, providing the high-resolution in a three dimensional stack of a multi-channel image which was needed to co-localize EGFP as well as Cy3 signal in structures as small as synapses. A 40x water immersion objective was used, combined with a digital 4x zoom and a step width of 0.3 µm. A green structure overlapping with or directly neighbored by a red dot in the same focal plane, one below or one above, was considered a synapse (Fig. 8D). Unfortunately, antibodies against GFP as well as the presynaptic markers were limited in penetrating the fixed and processed slice culture, restricting the analysis to the more superficial dendrites. Therefore, the number of analyzed dendrites was limited, and the detected signal was often very low.

3.9.4 Imaging dissociated cultures

Dissociated growing ESNs and primary hippocampal neurons were imaged either at the Axioplan2 microscope or the LSM5-Meta. Multi-channel single plane records were taken.

3.10 Cell lines

Cell line	Origin	Source	Genotype
M22	J1 murine ES cell line	K. Tucker, Basel*	WT, *tau*EGFP transgene
B7-15	R1 murine ES cell line	C. Annaheim, Basel*	$p75^{NTR-/-}$, *tau*EGFP transgene
MEFs	Bl6 mouse	Y.-A. Barde, Basel	$Puro^R$/Tbx2 transgene
COS7	African green monkey kidney fibroblasts	DSMZ Braunschweig	WT

Generation of the tauEGFP-expressing ES cell lines M22 and B7-15

Both ES cell lines were generated in the lab of Y.-A. Barde, Basel (CH). An 8.5 kb fragment from the Mapt (*tau*) locus was cloned by K.-L. Tucker and inserted into a plasmid containing EGFP as well as a neomycin resistance (plasmid A). By electroporation of J1 ES cells, this plasmid was brought into the genome as a multiple copy transgene, resulting in relatively intense EGFP fluorescence compared to the homologous integration approach. The deriving WT ES cell line, EGFP-positive upon *tau* promoter activation, was named “M22”.

In her dissertation, C. Annaheim generated an ES cell line homozygous for the lack of exonIV of the $p75^{NTR}$ gene (Annaheim, 2008; Plachta et al., 2007). This was done using a gene targeting vector (plasmid B) carrying a floxed version of exonIV as well as a neomycin resistance (Neo^R) in a first electroporation step. In a second step, positive clones were electroporated with a plasmid expressing Cre recombinase (plasmid C), leading to a heterozygous excision of the exon together with Neo^R. In a third step, the targeting vector (plasmid B) was used again to introduce loxP sites into the other unimpaired allele of $p75^{NTR}$. Positive clones were treated anew with the Cre vector (plasmid C) resulting in a $p75^{NTR-/-}$ ES cell line called “B7”. Subsequently, C. Annaheim used the *tau*EGFP plasmid (A) to introduce the EGFP transgene in multiple copies into the genome. The resulting $p75^{NTR-/-}$ ES cell line expressing EGFP in neuronal progeny was named “B7-15”.

4 RESULTS

4.1 Transplantation of ESNPs into hippocampal slice cultures

The first goal of the present study was to establish a reliable and reproducible transplantation method for ES cell-derived neuronal precursors (ESNPs) which would enable me to control transplanted region and cell number, and follow up single ES cell-derived neurons (ESNs). So far, a similar transplantation approach into hippocampal cultures had been used by C. Annaheim (2008) who started the work on the present project, transplanting a high number of cells to follow their collective projection. Another group has also brought ESNPs on the surface of slice cultures (Benninger et al., 2003; Husseini et al., 2008), although they were using a different system and focused more on the electrophysiological properties of glial precursors as well as neuronal precursors integrated into the hilar region of the dentate gyrus (DG).

4.1.1 Survival of transplanted precursors

In the first experimental setting, I found that ES cell-derived cells survived for 14 days within organotypic cultures (Fig. 9A). By their green fluorescence it could also be seen that they developed into neurons, as EGFP expression was driven by the *tau* promoter. The major fraction of ESNs was located within the region into which the cells had been transplanted (DG in Fig. 9A). Nevertheless, there were also a considerable number of green neurons that had moved toward other regions (the entorhinal cortex – left side of the image – or to the periphery of the culture). In order to estimate the transplanted cell number and define conditions for an optimal success rate of ESNs after 32 days of culture, slices were fixed two hours after transplantation and immunohistochemically stained against the EGFP protein and DAPI as well. Surprisingly, EGFP fluorescence was already seen at this early stage (see Fig. 9B-D). In parallel, precursors had been transplanted into the three regions of interest – DG, CA1 and CA3 – and were visible as green dots (DAPI is shown in red). An approximate number of 1000 injected cells per slice could be assumed ($5x10^6$ cells in 100 µl N2 medium results in $5x10^4$ per µl cell suspension; for the transplantation of 48 slices – two plates – about 1 µl suspension was needed, corresponding to 0.02 µl and 1000 cells per slice, respectively). Additionally, the survival of frozen and thawed ESNPs was generally very low. Plating ESNPs on cover slips after a freezing period of a few weeks in liquid nitrogen, about twenty times as many cells were needed to obtain a confluent layer of neurons than when freshly dissociated hippocampal neurons were used. Regarding these facts one can assume that of the transplanted 1000 cells per slice about 50 cells might have been viable. This number lies within the same range as the number of surviving cells after two hours of

incubation within the culture. In the DG, 22 cells were seen, 23 in CA1 and 18 in CA3, most of which in a spatially restricted area close to the injection site (single experiment, Fig. 9B-D). Furthermore, there were small-sized DAPI signals most likely corresponding to dead cells (red staining in C and D). However, whether these belong to precursors which had died upon transplantation or to host cells destroyed through the tissue penetration of the pipette cannot be stated.

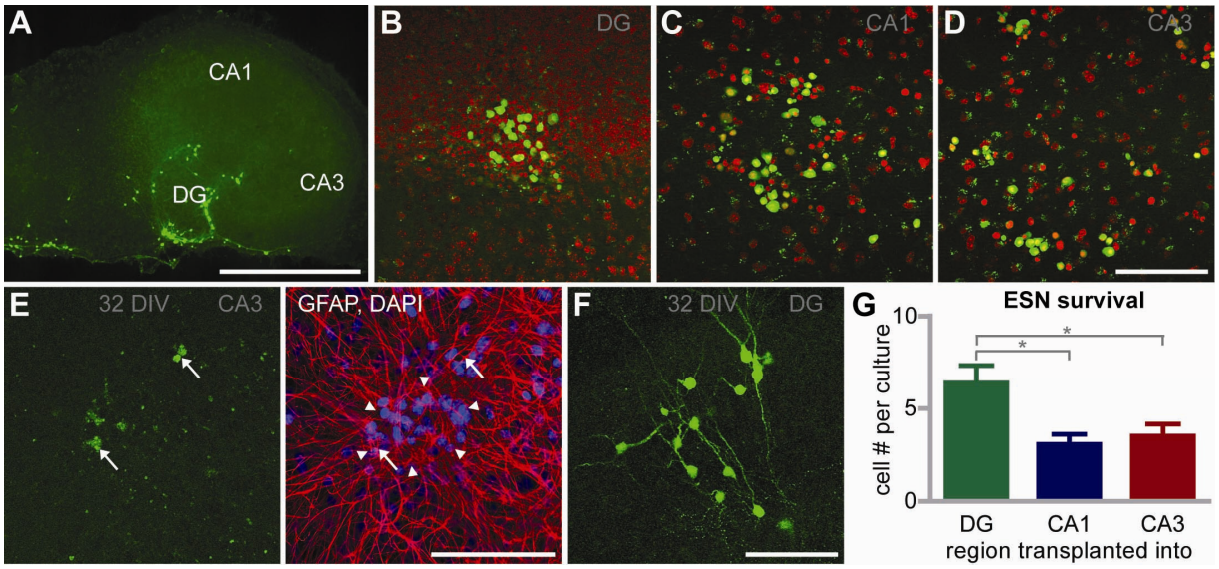

Figure 9 | Transplantation efficiency and survival of ESNs. A | After 14 days, EGFP-positive neurons can be seen in the fixed slice. **B-D** | Precursors transplanted into DG, CA1 and CA3 regions, fixed after two hours and stained for EGFP (green) and DAPI (red). **E** | Slice culture fixed 32 days post transplantation into CA3 and stained with αGFP, GFAP (glial fibrillary acidic protein) and DAPI. Arrows point to EGFP-positive debris; arrowheads mark the presumptive injection site. **F** | ESNs in the DG at 32 DIV, stained with αGFP. **G** | ESNs counted separately for slices transplanted into the respective regions; average ESN number at 32 DIV (DIV refers to days *in vitro* post transplantation; DG: 6.4 ± 0.9; CA1: 3.1 ± 0.5; CA3: 3.5 ± 0.6; n=80 slices per transplanted region). Error bars represent the standard error of the mean. Student's t-test, *p < 0.05. Scale bars 1 mm in **A**, 100 µm in **B-F**.

When the cells were injected into the hippocampal slices, tissue reorganization had to take place. This was seen in slices, which had been transplanted with ESNPs 32 days prior to fixation, and were stained with αGFP, the astrocyte marker GFAP (glial fibrillary acidic protein) as well as with DAPI (Fig. 9E). Clearly, astrocytic processes were more concentrated in a defined area, where an accumulation of DAPI-positive nuclei was seen as well. Close to this area EGFP signals were also found (arrows). The region with the accumulation of nuclei therefore might represent the injection site (arrowheads), and the EGFP-positive signals, which did not correspond to cells, most likely belonged to cell debris of ESNPs that had died upon transplantation.

After 32 days in culture, ESNs were seen in most of the slices (Fig. 9F). Remarkably, the number of surviving cells was dependent on the transplanted hippocampal region. While in cultures transplanted into the DG on average 6.4 ± 0.9 cells were found, only 3.1 ± 0.5 and 3.5 ± 0.6 cells survived in the CA1 and in the CA3 regions, respectively, the difference being

statistically significant (Fig. 9G; $p < 0.01$ for DG/CA1; $p < 0.05$ for DG/CA3). Altogether it can be said that transplantation using the presented setup and parameters fulfilled the criteria for the analysis: A relatively constant number of ESNs survived within the hippocampal slice cultures, and isolated ESNs were often found.

4.1.2 Growing up in a stimulating neighborhood

At the beginning, transplantation parameters such as injection time as well as the distance from which the suspension was dropped unto the slice culture were varied. This series of experiments included an injection deep into the slice culture. The needle was lowered until it touched the surface of the culture. From this point on it was pushed even lower, leading to a penetration of the outer cell layers. Subsequently, the needle was withdrawn again and the cell suspension was injected into the generated tissue cleft. 21 days after transplantation (21 DIV), different types of ESNs were found (Fig. 10A-C; all three images originate from the same culture preparation and the same precursors were used). Some neurons showed a very immature morphology with thin and short dendrites (Fig. 10A). On the other hand, their EGFP fluorescence (enhanced by αGFP-staining) was strong and their cell bodies were stained with an antibody against the microtubule associated protein 2 (MAP2) which is specific for neurons (Fig. 10A''). In contrast, other ESNs showed considerably lower fluorescence intensity (Fig. 10B,C). Maximum intensity projections of the different ESNs (left) also revealed that the morphologically immature neurons (Fig. 10A) were growing rather flatly and in parallel to the culture surface, whereas the other neurons (Fig. 10B,C) showed a highly complex and three-dimensional structure which was difficult to project to a single focal plane because of the faint signal. Comparing the latter ESNs (Fig. 10B,C) to a mature hippocampal pyramidal neuron (shown in Fig. 10D), complexity as well as dendritic length lay within the same order of magnitude. Antibody staining was very superficial as seen in many cases. Taking into account that this methodological constriction also underlay the described ESNs (Fig. 10), the neurons stained with MAP2 must have been located at the surface. This clearly applied to the morphologically immature ESNs (Fig. 10A), where a correlation between the EGFP signal and MAP2-positive cell body-like structures could be seen. The other ESNs showed a lower or no MAP2 signal (diminishing from A to C), suggesting that they were located deeper within the culture. Their low EGFP signal can accordingly be explained by a reduced staining with the αGFP antibody.

From these observations I drew the conclusion that an injection into a lesion site within the cell layers might help ESNPs to morphologically mature. Therefore, I routinely transplanted directly into the cell body layers of CA1 and CA3 regions as well as the dentate gyrus, respectively. According to culture quality and transplantation conditions, complex ESNs

resembling hippocampal neurons were found in nearly all preparations, with the frequency being rather low (2-12 neurons per 36 transplanted slice cultures; see below).

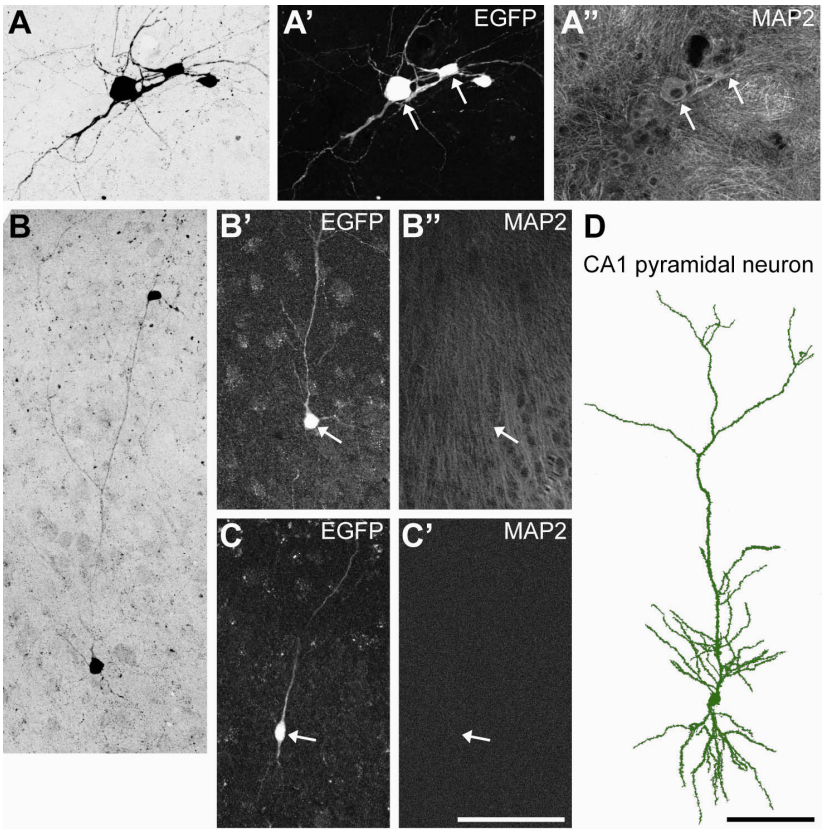

Figure 10 | ESNs adopting pyramidal structure are found deep within the slice. A | Neuron showing immature characteristics; **A'** stained with αGFP, and **A''** with αMAP2 antibody. **B,C** | ESNs found in the CA1 region of the same preparation. **A** and **B** Maximum intensity projections; **A'-C''** single sections. All three images were taken from cultures fixed at 21 DIV. **D |** Mature hippocampal CA1 pyramidal neuron. Scale bars 100 µm.

4.2 Characterization of ESNs

4.2.1 Morphology

Structurally defined ESN populations

After having established clear experimental procedures, I could continue with the characterization of ES cell-derived EGFP-expressing cells. First, the cells found in different compartments of the hippocampus were counted separately, and categorized according to the respective hippocampal region CA1, CA3, CA4 and DG (Fig. 11A). If a neuron was found in the centre of the slice and could not be clearly attributed to one of the hippocampal subfields, it was named "HF" for hippocampal fissure. A considerable number of neurons could be seen either in the entorhinal cortex (EC) or in the periphery (P) surrounding the complete slice beyond the pyramidal cell body layers. Different morphologies of cells were

found throughout the hippocampal slice culture (Fig. 11B). Besides the pyramidal neuron-like phenotype (e.g. CA1, upper middle panel), also reported in 4.1.2, different types of smaller cells were present. Many of them showed an undirected dendritic growth as described earlier (Fig. 10A) as well (e.g. EC left bottom panel), but on the other hand some appeared to share similarities with granule neurons (DG, top left neuron). Unexpectedly, 1.5% of the EGFP-positive cells (out of 1036 cells found in 240 slices) were relatively small and carried highly branched processes, resembling those of glial cells (CA3). Some of the most complex ESNs showed a rounded cell body lacking the clear polarization of pyramidal neurons, thus constituting an additional population (e.g. CA3, bottom right neuron). To determine the percentage of green fluorescent cells found in the different hippocampal subdivisions (see Fig. 11A), 68 wells (four slice cultures each) from twelve independent preparations were analyzed (Fig. 11C). While transplantation had only occurred into CA1, CA3 and DG regions (Fig. 11A, arrows), the progeny of transplanted precursors could be found in all subfields of the slice culture. 43.7 ± 4.5% of ESNs were present in the DG, although the same amount of precursors had been injected into the three regions. This value significantly differed from the percentage of cells seen in CA1 (12.6 ± 1.9%) and CA3 (15.0 ± 2.4%), respectively ($p < 0.00001$; $p < 0.0001$), pointing toward survival-supporting conditions in the DG. Other regions containing a relatively high number of ESNs were the hippocampal fissure and the periphery, both neighboring all three targeted subfields.

The immense diversity of neuronal and glial morphologies (Fig. 11) was paired with the varying fluorescence intensity of ESNs. In many cases the more complex neurons showed a lower EGFP signal leading to difficulties in performing a morphological analysis (also seen in Fig. 10). Furthermore, a high heterogeneity even within the group of pyramidal-like ESNs was found (see below).

Taken together, the first conclusion can be drawn: **Transplantation of a population of ESNPs into the hippocampal slice culture results in a variety of neuronal and glia-like cell shapes, differing in size and complexity, and transplanted ESNPs survive best in the DG.**

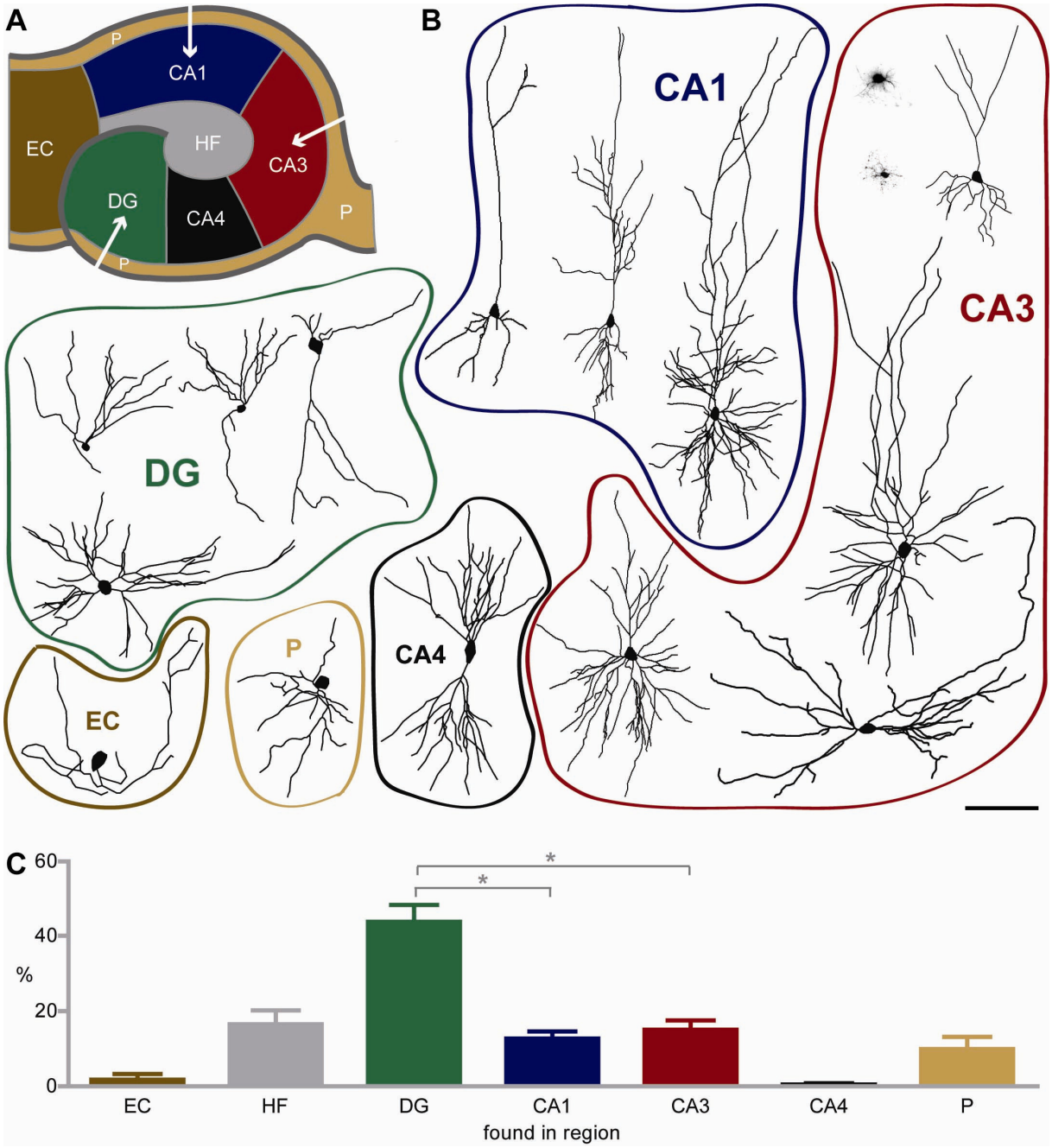

Figure 11 | Overview over morphologies of ES cell-derived fluorescent cells. A | Hippocampal subfields the found ESNs were attributed to. EC – entorhinal cortex; P – periphery; DG – dentate gyrus; CA1/2/3/4 – cornu ammonis 1/2/3/4; HF – hippocampal fissure. Transplantation was only performed into the DG, CA1 and CA3 (arrows). **B** | Tracing examples of cells found after 28-32 days in the respective subfields seen in **A**. Scale bar 100 µm. **C** | Percentage of cells present in the regions of the slice culture (EC: 1.76 ± 1.47; HF: 16.51 ± 3.49; DG: 43.71 ± 4.50; CA1: 12.56 ± 1.87; CA3: 15.03 ± 2.36; CA4: 0.46 ± 0.31; P: 9.87 ± 3.10) from 12 independent transplantations; n = 68 wells containing four slice cultures each. Average and standard error of the mean are shown. Two-tailed student's t-test; *p < 0.05.

Despite the high diversity which was observed, a regularity of neuronal phenotypes was noted. Pyramidal ESNs were only found within CA regions, on the other hand granule cells only developed within the DG (in 572 slice cultures 1970 EGFP-positive cells were analyzed in total). However, the morphological transition between granule cells and the very diverse group of "immature" ESNs was not sharp and hard to determine. Glia-like EGFP-positive

cells were mainly seen close to the CA regions or the DG. In contrast, the immature neurons, but also the group of extremely “complex” ESNs were encountered anywhere, ranging from CA and DG to the entorhinal cortex to fissure and periphery. Following this observation, the question arose whether the position as well as the environment may have an influence on cell fate. In order to position ESNs more precisely in relation to the intrinsic hippocampal neurons that had been growing in the hippocampus already before culture preparation, slice cultures transplanted with ESNPs were stained with DAPI after GFP-immunohistochemistry. ESNs closely associated to the intrinsic neuronal cell body layer of CA1, CA3, CA4 or the DG (Fig. 12A-D) appeared to reproduce the characteristics of hippocampal neurons from the respective regions. By contrast, cells not embedded in a neuronal cell body layer (Fig. 12E-G) did not match the intrinsic hippocampal pattern. Thus, it can be concluded that ESNs with hippocampal neuron-like morphology were matching cells in the respective hippocampal regions they were located in, whereas structurally aberrant ESNs occurred anywhere.

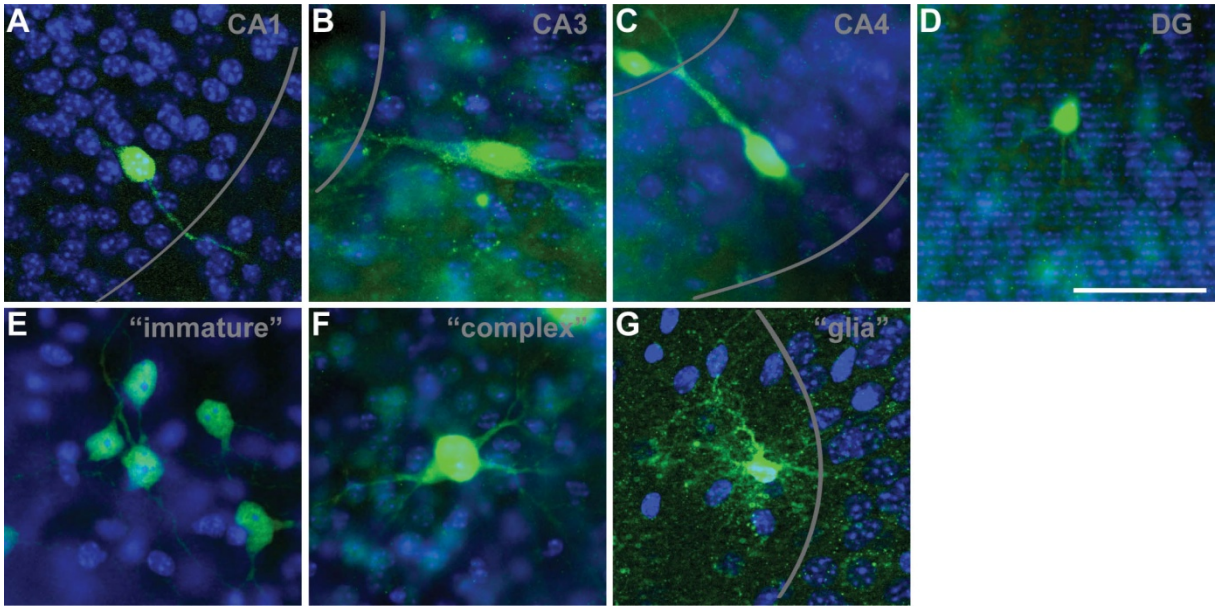

Figure 12 | DAPI staining of morphologically different ESN types show their spatial relationship to intrinsic nuclei. Grey lines indicate pyramidal cell layers of the CA regions. **A-C** | Pyramidal-like ESNs found within the cell body layers of CA1, CA3 and CA4, respectively. **D** | ESN surrounded by DG granule cell nuclei. **E** | Five ESNs lacking signs of morphological maturation do not show an association with a neuronal cell layer. **F** | Complex ESN in the hilar region of the DG. **G** | EGFP-positive cell with glia-like morphology found close to CA3. Single section images, scale bar 50 µm.

In order to address the overall question whether ESNPs are able to integrate into a neuronal circuit, a clear distinction of different morphological types had to be undertaken. Resulting from the variety of morphologies combined with their occurrence, a classification can be suggested. Some ESNs closely resembled their surrounding hippocampal neurons – this was true for pyramidal and granule cell-like ESNs – and were never found outside their characteristic place of occurrence. Other ESNs, mostly the abundant immature type, did not

show region-specific morphology, and were even found for instance in the periphery where integration into the network is doubtful. These findings point toward the existence of two ESN types, one receiving and responding to local signals, therefore acquiring the local morphology, and another type which develops a shape unrelated to its environment. To distinguish between these two populations as accurately as possible, four exclusion criteria were established (Fig. 13B).

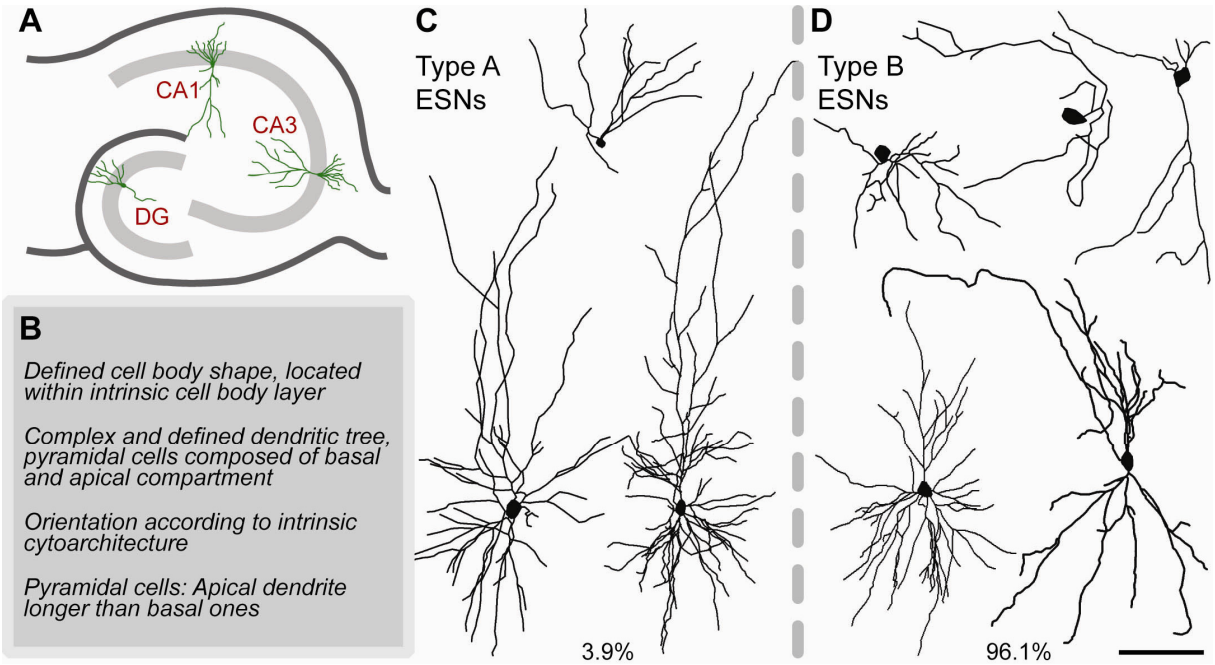

Figure 13 | Categorization into type A and type B ESNs. A | Schematic view of the hippocampal slice with its subfields CA1, CA3 and DG. The characteristic regional neuron types are indicated in green, intrinsic cell body layers of the CA regions and the DG are shown as broad grey lines. **B** | Criteria developed to distinguish between morphologically adjusted ESNs (**C**, type A ESNs) and unadjusted ESNs (**D**, type B ESNs). **C,D** | Neurolucida® tracings of ESNs found in different regions. Scale bar 100 µm. Quantification of type A *versus* type B was done from the 12 independent transplantations analyzed in Fig. 11 (1036 ESNs in n=240 slices).

The ESN type that supposedly had integrated and matured (type A, Fig. 13C) showed a defined cell body form with clear edges, and either round or pyramidal shape. Its fluorescence intensity was more pronounced than that of the dendrites, pointing toward a three-dimensional structure. Both the position within the slice and the DAPI staining indicate that their somas were surrounded by cell bodies of resident hippocampal neurons, showing that they grew embedded in the intrinsic cell body layer (see Fig. 13A, grey lines). In contrast, the more abundant type B (Fig. 13D) was characterized by a misshapen cell body which in most cases was not directly associated with the neuronal cell body layer, as revealed by a nuclear marker. The structure of the dendritic arbor was the second criterion. For type A neurons – the more mature cells – it had to be complex with branched dendrites that were relatively thick until the terminal was reached. ESNs were assigned to the pyramidal population if they showed a bipolar organization comprising a basal as well as an

apical dendritic compartment. Typically, the apical shaft was thicker than the basal dendrites. Type B neurons, on the contrary, often showed thin and unorganized dendritic arbors, which were difficult to distinguish from axons. Their dendritic organization was neither unipolar nor bipolar, but dendrites sprouted at random from the soma. The third criterion concerned the ESN orientation within the slice culture. As described, the hippocampus is highly organized and consists of defined subfields with a well-known composition of neurons. Pyramidal neurons present in the CA regions are all located in the same orientation (Fig. 13A), with their apical shafts growing in the direction of the centre, and their basal dendrites extending toward the periphery. Pyramidal-like ESNs had to reproduce this pattern in order to be attributed to type A ESNs. Accordingly, DG granule neurons also occur in one characteristic orientation, their unipolar dendritic trees located in the molecular layer in the direction of the entorhinal cortex and the CA1 region (suprapyramidal blade) and the periphery (infrapyramidal blade), respectively. Granule cell-like ESNs equally had to match this intrinsic cytoarchitecture. The forth criterion referred to pyramidal-like ESNs only. ESNs that matched all criteria but had a longer basal than apical dendritic tree were excluded from type A ESNs. Quantification of type A *versus* type B ESNs revealed that only 3.9% of all ESNs (a total of 1036 ESNs found in 240 slices were analyzed in 12 independent experiments) could be attributed to type A (this percentage corresponds to 3.3 type A ESNs per experiment, 0.6 cells per analyzed well and 0.17 cells per slice).

In the following chapters, this clear distinction between the two ESN types A and B will be maintained. In terms of morphological maturation and presumable integration, type A will be analyzed and dealt with in a more detailed way in the next paragraphs and chapters. Nevertheless, some experiments will also refer to the more abundant and less mature type B of ESNs (see 4.2.4).

Morphological characterization of type A ESNs

After establishing the exclusion criteria for ES cell-derived cells comparable to original hippocampal neurons, I examined to what extent the transplanted precursors were able to reproduce the structure and complexity of the principal hippocampal neuron types. To this aim, slice cultures containing ESNs were fixed after 32 days post transplantation, stained with αGFP antibody, and imaged. Sholl analysis was performed separately for the different hippocampal regions that were examined. Complexity curves for the apical and basal dendritic compartment were compared to intrinsic hippocampal neurons which had been transfected with a membrane-bound form of EGFP after 21 DIV, and fixed after 25 DIV for pyramidal neurons (transfected after 11 DIV, and fixed after 14 DIV for granule neurons). By comparing ESNs found in the CA1 region to intrinsic CA1 pyramidal cells (Fig. 14A,B), a high morphological similarity was visible. The statistical analysis also reflected this finding: The

complexity curves of apical (Fig. 14C) as well as basal dendrites (Fig. 14D) clearly showed that CA1 ESNs were indeed able to reproduce the pyramidal pattern of intrinsic CA1 neuronal morphology. However, since the ESN population was relatively heterogeneous and the weak fluorescence signal of many neurons complicated the analysis, variations of complexity were found. ES cell-derived CA1 neurons were less complex in both dendritic compartments with a statistically significant difference over almost the entire distance from the soma. While the reduction comprised the entire curve to the same extent for the basal dendrites (D), the apical compartment was even less complex at the more distal parts, and was also shorter in ESNs. This overall tendency was also reflected in the total dendritic complexity panels (C and D, right), again indicating that the difference was more pronounced for the apical than for the basal dendrites.

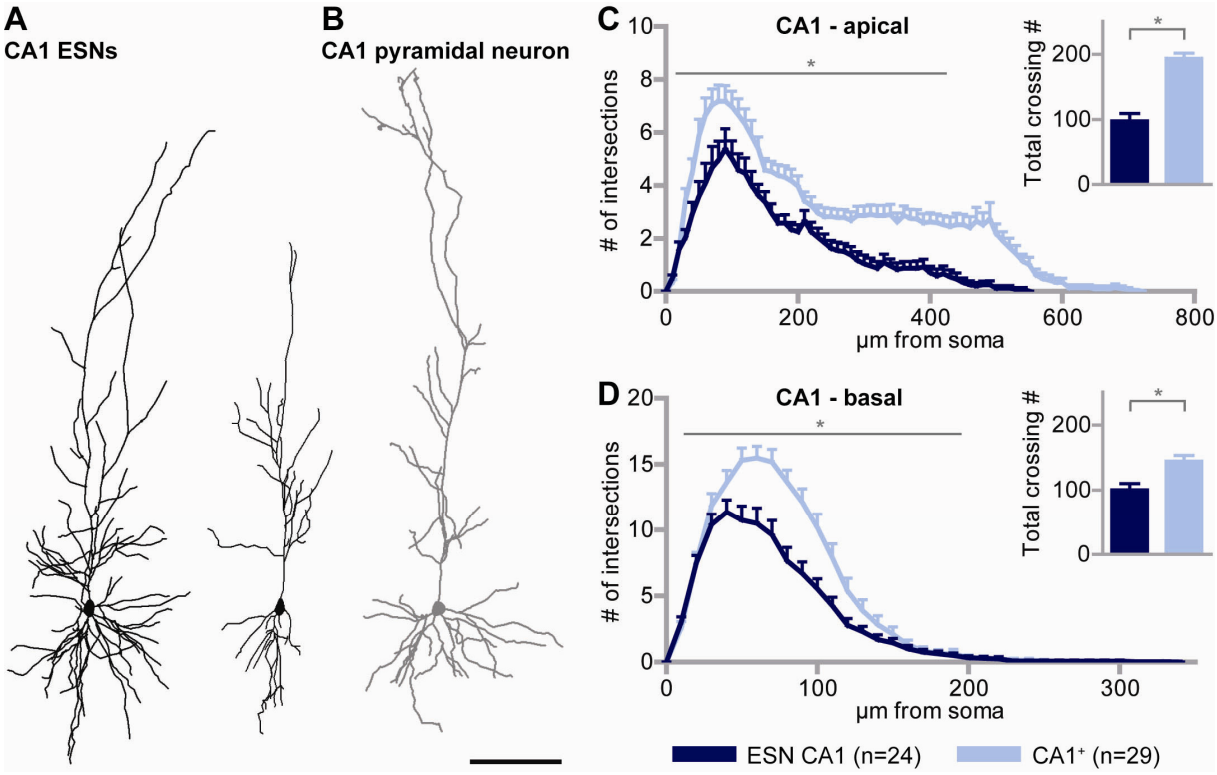

Figure 14 | Morphological analysis of CA1 ESNs compared to intrinsic hippocampal neurons. A | Tracing examples of ESNs found in the CA1 region. **B** | Original hippocampal CA1 pyramidal cell. Scale bar 100 µm. **C,D** | Sholl analysis and total dendritic complexity of CA1 ESNs *versus* original CA1 pyramidal neurons for (**C**) apical and (**D**) basal dendritic compartment. Average and standard error of the mean are shown. Two-tailed student's t-test; *p < 0.05. [+]Intrinsic neurons at 25 DIV: M. Zagrebelsky.

The same analysis was also performed for ESNs present in the CA3 region of the hippocampal slice after 32 days in culture (Fig. 15). It has to be mentioned that there was an even higher heterogeneity between cells within CA3 (see Fig. 11). Nevertheless, a comparison of tracing examples already pointed toward a high morphological similarity between CA3 ESNs and intrinsic pyramidal neurons (Fig. 15A and B). Additionally, the Sholl analysis for apical (Fig. 15C) as well as basal dendrites (Fig. 15D) confirmed that CA3 ESNs

closely resembled original CA3 pyramidal neurons of the hippocampus. Nevertheless, the difference from the hippocampal control neurons was even higher than seen for CA1. The most pronounced discrepancy was found in the apical compartment around 150 µm from the soma where the number of intersections was approximately half of the one in control neurons.

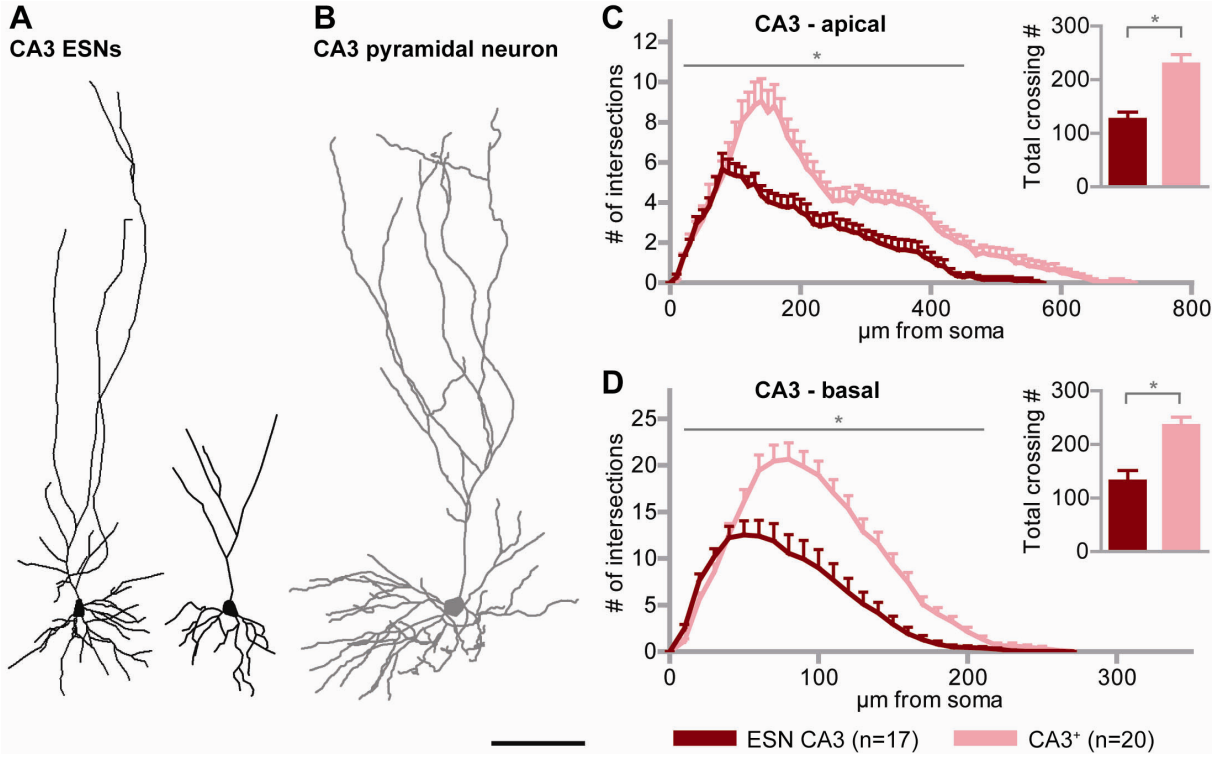

Figure 15 | Morphological analysis of CA3 ESNs compared to intrinsic hippocampal neurons. A | Tracing examples of ESNs found in the CA3. **B** | CA3 pyramidal cell. Scale bar 100 µm. **C,D** | Sholl analysis and total dendritic complexity of CA3 ESNs *versus* original CA3 pyramidal neurons as described in Fig. 14.

As a next step it was of special interest whether the ESNs in CA1 and CA3 regions produced one uniform pyramidal phenotype or if they were able to react to local information and express characteristic features of neurons in the two distinct CA subdivisions. For this purpose the complexity curves of both, CA1 and CA3 ESNs were plotted against one another to find out whether they actually represented two separate populations. Intrinsic pyramidal CA1 and CA3 neurons showed two significantly different curves for the apical (Fig. 16C), and the basal compartment (Fig. 16D). In both ESN graphs (Fig. 16A and B), the proximal part of the tree seemed to show the same degree of complexity (A for the apical and B for the basal dendrites). During the subsequent course, however, statistically significant differences between both neuron groups arose (see asterisks). This applied to the apical as well as the basal dendrites, and led to the conclusion that CA1 ESNs indeed differed from CA3 ESNs in terms of their dendritic complexity pattern, in a way that is comparable to original hippocampal pyramidal cells.

Taking all of this into account, it can be concluded that **embryonic stem cell-derived neuronal precursors transplanted into hippocampal slice cultures are able to acquire the region-specific morphology of mature hippocampal pyramidal neurons.**

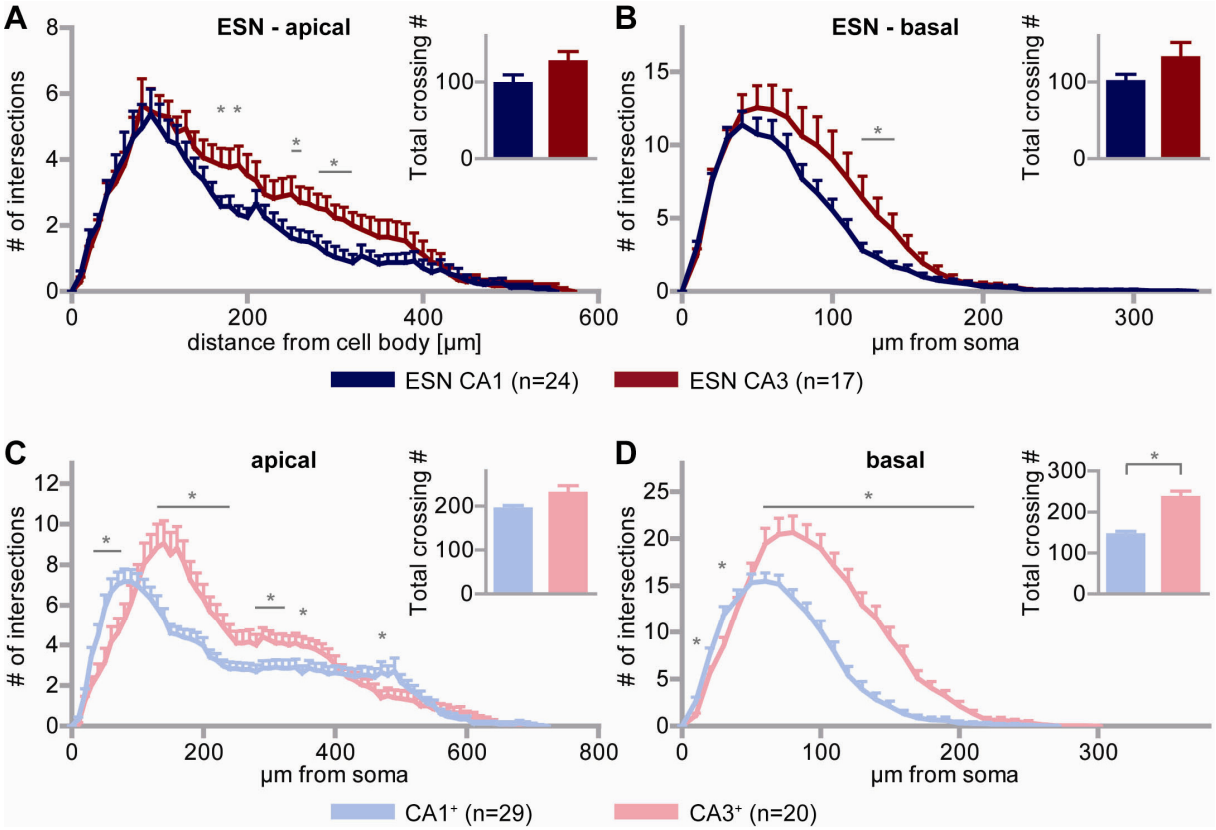

Figure 16 | CA1 ESNs are significantly less complex than CA3 ESNs. A,B | Sholl analysis and total dendritic complexity, **A** for the apical and **B** for the basal compartment. Curves and columns represent average values; error bars represent the standard error of the mean. **C**,**D** | Sholl analysis and total dendritic complexity, **C** of apical and **D** of basal dendrites of intrinsic hippocampal neurons. Two-tailed student's t-test, *p < 0.05. $^{+}$Intrinsic neurons in **C** and **D** – M. Zagrebelsky.

The previous results are in line with the known identity of the precursors as radial glia (RG) that express Pax6 and give rise to a population highly enriched of pyramidal neurons (Bibel et al., 2004). All the same, precursors were also transplanted into the DG, and surviving ESNs were detected, some of which were considered to be type A ESNs and were included into the morphological analysis (Fig. 13). Although there were fewer type A ESNs found in the DG than in the CA regions (8 compared to 24 and 17, respectively), a morphological analysis comparing these DG ESNs to intrinsic hippocampal granule cells was performed (Fig. 17). In contrast to pyramidal ESNs which were less complex than their intrinsic counterparts, DG ESNs adopted the structure of intrinsic granule cells almost completely. According to the tracing examples (Fig. 17A,B), they were indistinguishable. Sholl analysis and total complexity (Fig. 17C) also reflected this tendency with only minor differences (around 60 µm to 100 µm from the soma) that were not statistically significant. Thus, ESNPs

were able to morphologically develop into granule cells when injected into the DG, regardless of their pyramidal pre-differentiation.

From this results the following conclusion: **Despite their homogenous pre-differentiation, ES cell-derived precursors are responsive to local cues that influence their ultimate fate corresponding to regionally different hippocampal neuron populations.**

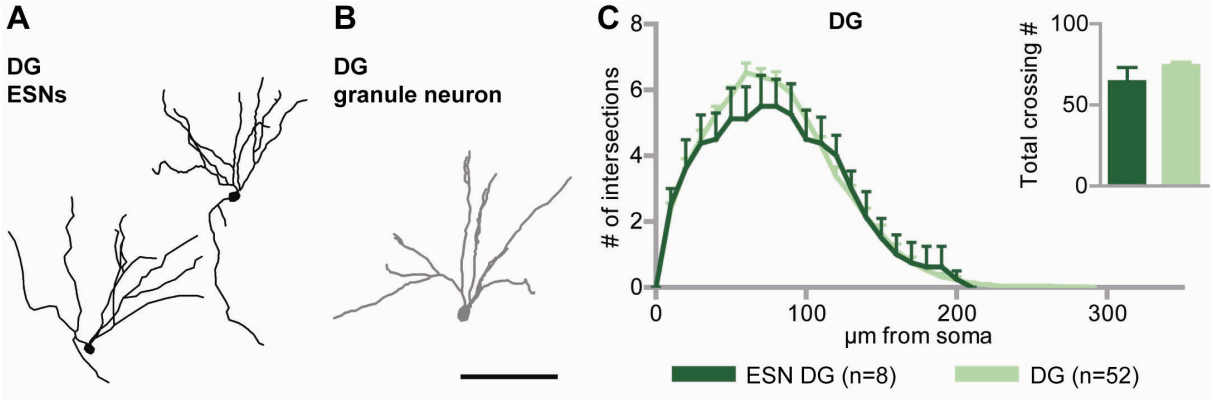

Figure 17 | ESNs in the DG depict granule cell-like morphology. A | Tracing examples of ESNs found in the DG; **B** | Dentate gyrus granule cell. Scale bar 100 µm. **C** | Sholl analysis and total dendritic complexity of DG ESNs *versus* original DG granule cells as described in Fig. 14. Control neurons were fixed at 14 DIV.

Fast morphological maturation into pyramidal ESNs

By repeatedly imaging a single developing ESNP, it was possible to follow its maturation one to four days after transplantation into the hippocampal slice culture (Fig. 18A). While an extremely weak EGFP signal was seen on the first day, fluorescence increased over time, revealing a rather complex dendritic tree as early as three days after injecting the precursor into the tissue. At this stage the cell already showed the typical characteristics of a pyramidal neuron, including a pyramidal cell body and clearly defined apical and basal dendritic compartments. The presence of an axon could already be detected after 48 hours (Fig. 18; shown as a red thin line emanating from the left side of the cell body) suggesting successful polarization of the newly formed neuron. Although its architecture already closely resembled a mature pyramidal cell, the dendritic tree at DIV 4 was found to be shorter. The apical dendrite showed a length of about 250 µm, whereas CA3 ESNs after 32 days of incubation were 379 ± 24 µm long. Furthermore, the dendrites were relatively thin, making their morphological analysis difficult (see Fig. 18A; bottom row). The maturation from a precursor into a hippocampal-like ESN could only be followed in this single case. Nevertheless, this example shows that the main steps of morphological maturation an ESNP undergoes to become a pyramidal ESN happened extremely fast – over the period of four days. The result was an immature and fairly small neuron with thin dendrites, which was on the other hand by means of dendritic characteristics clearly attributable to the group of pyramidal neurons.

Live imaging was also performed at later stages and pyramidal ESNs were frequently detected after 28 DIV (Fig. 18B). The dendritic trees of these older ESNs were rather complex and longer than those of the four days old ESN (it cannot be seen completely in the single section view in Fig. 18B).

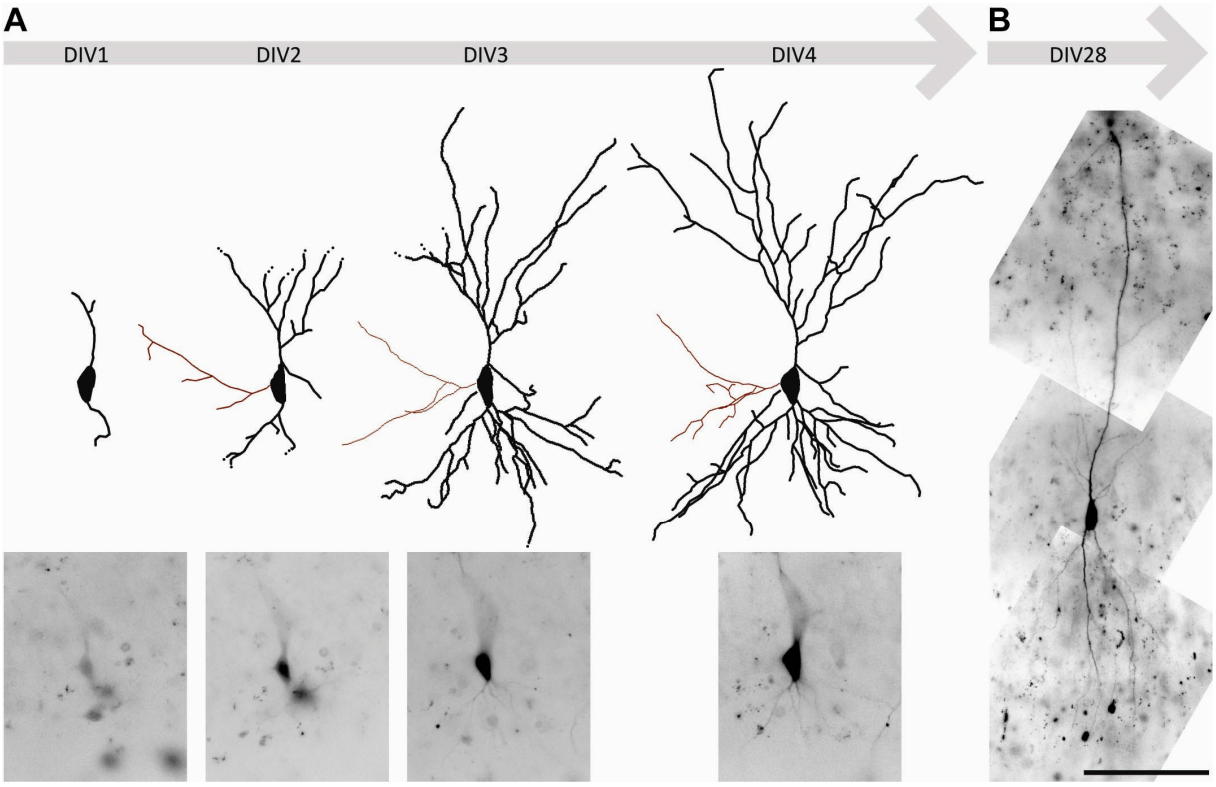

Figure 18 | Maturation into a pyramidal-like cell occurs within 4 days. A | Live imaging time course 1-4 days after transplantation of ESNPs into hippocampal slice culture, CA3 region. Top row – tracings of the same neuron, the axon is shown in red. Dots indicate that some dendrites were not completely imaged. Bottom row – sections of live images at the respective DIV. Increasing fluorescence intensity is clearly visible over time. **B** | Example of a different CA3 ESN imaged live after 28 DIV, single section. Scale bar 100 µm. Time lapse imaging in **A** was done by S. Janßen (2010).

4.2.2 Connectivity of type A ESNs

Besides the morphological signs for maturation, type A ESNs also presented a further quality: Their dendrites carried dendritic spines, a hallmark of excitatory post-synapses (Fig. 19; n=9 ESNs from 9 cultures in which spines were unambiguously detected. In most cases, a distinction between spiny and aspiny ESNs was not possible because of the low EGFP signal. Therefore, spine growth could not be quantified). This was found for ESNs in the three examined regions of the hippocampus DG (Fig. 19A), CA1 (D) and CA3 (B, C, E-J) and for the apical (B) as well as the basal part of the dendritic tree (C). Imaging dendrites of CA3 ESNs at different time points revealed that spine growth was age-dependent: While at 14 and 21 DIV spines were never seen, the spiny dendrites were present in ESNs at 28 and 32 DIV (Fig. 19). On the other hand not every ESN at this stage was found to exhibit spine

growth (see Fig. S1C). In many cases, however, this could be attributable to the difficult imaging conditions (Fig. S1B).

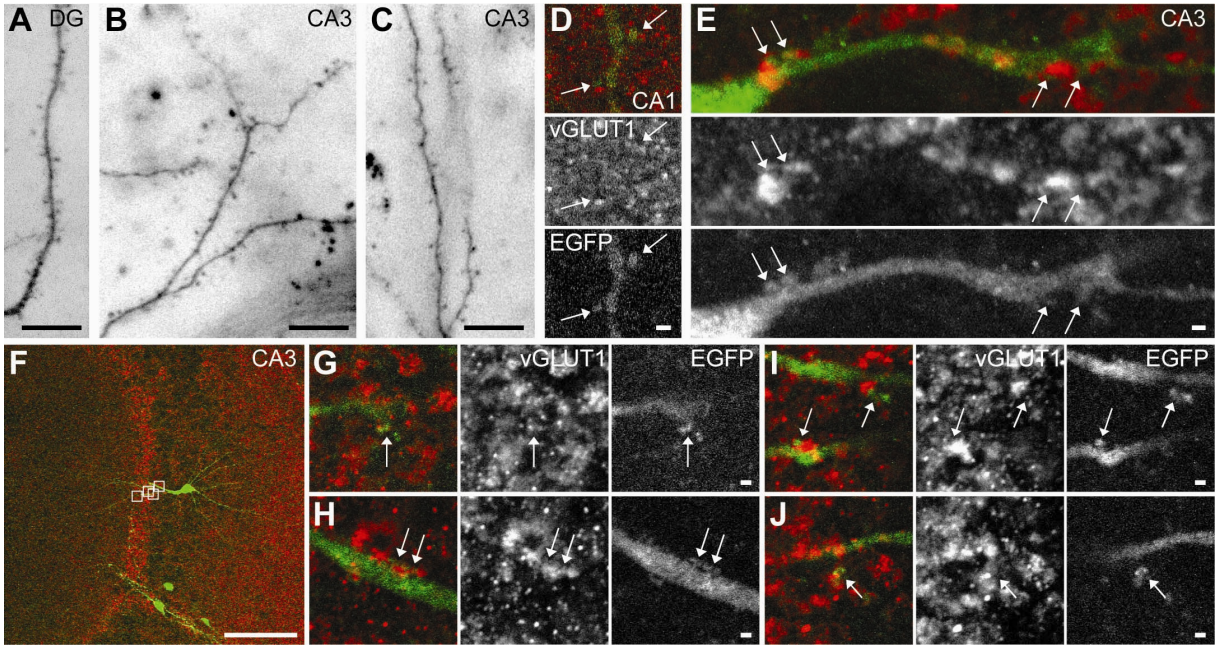

Figure 19 | ESNs carry spines co-localizing with presynaptic markers. A | DG ESN filled with Alexa 488 via single cell electroporation, imaged after fixation. **B,C** | Live image of a CA3 ESN, **B** in the proximal apical and **C** in the basal compartment – EGFP fluorescence. **D-J** | Co-stainings of ESNs, **D** in the CA1 region and **E-J** in the CA3 region; immunohistochemistry against EGFP and vGLUT1. Arrows point to co-localizations of both markers. **G-J** Detailed images of CA3 neuron shown in **F** – zoomed-in view of white boxes. Scale bars in **A-C** 10 µm; **D, E, G, H, I, J** 1 µm; **F** 100 µm.

ESNs carrying dendritic spines were co-stained with αGFP and an antibody against vGLUT1, a vesicular glutamate transporter found in the glutamatergic pre-synapse. Co-localizations of presynaptic red vGLUT1 puncta with the postsynaptic spine-like structure of ESNs in the CA1 and CA3 region were found (Fig. 19D-J). This was especially striking in terms of some CA3 neurons which reproduced the pyramidal cell-specific position within the CA3 region. A red belt of vGLUT1 signal represented the highly innervated *stratum lucidum*, where mossy fibers, the axons of DG granule neurons, project on the proximal apical dendrites of CA3 pyramidal neurons (Fig. 19F). Although not being as complex as expected for mature intrinsic CA3 neurons, the ESNs shown here clearly carried spines in the corresponding innervated region. Some of the protrusions were branched and co-localized with vGLUT1-positive puncta (Fig. 19G,I).Taken together, these data suggest that the spines found on ESN dendrites represented active excitatory synapses.

Therefore it can be concluded that **a fraction of ES cell-derived neurons receives synaptic input from the host circuitry.**

4.2.3 Associated type A ESNs

During the process of tracing and analyzing the morphologically mature ESNs (4.2.1) a puzzling finding caught my attention. A major part of the type A ESN population appeared to be cytoplasmically connected with other EGFP-positive neurons. The secondary cell could also be type A, or belong to the morphologically immature group of type B cells. EGFP-positive processes could be followed from one cell body directly to another one. This was observed at the ApoTome system as well as in confocal stacks, and resulted in a difficulty in terms of the morphological analysis. If the putative secondary cell body was attached to a process that seemed to be additionally added to the more or less complete dendritic tree of the neuron (Fig. 20A), the respective type A ESN was included, and tracing was stopped when the additional cell body was reached. On the other hand, in some cases the cell body-like swelling seemed to be directly linked to the dendritic arbor of the neuron, e.g. it was located within the proximal apical dendrite (Fig. 20B). If a situation like this was faced it was impossible to attribute the processes to either one of the cell bodies, and the neuron was excluded from the morphological analysis.

It should also be mentioned that connections were often seen in the very distant parts of the dendritic tree where the fluorescence intensity was extremely low, and therefore complete tracing of the terminals was uncertain. This is the reason why – when quantifying connected *versus* unconnected ESNs (Fig. 20C) – a third group of neurons had to be added, in which an association was ambiguous. Many type A ESNs were found in cultures where also numerous other EGFP-positive neurons were seen in close proximity (especially type B ESNs), and because of the difficult imaging conditions thin cytoplasmic connections could have been missed. The quantification of the type A ESNs refers to all ESNs included into the morphological analysis seen in 4.2.1. In 44.9% of the included neurons a connection was found, and only 25.5% of the cells could be shown not to exhibit any additional cell body-like structures, because surrounding EGFP-positive neurons that could possibly be linked to them were lacking. Besides in the DG (Fig. 20D) and the CA3 region (Fig. 20A,B,F) the phenomenon was also found in CA1, the percentage of association not differing from the other regions.

In some remarkable cases two fairly complex ESNs were seen, resembling hippocampal DG and pyramidal neurons, respectively (Fig. 20 D-G; see red and green tracings in E and G). Presumably immature neurons which were also EGFP-positive, extended processes toward or even into both somas of the type A ESNs (shown as blue tracings in Fig. 20E and G). It was difficult to attribute the connecting processes to one partner only. What seemed to be dendrites of these neurons could be rudimentary (as seen in E) but on the other hand as complex as an entire second neuron (G). In many cases the swellings were found to be

associated with the cell body of the primary neuron but on the other hand they could also be seen in contact with the apical or basal dendritic tree.

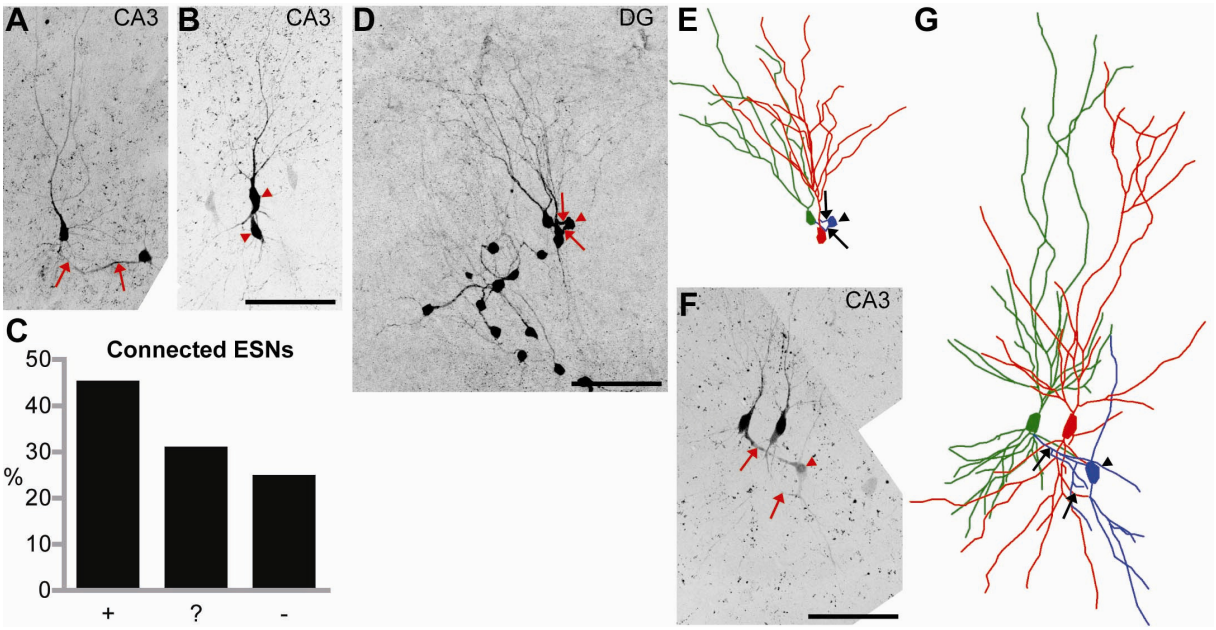

Figure 20 | A high percentage of type A ESNs appears to be connected to other cells. A | CA3 ESN showing a connection to a type B ESN emanating from the base of its soma. It was included in the Sholl analysis. **B** | Two associated CA3 ESNs with intermingled dendritic trees that had to be excluded. **C** | All type A ESNs included in the morphological analysis in 4.2.1 were examined for potential associated cells, and the percentage of ESNs with a visible connection (+ = 44.9%), possibly connected ESNs in the neighborhood (? = 30.6%), and ESNs where a connection could be excluded (- = 24.5%) were plotted; n=49 ESNs. **D,E** | ESNs in the DG, many of which seem to share processes. **F,G** | Two type A CA3 ESNs associated with an immature EGFP-positive cell extending processes into both somas. **A,B,D,F** Maximum intensity projections. **E,G** Neurolucida® tracings of ESNs shown in **D** and **F**. Type B ESNs are depicted as blue tracings. Arrows point to linking processes, arrowheads to secondary cell body-like structures. Scale bars 100 µm.

The occurrence of cells with two cell body-like swellings raised the question if a second nucleus could be detected. Therefore, nuclear staining using DAPI was performed on a routine basis. It was found that in every examined case a second swelling was attached to a dendritic tree, it carried a separate nucleus (Fig. 21A; n=10). Furthermore, while type A ESN somas were located within the intrinsic cell body layers (as shown in Fig. 21A for the CA1 ESN on the right side by the numerous densely packed nuclei surrounding it) associated secondary type B cells did not reside within these layers (sparsely scattered nuclei in the neighborhood of the left cell). Secondary type B cells often showed a rudimentary dendritic tree and clearly visible DAPI-positive chromatin aggregations (Fig. 21A).

These observations resulted in the question how associated cells might develop. My first strategy was to analyze ESNs in a more immature stage to see whether some kind of intermediate stages could be found. Slices were fixed five days after transplantation and stained with αGFP antibody and DAPI. A long immature ESN which was restricted to a few focal planes (in contrast to the cell in A) was seen to contain as many as three nuclei

(Fig. 21B). One of those nuclei was not located in the direct neighborhood of the other two, connected by a broad cytoplasmic bridge.

If this snap-shot is interpreted as a potential intermediate stage of immature ESNPs on their way to becoming mature, associated ESNs might have derived from an incomplete cell division, more precisely an unfinished cytokinesis after mitosis. Alternatively, cell fusion could have been the cause for the phenomenon.

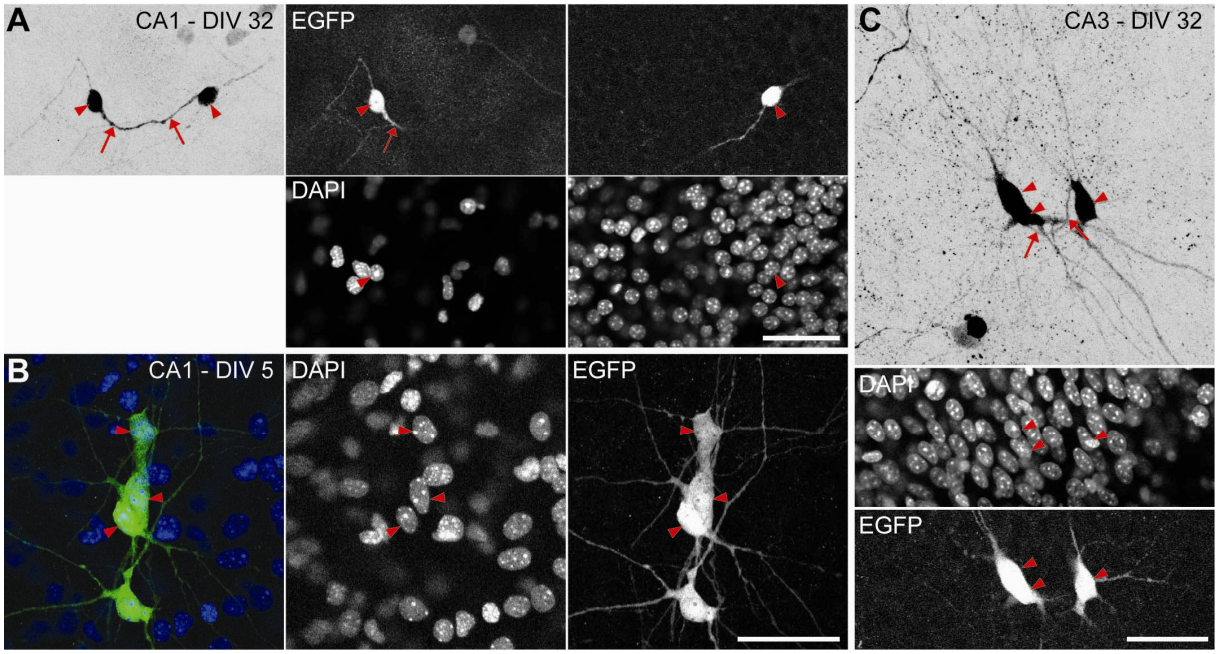

Figure 21 | Associated soma-like structures contain nuclei. A | CA1 ESN (right cell) 32 days after transplantation. Maximum intensity projection of confocal Z stack (grey) and single sections of two different focal planes. Both connected cell bodies contain nuclei. **B** | Immature ESNs five days after transplantation, single sections. **C** | Two CA3 ESNs after 32 DIV with some characteristics of type A ESNs. Maximum intensity projection (grey) and single confocal sections. Cells are connected; the left soma contains two nuclei. Arrows – connecting processes; arrowheads – nuclei. Scale bars 50 µm.

Furthermore it was found also at later stages that some neurons were harboring two nuclei within their primary soma. This especially applied to ESNs expressing some, but not all features of pyramidal neurons – sometimes being more complex than an intrinsic cell. One CA3 ESN showed an atypically shaped cell body containing two DAPI-positive nuclei (Fig. 21C; left soma). It was located near a second CA3 ESN within the CA3 pyramidal layer and therefore densely surrounded by other nuclei. Both cells had a rather complex basal dendritic tree, whereas the apical part showed abnormalities in missing a defined apical shaft and being too short. Their orientation, however, was the one of intrinsic pyramidal neurons, which was rarely seen among type B ESNs. Finally, both cells were connected by a thin cytoplasmic belt from one apical soma to the other in a different focal plane (Fig. 21C, arrows).

4.2.4 Characteristics of type B ESNs

Although the present study mainly focuses on the examination of ESNs that were able to adopt hippocampal morphology (type A ESNs), the other and more abundant group of ESNs was also investigated. I was interested, whether this fraction of the ESN population also underwent developmental maturation stages and whether it received synaptic input. Furthermore, the question arose if the group of type B ESNs would be homogenous enough to be compared with type B neurons of another cell line, e.g. one lacking the gene for a protein of interest. For this purpose, dendritic complexity was examined at different time points using live microscopy. Since no difference was found between ESNs growing in the different subfields of the hippocampus, all ESNs were pooled for analysis, except for those in the periphery (which were excluded). Images of ESNs were taken at 1, 7, 14, 21 and 28 days after transplantation, and Sholl analysis was performed (Fig. 22A). It has to be noted, however, that the time course does not represent a fixed population of ESNs over time, since repeated imaging was restricted to a time period of four days to avoid phototoxic damage. Therefore, at each imaging time point, a new population of cells was subject of investigation. Nevertheless, a clear course of morphological events was followed while a precursor developed from a rather simple structure at 1 DIV to a morphologically stable neuron with a defined dendritic tree at 28 DIV. The onset of dendritic outgrowth occurred mostly before 1 DIV, as many precursors by then already carried one or even two tiny processes. On the other hand some cells were devoid of neurites at this stage. Not to be underestimated was the number of cases in which no clear cell structure could be defined after one day of growth. In these cases, the cultures were analyzed again after another 24 hours of incubation.

The most remarkable dendritic outgrowth was observed within the first week in which the dendritic tree developed anew. This finding was also reflected in the total dendritic complexity (Fig. 22B), showing a significant increase during the first week (DIV1-7; $p < 0.00001$). At DIV 7, most of the highly branched dendrites were still located in the proximity of the soma (Fig. 22A). In the following week this tendency shifted, and the highest complexity was seen toward the distal portion of the dendritic tree (DIV 14), although total complexity was not changed (Fig. 22B).The third week appeared to be a period of extensive elongation with dendrites longer than 400 µm, accounting for an increase in total dendritic complexity (Fig. 22A and B). All the same, the variability between cells was high in the proximal compartment (especially between 80 µm and 140 µm from the soma). Subsequently, at 28 DIV complexity slightly decreased (Fig. 22B), due to retraction of the most distant processes. Furthermore, the variability was reduced over the entire length of the complexity curve. Comparing type B morphological maturation to the complexity of type A ESNs (Fig. 16 and 17), it was clear that they represented different and distinct populations. Pyramidal ESNs were longer in their apical compartment and significantly more complex in

their basal compartment than type B ESNs. Granule ESNs, however, lay within the same complexity range, although their number of intersections peaked around 70 µm to 90 µm from the soma (Fig. 17C), compared to about 30 µm for type B ESNs (Fig. 22A, DIV 28), suggesting a less mature morphology or a different cell type.

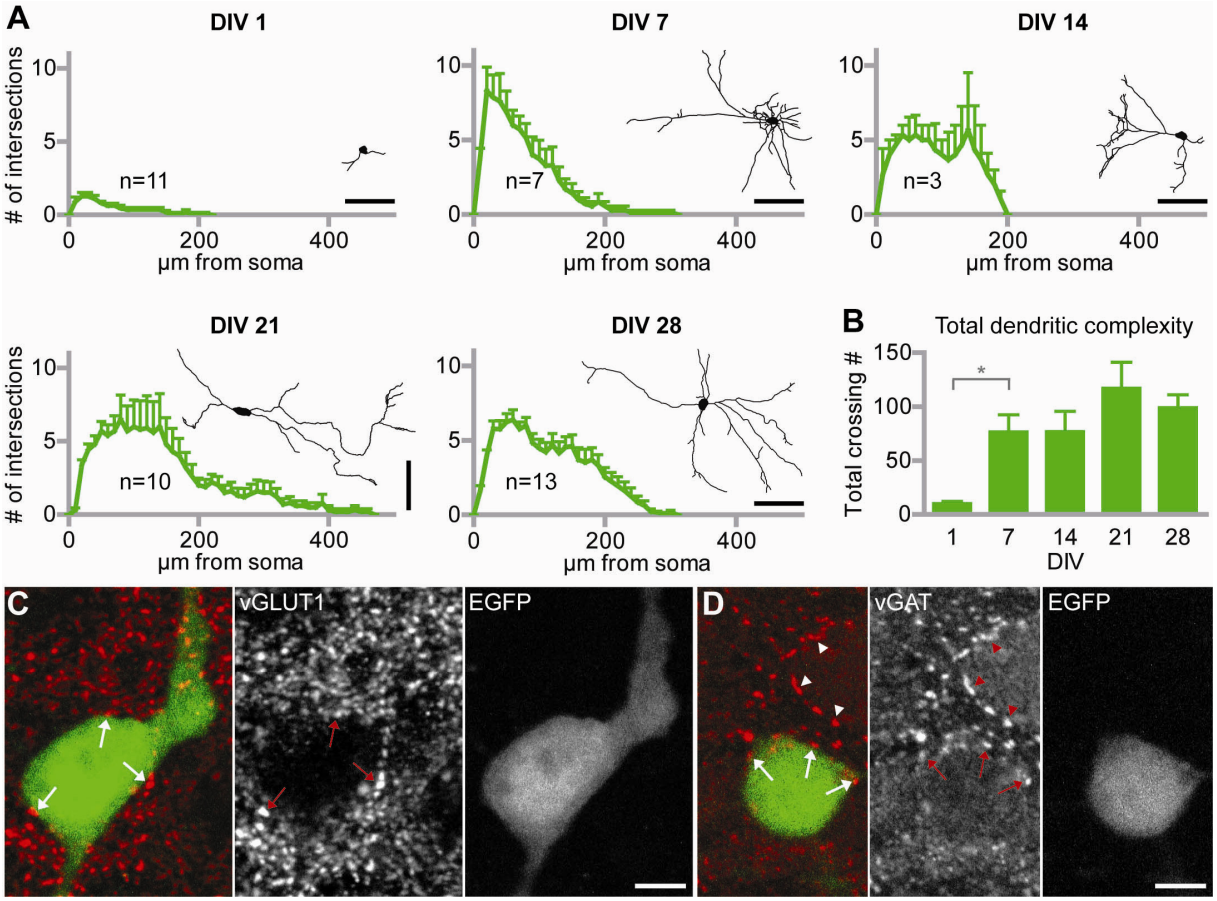

Figure 22 | Type B ESNs morphologically develop and receive excitatory as well as inhibitory synaptic input. A | Maturation time course of type B ESNs. Different groups of neurons were analyzed at the respective ages. Sholl analysis was performed as described earlier; tracing examples are shown. **B** | Total dendritic complexity for type B ESNs after 1, 7, 14, 21 and 28 DIV. A significant complexity increase was found between DIV 1 and DIV 7 (two-tailed student's t-test, *p < 0.05). Averages as well as standard errors of the mean are shown. Time course depicted in **A** and **B** was done by S. Janßen (2010). **C** | Co-staining of an ESN with vGLUT1. Arrows point to presumptive synapses on the ESN soma. **D** | Co-staining of an ESN with the inhibitory presynaptic marker vGAT. Arrows point to presumptive synapses on the ESN, arrowheads on an adjacent EGFP-negative intrinsic cell body. Scale bars in **A** 100 µm; in **C** and **D** 5 µm.

Having detected a clear maturation process for type B ESNs, the question arose if these cells also received synaptic input. Because their fluorescence intensity in most of the cases was stronger than in type A ESNs, dendritic fine structure could readily be examined. The first finding was that type B ESNs did not carry dendritic spines except for a few cells in which isolated spiny protrusions could be detected. Type B ESN dendrites were mostly thin and often discontinuous after fixation (Fig. S1D). Therefore, the growth of protrusions could not be quantified. Knowing that spine growth is a sign but not a prerequisite for the presence of synapses, immunostainings against vGLUT1 (excitatory presynapse) and the inhibitory

presynaptic marker vGAT were performed (Fig. 22C and D). Presynaptic accumulation of the markers indicated the presence of active presynaptic excitatory and inhibitory terminals, respectively. The fact that it was possible to find vGLUT1 (Fig. 22C; 3 clearly positive ESNs out of n=7) as well as vGAT-positive puncta (Fig. 22D; 1 positive ESN out of n=2) on the surface of ESN cell bodies suggests that, although showing many features of immature neurons, type B ESNs were targeted by excitatory as well as inhibitory projections of host neurons (additionally, synapsin-positive puncta were found on 3 out of n=5 ESNs).

4.2.5 Identity

The morphological and positional heterogeneity led to the question, what the identity of ESNs in slice cultures might be. By using the differentiation protocol of Bibel et al. (2004; 2007) the outcome in theory should be defined, as precursors were reported to develop into a homogenous population of 95% glutamatergic pyramidal-like neurons. The cells were shown to express high levels of Pax6 in the precursor stage, a hallmark for radial glia (RG) representing the progenitors for pyramidal neurons in the CNS. Also during later development, dissociated ESNs were found to contain the same neuronal markers (AMPAR subunit 1 (GluR1), synaptophysin, amyloid precursor protein (APP), panTrk and $p75^{NTR}$) in a synchronous time course (Bibel et al., 2004). Furthermore, testing with hippocampal subtype-specific antibodies was performed in order to determine their ability to also acquire the molecular phenotype of hippocampal neurons.

Three different antibodies were used. Ca^{2+}/calmodulin-dependent protein kinaseII (CaMKII) is a serin/threonin kinase known to play an important role in synaptic plasticity, mediating the cellular answers to activity-dependent Ca^{2+} influx (reviewed in Lisman et al., 2002). CaMKII is found in the cytoplasm of all excitatory neurons in the hippocampus. In primary hippocampal cultures, the enzyme is expressed in many neurons, distributed in soma and dendrites (Fig. 23D). ESNs transplanted into organotypic slice cultures were also tested for CaMKII immunoreactivity (Fig. 23A). All ESNs examined belonged to the group of type B ESNs, and were not stained with the αCaMKII antibody. By contrast, intrinsic CA3 pyramidal neurons showed a strong signal in soma and dendrites (Fig. 23B). When ESNs were plated on cover slips, only a minor fraction was positive for CaMKII (Fig. 23C; the neuron presented here being negative for the *tau*-driven EGFP). This was the case after 15, 21 and 28 DIV, ruling out the possibility that with progressive maturation more ESNs would express the marker for excitatory neurons.

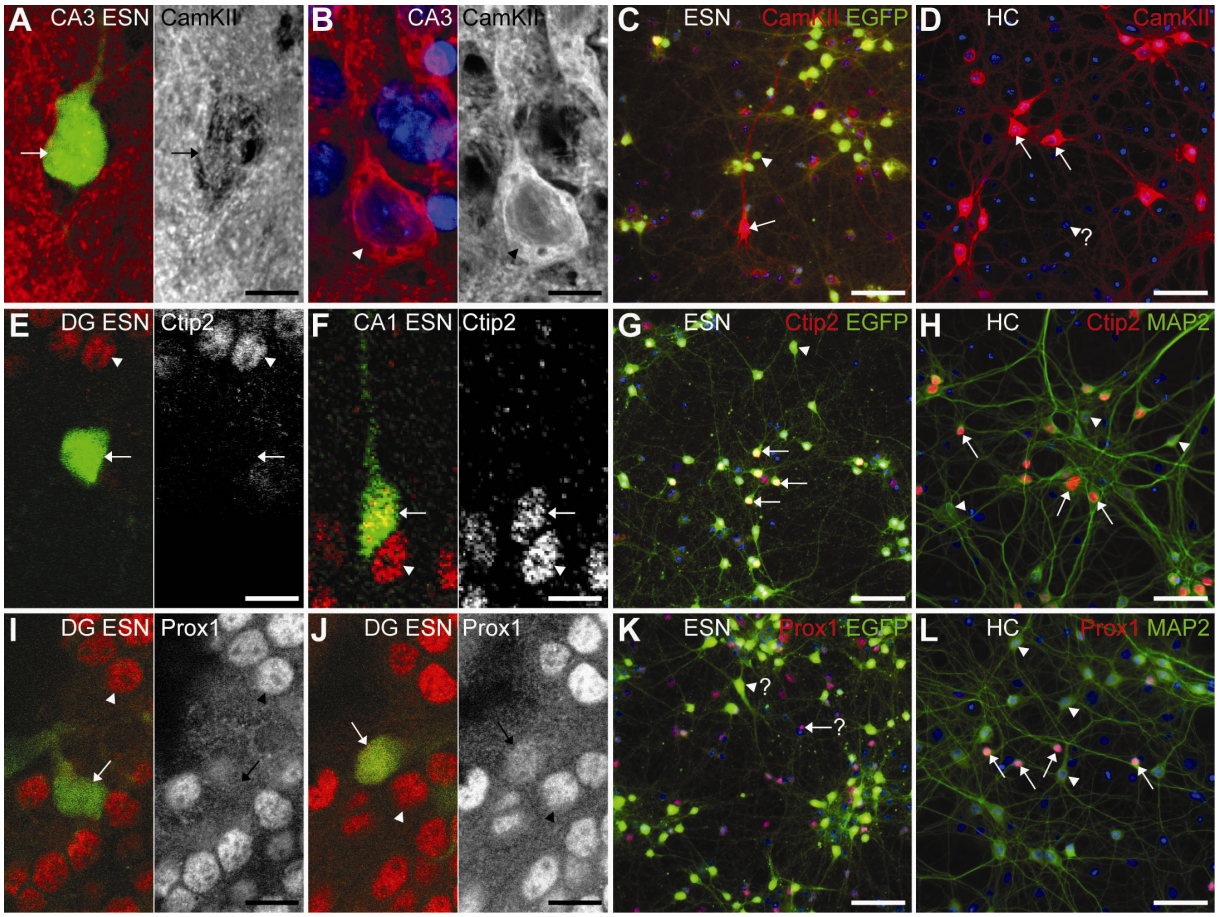

Figure 23 | ESNs partially adopt the immunohistochemical identity of resident hippocampal neurons. **A** | Type B CA3 ESN is CaMKII-negative (arrow). **B** | Intrinsic CA3 pyramidal neuron shows CaMKII immunoreactivity (arrowhead). **C** | Only a minor portion of plated ESNs is positive for CaMKII (arrow); arrowhead points to negative ESN. **D** | Primary hippocampal neurons expressing CaMKII (arrows); arrowhead – presumptive CaMKII-negative neuron. **E** | Type B DG ESN is Ctip2-negative (arrow). Arrowhead points to Ctip2-positive intrinsic granule neuron. **F** | Type A CA1 ESN shows Ctip2 immunoreactivity (arrow) like intrinsic CA1 pyramidal neurons (arrowhead). **G** | Plated ESNs are divided in Ctip2-positive (arrows) as well as negative neurons (arrowhead). **H** | Primary hippocampal neurons can be found expressing (arrows) or not expressing Ctip2 as well (arrowheads). **I** | Type B DG ESN is Prox1-negative (arrow); in the same section, Prox1-positive intrinsic granule neurons were seen (arrowhead). **J** | DG ESN associated to the cell in **I**. It shows a weak Prox1 signal (arrow). **K** | Growing ESNs on cover slips, a Prox1 signal is hard to distinguish from the background. Arrow – presumptive Prox1-positive cell; arrowhead – presumptive Prox1-negative pyramidal neuron. **L** | In primary hippocampal culture, Prox1-positive granule neurons (arrows) can easily be distinguished from negative cells (arrowhead). Cryosections (**A, B, E, F, I, J**) were made 32 days post transplantation; Scale bars 10 µm. Neurons in **D, G, H, K** and **L** were fixed at 15 DIV, neurons in **C** at 21 DIV; Scale bars 50 µm.

Ctip2, a transcriptional repressor, is expressed in the nuclei of cortical neurons with subcortical projections (Arlotta et al., 2005), and specifically in the CA1 region as well as the dentate gyrus of the hippocampus (Leid et al., 2004). When using Ctip2 antibody to characterize primary hippocampal cultures (Fig. 23H), hippocampal neurons were clearly divided into a Ctip2-negative and positive population. The latter could either have small and round cell bodies or show a pyramidal shape (arrowheads). Similarly, in ESNs growing in a dissociated state (Fig. 23G), one portion of neurons was clearly Ctip2-positive (arrows) and another portion was not (arrowhead). Again, no difference was found after longer periods in culture. Interestingly, when examining transplanted ESNs, Ctip2-positive as well as negative

donor neurons were seen (Fig. 23E and F, respectively). The first cell belonged to type B ESNs and was negative (Fig. 23E); the second cell belonged to type A ESNs and was positive (Fig. 23F, arrow). A third neuron, belonging to type B ESNs and found close to the CA1 region, showed a weak signal, barely above background level (not shown). Because the analyzed cell number was very low and both fluorescence signals, for EGFP and Ctip2 were difficult to detect, no clear conclusion can be drawn. However, it can be stated that the morphologically integrated neuron showed the region-specific molecular identity, whereas an immature neuron was not able to acquire the molecular phenotype of the surrounding tissue.

Prox1 is a homeobox transcription factor expressed in many different organs during development. In the adult mouse, however, it is only present in the cerebellum and the dentate gyrus of the hippocampus (Lavado and Oliver, 2007). Therefore, in primary hippocampal cultures, only the small and round nuclei of granule neurons were stained with αProx1 antibody (Fig. 23L). In dissociated growing ESN cultures, Prox1 immunofluorescence was ambiguous (Fig. 23K). All neurons were faintly positive, suggesting an unspecific staining, although, in some of the cases, the signal resembled a granule cell nucleus (arrow/question mark). On the other hand, pyramidal neurons showed the same weak signal (arrowhead), making it impossible to draw a conclusion. After transplantation into the DG of hippocampal slices, different phenotypes of ESNs were seen. Some ESNs expressed Prox1 (Fig. 23J), others did not (Fig. 23I).

Immunostainings of dissociated growing ESNs were further performed with antibodies against the neuronal antigen N (NeuN), a marker for mature neurons, vGAT and synapsin (Fig. S2E-G). Using αNeuN and αCaMKII antibodies revealed that not all ESNs expressed EGFP. Apparently, many of the EGFP-negative or weakly expressing ESNs showed a rather complex dendritic tree which, in single cases, clearly had pyramidal morphology (Fig. 23C). Conclusively it has to be said that the precursors used for transplantation did not represent a homogeneous population, as seen by the examination of plated ESNs. Accordingly some, but not all transplanted ESNs adopt the local molecular identity.

Besides the presence of morphologically differing neuronal ESN progeny within the slice culture, another point still needs to be elucidated. As already mentioned in 4.2.1, not only neuronal EGFP expressing cells were found after transplantation, but also green fluorescent glia-like cells (Fig. 11, Fig. 12, and Fig. 24A). This observation resulted in many open questions. The most important one was whether the glia-shaped cells represented astrocytes, possibly ESNP progeny, and therefore derived from donor cells expressing EGFP. Alternatively, they might have represented microglia, a cell type similar to macrophages, which are responsible for phagocytosis of dying neurons in the CNS and are generated in the bone marrow (Chan et al., 2007). In this case, EGFP-positive glia-like cells

most likely would have been of host-origin, and carry EGFP protein adsorbed from dying ESNs. In order to address this question, firstly dissociated ESNs were stained with antibodies against astrocytic and microglial markers. In parallel, also dissociated hippocampal cultures were examined. In ESN cultures, GFAP-positive glial cells were found (Fig. 24B), showing the same appearance as GFAP-positive glia in primary hippocampal cultures (Fig. 24D). Also Bibel *et al.* reported the presence of astrocytes in their ESN cultures, but the portion of glia in the present study was higher than their obtained 1%. Staining with Isolectin B4, which is used to detect macrophages and microglia, ESN cultures did not show any specific signal, whereas hippocampal cultures contained IB4-positive cells on most wells examined (Fig. 24F; n=7 wells, 5 wells showed IB4 signal), as well as in many slice cultures processed for microglia detection (Fig. 24G; n=36 analyzed slices, all were IB4-positive and in 8 slices (22%) single microglial cells could be detected). Therefore, it is unlikely that microglia were produced by the ESNPs that were transplanted into the slice cultures.

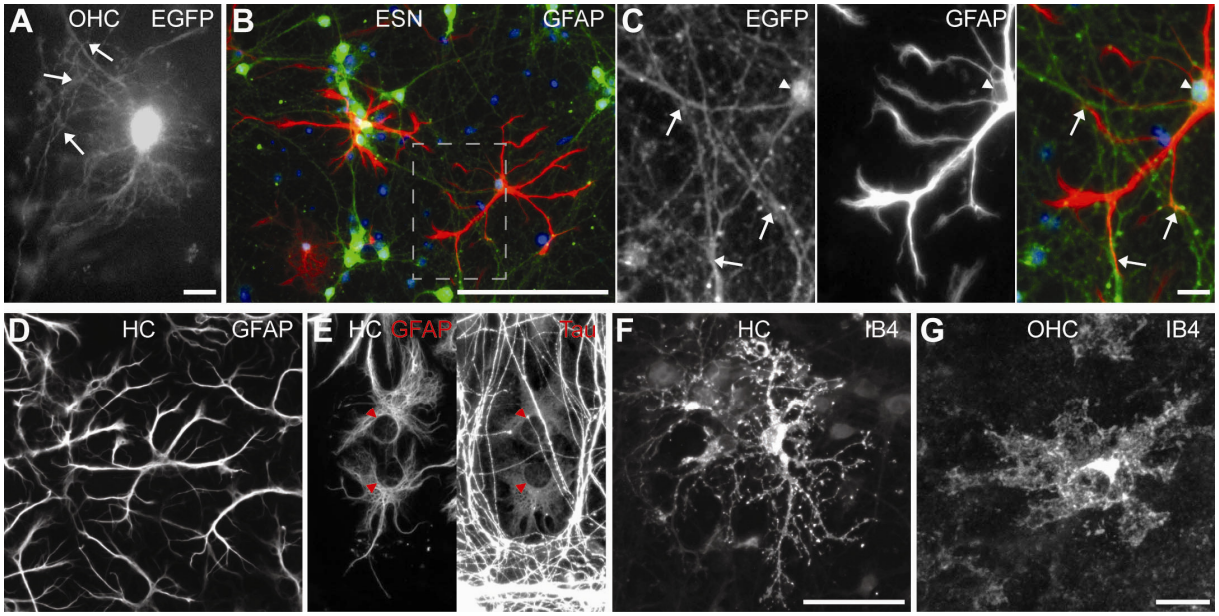

Figure 24 | Glia-like ESNP-derived cells resemble astrocytes. A | Glia-like EGFP-positive cell imaged live in the slice culture at 28 DIV. Its processes are in contact with thin EGFP-positive fibers, presumably ESN axons (arrows). **B** | Dissociated growing ESN culture at 15 DIV. GFAP (glial fibrillary acidic protein) expression is shown in red. **C** | Higher magnification view of boxed region in **B**. Arrows point to association sites of GFAP-positive glial processes with GFAP-negative EGFP-positive fibers. The cell body of the glial cell shows a faint EGFP staining (arrowhead). **D-F** | Primary hippocampal cultures, detection of GFAP alone in **D**, GFAP and tau in **E**, and a microglial cell in **F**. **E** shows that astrocytes contain tau protein. **G** | Microglial cell in organotypic slice culture; maximum intensity projection of confocal stack. Scale bars in **A, C** and **G** 10 µm; in **B** 100 µm; in **D-F** 50 µm.

Strikingly, on the other hand, ESNP-derived astrocytes showed a faint EGFP signal both in the cell body as well as in the processes (Fig. 24C), suggesting that the *tau* promoter must be active in astrocytes. To further proof this hypothesis, dissociated hippocampal cultures were stained with GFAP and tau antibodies at the same time (Fig. 24E). Although much

fainter than the surrounding neurons, GFAP-positive glial cells showed a tau signal clearly above background level (arrowheads). Furthermore it had been reported by Couchie et al. (1988) that cultivated astroglia are able to express *tau* mRNA. Thus, EGFP fluorescence of glia-like cells might have derived from astrocytic cells originating from ESNPs that express low levels of tau protein, and are therefore able to produce some EGFP transgene.

To determine glial identity within the organotypic culture, slices in which the presence of EGFP-positive glia had been detected by live microscopy were stained with IB4. Within the same slice, IB4-positive microglia and green fluorescent glia-like cells were detected, the latter clearly being IB4-negative (see Fig. S3A). Unfortunately, no co-localization of EGFP-positive glia with GFAP could be seen. On the other hand, even a clear co-localization with the astrocytic marker GFAP would not have been sufficient to rule out microglial identity, since microglia where also found to express GFAP under certain conditions (Fig. S3C).

Altogether, the presented facts point toward an astrocytic donor identity of glia-like cells. Nevertheless, it remains elusive why these cells were mostly found in the vicinity of EGFP-positive ESNs. In some cases, glia-like cells even seemed to be directly associated with an atypically shaped neuronal cell body (Fig. S3B). The possibility that microglial host cells might adsorb EGFP protein from dying ESNs is of special interest since cell fusion of microglia with pyramidal neurons has been reported under special conditions (Ackman et al., 2006).

4.3 The role of $p75^{NTR}$ during maturation and integration

In the preceding paragraphs the establishment of a model system was described. ESNPs were transplanted into hippocampal slice cultures, and their maturation was followed and analyzed. It could be shown that ESNs were able to adopt hippocampal neuron morphologies in a region-specific manner. The uniqueness of this model system lies in the ability to analyze a single developing (genetically altered) neuron in a wild type context. In contrast to conventional knockout models, where the entire system is altered, the present method provides an unimpaired neighborhood leading to the possibility to analyze cell-autonomous effects. In a second step, I applied the transplantation protocol to a first protein of interest and its respective knockout neurons to proof its value in revealing protein function during neuronal maturation.

As a first candidate protein the $p75^{NTR}$ was used. This multifunction transmembrane receptor is involved both in synaptic plasticity, regulating long-term depression (LTD), and in controlling apoptosis (see introduction; reviewed in Lu et al., 2005). On the other hand, the receptor has also been linked to neuronal structure. It has been shown in organotypic

hippocampal slice cultures from $p75^{NTR-/-}$ mice that the dendritic complexity of pyramidal neurons was increased. Conversely, $p75^{NTR}$ overexpression decreased complexity (Zagrebelsky et al., 2005).

According to the method described above (Bibel et al., 2007), $p75^{NTR-/-}$ ES cells were differentiated into neuronal precursors. The used homozygous ES cell line lacked exonIV of the $p75^{NTR}$ gene (Annaheim, 2008) and additionally carried multiple copies of the same *tau*EGFP transgene as the wild type line M22 used in this study. In the precursor state as well as shortly after plating onto coated cell culture plates or cover slips, no severe abnormalities could be detected in cells lacking $p75^{NTR}$. Nevertheless, C. Annaheim who analyzed cell death directly after plating saw a surprising increase in cell death for $p75^{NTR-/-}$ cells. Furthermore, the number of primary dendrites was found to be increased as well, corresponding to the earlier mentioned role of the receptor in restricting neuronal complexity. Transplanted into hippocampal cultures, green fluorescent ESNs were seen after a few days as expected, due to the expression onset of the tau protein. As described for the wild type in 4.2.1, a wide range of neuronal morphologies was found revealing no obvious difference in ESN fate. The most abundant group was again represented by the morphologically immature type B ESNs, but also pyramidal as well as granule cell-like ESNs occurred. Similar to the wild type, a fraction of type A $p75^{NTR-/-}$ ESNs showed spiny dendrites, which could not be quantitatively analyzed due to the weak EGFP signal (two ESNs showed spines co-localizing vGLUT1; included in 4.2.2). The following experiment focused on the structural analysis of type A ESNs. A careful exclusion of type B ESNs, according to the aforementioned criteria (Fig. 13), was performed in advance.

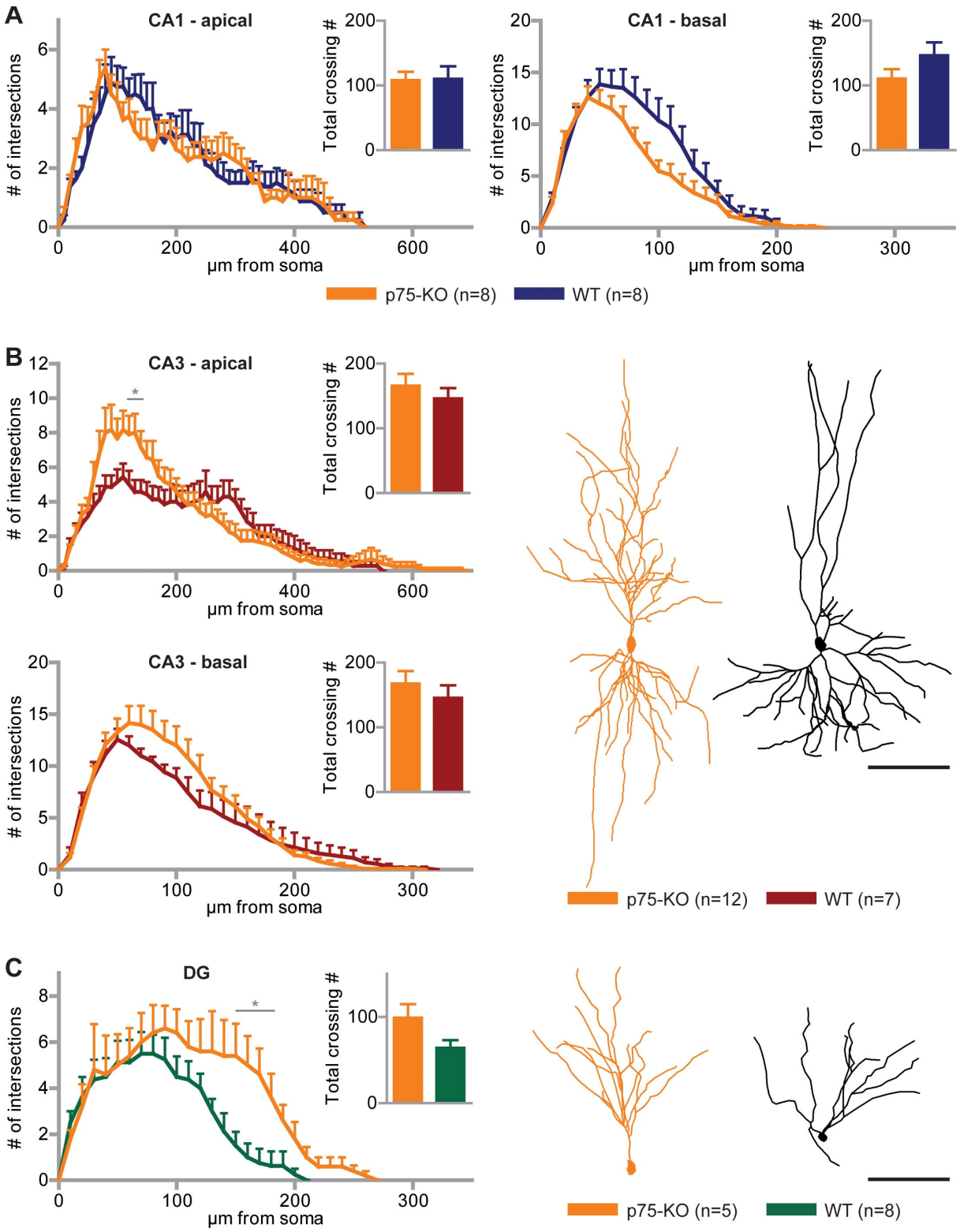

Figure 25 | P75$^{NTR-/-}$ ESNs are more complex than the wild type. A | Sholl analysis and total dendritic complexity for CA1 pyramidal ESNs, p75$^{NTR-/-}$ compared to WT. Apical and basal dendrites are shown separately. **B** | Sholl analysis, total dendritic complexity and tracing examples for CA3 pyramidal ESNs. p75$^{NTR-/-}$ CA3 apical dendrites are significantly more complex than the ones of the respective wild type ESNs. Analyses in **A** and **B** were performed by C. Gonschior (2009). **C** | Sholl analysis, total dendritic complexity and tracing examples for DG ESNs. Also in this case a significant difference is displayed. Average values are depicted together with the standard error of the mean. Two-tailed student's t-test; *p < 0.05. Scale bars 100 µm.

Populations of pyramidal- as well as granule-like ESNs (type A ESNs) lacking $p75^{NTR}$ were compared to respective populations of wild type ESNs, found in the same hippocampal regions. Sholl analysis and total dendritic complexity of $p75^{NTR-/-}$ *versus* wild type CA1 pyramidal ESNs only revealed a non-significant reduction in complexity of the knockout basal dendrites (Fig. 25A). In case of CA3 ESNs, the $p75^{NTR-/-}$ cells (n=12 $p75^{NTR-/-}$ neurons from 10 cultures) showed an increase in complexity compared to the wild type (n=7 WT neurons from 7 cultures) both for the apical and basal dendritic tree (Fig. 25B). However, the only statistically significant difference occurred apically (at a distance of 130 µm from the soma; $p < 0.05$). The tracings also reflected a higher extent of branching in the proximal apical region of CA3 pyramidal-like ESNs lacking the receptor. An even stronger phenotype was found for granule cell-like ESNs (Fig. 25C). Again, knockout ESNs (n=5 $p75^{NTR-/-}$ neurons from 3 cultures) turned out to be significantly more complex than the wild type (n=8 WT neurons from 5 cultures; the differences were found 150 µm to 180 µm from the soma, as well as 200 µm and 210 µm from the soma; e.g.: $p < 0.01$ at 170 µm). These regions represent the more distally located part of the granule cell dendritic tree, suggesting that knockout ESNs were longer, but also showed a more pronounced dendritic branching. The phenotype was visualized by tracing examples of wild type and knockout DG ESNs, although the total dendritic complexity diagram again did not show a statistically significant difference. Altogether, the analysis of $p75^{NTR-/-}$ ESNs revealed a similar phenotype as described before (Zagrebelsky et al., 2005).

I would conclude from these results that **morphological maturation of ESNPs lacking the $p75^{NTR}$ is comparable to the one of the wild type. Comparison of both groups revealed a knockout phenotype in line with previous reports from conventional $p75^{NTR-/-}$ mice. Conclusively, the presented method serves as a model system for examining the roles of proteins during neuronal maturation and integration.**

In an additional analysis also type B ESNs were included. Survival and morphological maturation of $p75^{NTR-/-}$ neurons were analyzed using a time-lapse imaging approach (S. Janßen, 2010). Cell numbers of both, wild type and mutant neurons, showed a gradual decay over the examined time period of five weeks. After four weeks in culture, 26% of wild type ESNs (from 189 cells in 46 cultures at 1-2 DIV) and 8% of $p75^{NTR-/-}$ ESNs (from 53 cells in 19 cultures at 1-2 DIV) remained. In slices with transplanted knockout neurons the reduction of cell number was found to happen earlier compared to the wild type. Together with the afore-mentioned observation of C. Annaheim (2008), a survival-promoting role of $p75^{NTR}$ during early neuronal development of ESNPs can be postulated. This is in line with the results of others, showing that the receptor is needed to guarantee survival in an early period of neuronal life (Bui et al., 2002; Culmsee et al., 2002).

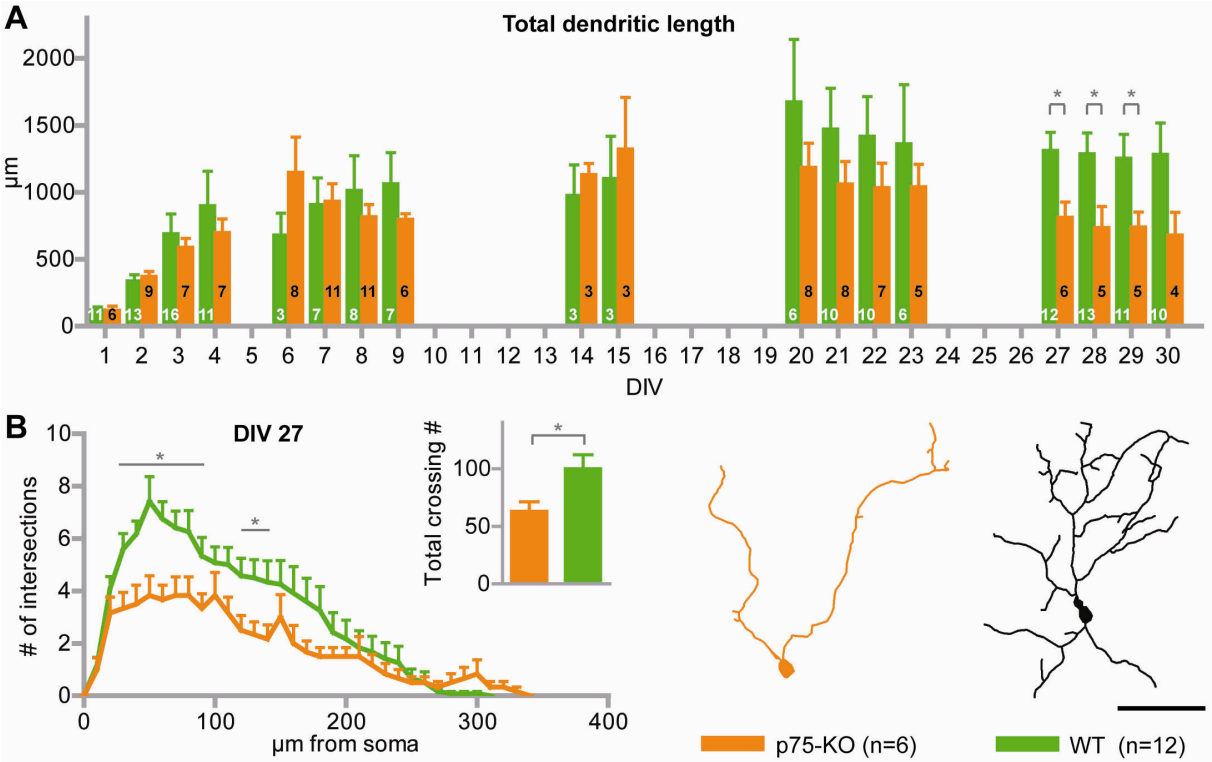

Figure 26 | With time, p75$^{NTR-/-}$ type B ESNs become less complex. A | Total dendritic length of p75$^{NTR-/-}$ *versus* wild type B ESNs. Different sets of ESNs were repeatedly imaged during the 1st (1-4 DIV), 2nd (6-9 DIV), 3rd (14+15 DIV), 4th (20-23 DIV) and 5th week (27-30 DIV). Cells were traced using the Neurolucida® software and the total dendritic length was determined. The numbers of analyzed cells (n) is indicated in the respective column. **B** | Sholl analysis and total dendritic complexity for p75$^{NTR-/-}$ *versus* wild type B ESNs at 27 DIV. Two-tailed student's t-test; *p < 0.05. Scale bar 100 µm. Taken from S. Janßen (2010).

Comparing the morphological maturation of wild type and mutant type B ESNs, the phenotype of p75$^{NTR-/-}$ neurons differed from the one described earlier for type A ESNs (Fig. 26). While the overall maturation course of both cell lines, wild type and knockout, was initially similar, a significant difference in total dendritic length could be seen four weeks after transplantation (Fig. 26A; $p < 0.05$ at 27 DIV). In contrast to the wild type whose complexity and dendritic length were stabilized, the distant dendrites of knockout neurons appeared to constantly shrink. Via Sholl analysis it was also shown that p75$^{NTR-/-}$ type B ESNs were significantly less complex in their proximal compartment after 27 DIV (Fig. 26B; 6 p75$^{NTR-/-}$ neurons from 5 cultures *versus* 12 WT neurons from 8 cultures; the differences were found 30 µm to 90 µm and 120 µm and 140 µm from the soma; e.g.: $p < 0.005$ at 60 µm). The length of primary dendrites, however, appeared to be unaltered (see complexity curve and tracing examples). Conclusively, complexity changes were most likely due to retraction or lacking stabilization of higher order dendrites. These results suggest a stabilizing role for p75^{NTR} in type B ESNs, which was not seen for type A ESNs in the present study (S. Janßen, 2010).

In parallel to wild type type B ESNs, also $p75^{NTR-/-}$ type B ESNs were examined for synapse formation. Although the analyzed cell number was low (n=3 for synapsin; n=2 for vGLUT1; included in 4.2.4), confocal analysis revealed synapsin- (2 cells) and vGLUT1-positive clusters (1 cell) on somas and proximal dendrites, suggesting that $p75^{NTR-/-}$ type B ESNs are innervated by the host circuitry, comparable to wild type type B ESNs (Fig. 22).

5 DISCUSSION

In the present work, I was interested in using pre-differentiated neuronal precursors to examine their integration into the hippocampal circuit. A major advantage of ES cells is the generation of knockout or transgenic cell lines. In combination with the used differentiation procedure of Bibel et al. (2004; 2007) and the presented transplantation approach, they provide a unique opportunity to observe a single modified neuron as it matures and tries to integrate into a functional neuronal network.

The discovery of adult neurogenesis at the end of the past century disproved the hundred year old dogma that no new neurons are added to the adult brain. The presence of stem cells which differentiate into mature neurons and continuously become integrated into pre-existing structures opened a new field of research. Initially, it was attempted to use stem cells to reconstitute the lost neuronal functions after injury or other pathological events. But the new idea of neurons integrating into a pre-existing network is also attractive for basic research. The maturation and integration of newborn neurons is being extensively studied (Lledo et al., 2006). Furthermore, stem cells from different sources are used for transplantation experiments.

In the current study, murine embryonic stem cells were used, which constitute the most plastic cell type available. They are capable of generating all cell types found in an organism. Cultured under specific conditions, defined populations of neurons can be generated, using retinoic acid (Rohwedel et al., 1999; Bibel et al., 2004; Glaser and Brustle, 2005). In order to prevent tumor formation and to direct functional integration into the circuitry, a precursor population restricted to a specific neuronal lineage was produced. The differentiation procedure of Bibel et al. (2004) has been reported to yield neuronal precursors expressing different proteins characteristic for Pax6-positive radial glia (RG), such as nestin, RC2 and the brain lipid binding protein (BLBP). It was further found that the precursors express the transcription factor Emx2 (Nikoletopoulou et al., 2007). This type of RG gives rise to pyramidal neurons in cortex and hippocampus, and to hippocampal granule cells. Previous transplantation studies of Pax6-positive RG into chick embryos revealed their fate restriction: Although being able to respond to local cues in the spinal cord, they did not adopt features of peripheral sensory neurons (Plachta et al., 2004). Equally it was found upon transplantation into the developing chick telencephalon that in contrast to undifferentiated ES cells, RG were limited to adopt a dorsal fate (Nikoletopoulou et al., 2007).

5.1 Survival and distribution of ESNs

Survival

Once the experimental procedure was established, I was able to reliably transplant a defined number of ESNPs. Transplantation was performed into the different regions of the slice cultures (CA1, CA3 and the DG), and surviving ESNs were detected irrespective of the transplanted subfield. However, the cell number found after 32 DIV was significantly higher in slices that had been transplanted into the DG than in slices transplanted into CA1 or CA3 (Fig. 9G). This could be explained by the fact that in contrast to pyramidal neurons which are generated prior to birth, DG granule cell generation continues during the postnatal period. Therefore, this region is prepared to incorporate new neurons. In rats, the initial phase of "normal" neurogenesis from the germinative layer in the hilar region has been reported to continue until p25 *in vivo* (Andersen et al., 2007). Later on, adult DG neurogenesis from a new germinative layer in the subgranular zone (SGZ) is maintained throughout life. There is some evidence that neurogenesis also occurs in organotypic cultures from rat (Kamada et al., 2004) and mice under specific conditions, the distribution of newly generated neurons closely resembling the *in vivo* situation (Raineteau et al., 2004). The so-called neurogenic niche in the SGZ supports proliferation of neural stem cells, neuronal maturation and integration (Alvarez-Buylla and Lim, 2004; Song et al., 2002). It can be assumed that factors promoting (adult) neurogenesis are also beneficial for the survival and maturation of ESNPs. The neurogenic niche might thus be the reason for the increased survival of ESNs in the DG.

Distribution within the slice culture

The DG also represented the region where most (43.7 ± 4.5%) of the ESNs were found after a period of 28-32 DIV, although ESNPs had been equally transplanted into all three subdivisions (Fig. 11). Besides the potential survival-promoting effect of the neurogenic niche, the transplantation procedure itself could account for the much higher cell number in the DG. Transplantation was always performed into the suprapyramidal blade of the DG, located more or less in the middle of the culture, where the tissue was thickest. Pyramidal cell layers, on the other hand, reside in the more peripheral regions that slightly flatten with time in culture. Therefore, when injected into the DG, cells might have stayed there more easily while the risk to flow out of the lesion site was higher in the CA regions (reflected in Fig. 9B-D). The fact that ESNs were not only found in the transplanted regions CA1 (12.6%), CA3 (15.0%) and the DG (43.7%), but also in the EC (1.8%), the hippocampal fissure (16.5%), the CA4 region (0.5%) and the periphery (9.9%; Fig. 11), could equally be explained by overflowing cell suspension during transplantation. Alternatively, migration could have occurred from the transplanted region into another hippocampal subfield. If migration would be the reason, it would have been mainly directed from CA1 and CA3 toward the DG and the

hippocampal fissure. In a time-lapse approach to examine ESN migration over a period of three days it could not be excluded that ESNPs migrate between 2 and 4 DIV, since their morphology at this stage was extremely plastic, making it difficult to follow a specific cell. However, between 7 and 9 DIV, migration was never observed (18 ESNs in n=6 slices, where ESNs could be continuously imaged, were analyzed; Janßen, personal communication). Therefore, large-scale migration from one subfield into another can be considered unlikely.

Injection as a prerequisite for morphological maturation

In other transplantation studies, precursors had been deposited on the surface of the hippocampal slice (Annaheim, 2008; Benninger et al., 2003). Benninger et al. reported that ESNs migrated into the slice and C. Annaheim could see the axons of a high number of transplanted ESNs unspecifically projecting toward the DG. When I initially used the same approach, ESNs displayed rather immature morphology and many were located at the very border of the culture. Thick axons were seen randomly crossing the slice, and sometimes even growing out of the culture. Indeed, only by injecting the ESNPs directly into the cell body layers, I was able to observe ESNs with pyramidal-like morphology and orientation (Fig. 10). Taken together, these observations led to the assumption that ESNs growing at the surface of the slice might not receive the appropriate signals promoting their proper maturation into hippocampal neurons. As an example, it is well-established that dendritic growth depends on neuronal activity (Wong and Ghosh, 2002). For ESNPs transplanted into the tissue (instead of just leaving them on top of the slice) it may therefore be more likely to be influenced toward a successful integration. Neuronal activity might be present, and their surrounding neurons and glial cells might create a stimulating environment supporting a neuronal precursor to survive, grow and become functional. The support could occur through the secretion of neurotrophic factors such as BDNF which has been implicated in survival and maturation of adult-born neurons (Rossi et al., 2006). Furthermore, the lesion occurring upon transplantation might promote integration, since it has been shown that under pathological conditions such as epilepsy or brain injury neurogenesis is increased (Urrea et al., 2007; Kernie et al., 2001; Parent, 2007). It was found in this study that the soma of all ESNs with pyramidal- or granule-like morphology was located within the principle cell body layer of the respective region, which was not the case for ESNs with immature morphology (Fig. 12). Position thus correlated with morphology, suggesting that a location within the cell body layer was a prerequisite for proper structural maturation. Accordingly, position and orientation within the slice were included into the criteria for type A ESNs (Fig. 13B).

5.2 Type A *versus* type B ESNs - two distinct ESN populations?

Type A and type B ESNs profoundly differed in many respects (summarized in table 1). The fact that two types of ESNs could easily be distinguished due to the establishment of specific criteria (Fig. 13) suggested that there might be one group of ESNs (type A) that received local signals and developed into hippocampal-like cells and another group (type B) that was less complex and did not succeed in developing a hippocampal morphology. The problem could either be the environment or the cell itself, meaning that either type B ESNs did not receive signals or were not able to respond to incoming signals. My first finding that transplantation into intrinsic cell body layers was necessary for ESNs to adopt hippocampal morphology suggested an influence of the surrounding cells and local cues. Nevertheless, a position within a cell body layer was not sufficient for the generation of a type A ESN. Even when directly injected into the cell body layers of the CA or the DG, only about 4% of the transplanted cells acquired the shape of pyramidal or granule neurons. This finding led to the assumption that type A and type B ESNs might differ in their physiological properties which could be reflected in their gene expression pattern. Therefore I wondered how homogenous the precursor population was, and I performed immunohistochemistry of plated ESNs growing in monolayer cultures. First, many non-neuronal cells were found, some of which were positive for glial markers (Fig. 24, discussed below). Second, some GABAergic neurons were generated as seen by vGAT staining (Fig. S2), and as reported by Bibel et al. before (Bibel et al., 2004). Third, neuronal markers against different subpopulations of hippocampal cells revealed major differences in expression levels.

Feature	Type A ESNs	Type B ESNs
Position (Fig. 12, S1)	Within cell body layer	Mostly outside cell body layer, sometimes close
Dendritic tree (Fig. 13)	Clearly structured, apical and basal part clearly defined	Unstructured
Spines (Fig. 19, S1)	Partially covered with spines	Single isolated spines on single cells
Signal intensity (Fig. 10)	Often very weak	Mostly strong
Nucleus (Fig. S1)	Resembles nuclei of pyramidal or granule neurons	Single big DAPI-positive chromatin structures
Connections (Fig. 20, 21, S1)	Yes	Yes

Table 1 | Summary of type A *versus* type B ESN characteristics.

CaMKII and NMDAR in neuronal plasticity

Most strikingly, only a minor portion of ESNs expressed CaMKIIα, an enzyme present in all excitatory hippocampal neurons. Furthermore, the CaMKII-positive ESNs appeared to be more complex than the major fraction of ESNs on the plate (see Fig. 23, Fig. S2). CaMKII is highly abundant in the brain and exerts multiple roles in response to NMDAR-mediated Ca^{2+} influx into the post-synapse (reviewed in Lisman et al., 2002). One isoform, CaMKIIα, is necessary for LTP induction (Otmakhov et al., 1997), since it promotes AMPAR phosphorylation. Furthermore CaMKII physically interacts with NMDARs (Shen and Meyer, 1999), anchoring them at the synapse, and establishing the organization of the postsynaptic density. Therefore, the lack of CaMKII in my ESNs could prevent their plastic response to activity.

In my study, one major difference between type A and type B ESNs was their dendritic structure which appeared to be immature in type B ESNs. Interestingly, CaMKII has been shown to have a direct influence on dendritic development. Fink et al. reported that upon selective overexpression or knockdown of CaMKIIβ in rat primary hippocampal neurons, neurite extension was increased and reduced, respectively (Fink et al., 2003). Furthermore, this process was dependent on direct binding of CaMKIIβ to filamentous actin (f-actin). Accordingly, f-actin bundled by CaMKIIβ (Okamoto et al., 2007), plays a major role in stabilizing dendritic spines during LTP, and mediates surface receptor diffusion (reviewed by Cingolani and Goda, 2008). In another study, heterozygous CaMKIIα mutant mice were used. In the DG of the hippocampus, dendritic length and branching of granule neurons were significantly decreased, concomitant with an increase in the expression of immature neuronal markers and immature electrophysiological features. Interestingly, transcriptome analysis revealed an altered expression of 2000 genes, amongst others a down regulation of the NMDAR (Yamasaki et al., 2008). These reported data point toward a major influence of CaMKII on downstream targets such as f-actin and NMDARs, involved in neuronal maturation. If CaMKII is lacking, as in a major portion of plated ESNs in the current study, morphological maturation via CaMKII signaling and actin stabilization would be heavily impaired. Furthermore, CaMKII has also been shown to be involved in microtubule stabilization via phosphorylation of the microtubule-associated protein 2 (MAP2), which promotes growth and maintenance of the dendritic arbor of cultured rat sympathetic neurons (Vaillant et al., 2002). This report also undermines the impact of CaMKII on dendritic structure.

On the other hand, NMDARs could also be the cause for the described lack of type B ESN plasticity. Lack of functional NMDAR would have the potential to reduce or even prevent Ca^{2+} influx into the cell. In this case, plastic processes could be largely inhibited. Earlier

transplantation studies showed that ESNs (generated with a different procedure) expressed the NMDAR subunit 1 (NR1), but were nevertheless devoid of NMDAR-dependent synaptic currents (Benninger et al., 2003; Wernig et al., 2004; Finley et al., 1996). Plated cultures of ESNs generated with our protocol were only examined in terms of glutamate-evoked activity without a distinction between AMPAR and NMDAR-mediated currents (Bibel et al., 2004). It has been suggested that the NMDAR itself is also involved in spine growth, since the latter could be induced by NMDAR-dependent presynaptic remodeling (Nikonenko et al., 2003). Others, however, reported that intrinsic new-born granule cells lacking the essential NR1 subunit of the NMDAR were capable of generating dendritic spines which were contacted by presynaptic terminals (Tashiro et al., 2006). Nevertheless, the reported lack of NMDAR-mediated synaptic transmission in ESNs (Benninger et al., 2003; Wernig et al., 2004) could be linked to the absence of CaMKII found in this study. Functional NMDARs should be present at all times; the NR1 subunit acts in a heteromultimer with NR2B in an immature stage, which is gradually replaced by NR2A during maturation (Monyer et al., 1994). It has been described that in the hippocampus the mechanism of LTP is strongly dependent on the developmental stage. During the first postnatal week, it is independent of CaMKII (Yasuda et al., 2003). However, at around p14, activity-dependent synaptic potentiation strongly depends on the direct interaction of CaMKII with NR2B, expressed in the immature system (Barria and Malinow, 2005). This is consistent with an upregulation of CaMKIIα expression around p5, concomitant with dendritic maturation and synapse formation (Bayer et al., 1999). Barria et al. showed that the affinity of CaMKII to NR2B is higher than to NR2A, the predominant form in the adult hippocampus, and that binding of CaMKII to NR2B is necessary for synaptic plasticity during maturation (Barria and Malinow, 2005). In the absence of CaMKII, the CaMKII-dependent stage of activity-dependent potentiation during the second postnatal week would not be reached, which could be an explanation for the undirected growth of ESNs in the present study.

Nuclear appearance

In addition to the aforementioned differences between type A and type B ESNs, their nuclei displayed different morphologies. Type A ESN nuclei resembled the surrounding cell layer (Fig. S1; Fig. 21): They showed small dots of dense chromatin. By contrast, type B nuclei after 32 DIV mostly contained one or two strongly stained areas, which was found neither in precursors directly after transplantation nor in immature neurons after 5 DIV (see Fig. 21). The aberrant nuclear appearance of type B ESNs after 32 DIV could be due to a different DNA organization within the nucleus. Chromatin re-organization might be a consequence of processes blocking maturation. Vice versa, chromatin remodeling (induced by an unknown process) could inhibit transcription and the capability of a cell to respond to its environment (Borrelli et al., 2008; Felsenfeld and Groudine, 2003).

Presumptive generation of type A and type B ESNs

Altogether I conclude that the different features that distinguish type A from type B ESNs (summarized in table 1) might be connected to one another. The starting point from which on each type develops separately cannot be clearly determined. Nevertheless the following model can be suggested (Fig. 27): The heterogeneity observed in the dissociated culture points to heterogeneity among the precursors which were plated and transplanted (Fig. 27A). I hypothesize that, for an unknown reason, only a minor fraction of precursors is able to express an unknown effector protein in response to activation (Fig. 27C). The effector protein could be CaMKII; however it is more likely that CaMKII represents one of its downstream targets. The few affected ESNs would accordingly be able to respond to incoming signals in a plastic way: AMPAR would be phosphorylated and new receptors would be recruited to the synapse. NMDARs would be guided to the postsynaptic density and become functional. Structural changes would occur in response to incoming signals: This could include dendritic growth via the actin cytoskeleton (and possibly the microtubules), according to the specific cytoarchitecture of the region where the ESN is located. Upon strong innervation, the presence of CaMKII could lead to the generation of postsynaptic spines. Reacting to local signals and activity, the developing ESN would acquire most features of intrinsic hippocampal neurons, including nuclear organization. The result would be a type A ESN (Fig. 27D). On the other hand, lack of the unknown effector protein would have the opposite effect. Upon activation, no synaptic potentiation would take place. AMPARs would not be phosphorylated, no new AMPARs would be recruited, and NMDARs would not become organized within postsynaptic densities. This might lead to a lack of NMDAR-mediated currents, although NR1 could be immunohistochemically detected (Benninger et al., 2003; Wernig et al., 2004; remains to be shown for ESNs according to Bibel et al., 2004 that I used). Structural changes might also be blocked by the lack of CaMKII. In the absence of dendritic spines, synapses would form at dendritic shafts and somas, containing functional AMPARs (as seen in Fig. 22 for type B ESNs). Altogether, the generated ESN would belong to type B ESNs (Fig. 27).

Expression of region-specific markers

Wernig et al. (2004) reported that in their *in vivo* approach ESNs displayed AMPAR-mediated EPSPs and the presence of synapses, suggestive of functional integration. However, no clear correlation between position, morphology and marker expression could be found. Therefore, a reasonable contribution to the host circuitry could be doubted. To explore the question whether type A and type B ESNs express region-specific markers, I stained ESNs growing in the slice. Because of staining difficulties in slice cultures, the examined cell number was low. Nevertheless, type B ESNs negative for CaMKII were found. A single type A ESN in CA1 expressed Ctip2, while a type B ESN was negative (Fig. 23). These very

preliminary data support the hypothesis that type A ESNs are capable of acquiring regional identity whereas type B ESNs are not, but the number of examined ESNs needs to be significantly increased.

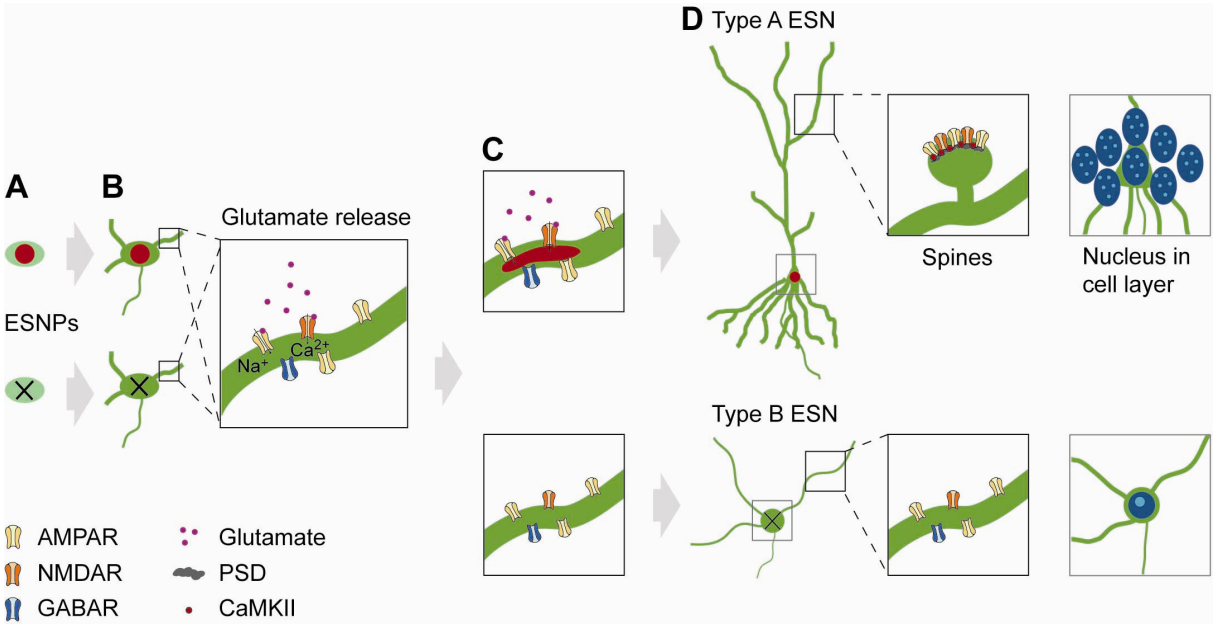

Figure 27 | Presumptive generation of type A and type B ESNs. A | A heterogeneous population of precursors is transplanted. **B** | Neurite outgrowth and insertion of NMDA, AMPA and GABA receptors take place in both precursor types. **C** | Upon stimulation by glutamate, Na^+ and/or Ca^{2+} influx mediated by the present receptors causes a cellular response in one of the two example ESNs. **D** | The affected ESN shows several distinct signs of maturation such as dendritic outgrowth, spine growth potentially accompanied by the presence of CaMKII and functional NMDARs, as well as the typical nuclear morphology of mouse hippocampal neurons. The ESN which remains unaffected by the initial activation does not show criteria for maturation.

Weak EGFP signal of type A ESNs

In many cases type A ESNs showed a low fluorescence intensity complicating the morphological analysis. Furthermore, the immature-appearing type B ESNs often showed a stronger signal. This difference could be due to the restricted penetration of the αGFP antibody in combination with the differing position of type A and type B ESNs within the slice (Fig. 10). However, while examining the dissociated ESN cultures, another potential reason attracted my attention: Some ESNs positive for CaMKII or NeuN did not express EGFP or only showed a low EGFP signal (Fig. 23; Fig. S2). ESNs expressing CaMKII were more complex and pyramidal-like than the remainder of cells on the plate (Fig. S2A-D). Additionally, staining against vGAT and synapsin also revealed that some EGFP-negative cells were innervated stronger than their EGFP-positive counterparts (Fig. S2F and D). Their presumptive pyramidal-like structure could be seen outlined by vGAT-positive puncta. These findings suggest that the responsive fraction of ESNs (that expresses CaMKII and might be strongly innervated by inhibitory and possibly excitatory presynaptic terminals) loses EGFP fluorescence. If this fraction corresponds to type A ESNs, they could be missed in the slice

culture, a possible explanation for the low number of type A ESNs. Consequently, the question was why the expression of the transgene would be down-regulated. One potential explanation could be that expression of the transgene (which is randomly inserted in multiple copies) interferes with the expression of plasticity-related proteins. However, Benninger et al. and Wernig et al. used an ES cell line that expressed EGFP directly from the *tau* locus (Benninger et al., 2003; Wernig et al., 2004), and therefore should not hinder the expression from other loci. Nevertheless, they did not detect NMDAR-mediated synaptic transmission. It is therefore unlikely that the insertion of the transgene is the reason for *tau*EGFP down regulation. Alternatively, tau expression could be down-regulated in a specific developmental stage. To address this question, primary hippocampal cultures were stained with tau antibody at different DIV. Tau was highly expressed at 8 DIV to 28 DIV (Fig. S2H), and could be observed in axons and dendrites. Some labeling differences were seen in cell bodies but it was hard to determine whether these were due to differential expression levels of the protein or the position of the cell body. Indeed, the *tau* locus has a complex gene structure containing multiple exons which are alternatively spliced according to developmental stage and tissue type. The question whether all splice variants depend on the same promoter is not yet resolved (Andreadis, 2005). Furthermore, it has been suggested that tau isoform expression switches from an immature to a mature form around p8, when neuronal structure is stabilized and plastic cytoskeletal processes are down-regulated (Kosik et al., 1989). Expression of EGFP in my experiments strongly depends on the cloned *tau* promoter sequence preceding each copy of the transgene. It is conceivable that this cloned promoter sequence does not drive the expression of the mature isoform of tau and therefore could explain why mature cells lose their EGFP fluorescence.

Pyramidal and granule ESNs

Despite the often low EGFP signal, different subpopulations could be distinguished among type A ESNs. The capability of ESNPs to respond to environmental cues included a differentiation into pyramidal neurons or granule cells, cell types that differ profoundly (Fig. 3). This was surprising since it has been reported that the differentiation procedure produces a homogenous population of Pax6-positive neuronal precursors, developing into neurons with pyramidal-like morphology (Bibel et al., 2004). Thus, besides mere survival and differentiation-promoting signals, there must be region-specific cues, directing ESNPs toward the acquisition of a region-specific morphology (and possibly also function). Pax6 expression, however, does not hinder granule cell formation, since granule neuron precursors were also shown to be Pax6-positive (Nacher et al., 2005). Interestingly, despite the aforementioned neurogenesis-promoting conditions in the DG, less granule type A ESNs than pyramidal ESNs were found (8 in the DG, 24 in CA1 and 17 in CA3). A possible explanation could be the presence of intrinsic granule cell precursors at the time point of transplantation. Since

new granule neurons are permanently integrated into the granule cell layer, there might be a competition between newly generated precursors so that only a minor part finally manages to mature. While ongoing neurogenesis in organotypic cultures has been shown in rat (Kamada et al., 2004), the conditions under which it also occurs in mouse cultures are under debate (Raineteau et al., 2004). In this context it is important to note that *in vivo* in the mature DG not all newly generated neurons survive and are integrated into the circuitry. In fact, only about 30% of mouse adult-born neurons have been shown to survive and mature between 1 and 10 weeks after the neurogenic cell division (Snyder et al., 2009). Thus, it appears to be natural that a fraction of new neurons is not capable of integrating into the pre-existing network.

Significance of type A versus type B ESNs

Altogether I conclude that based on morphological criteria, type A and type B ESNs represent two different cell populations. Although originally deriving from a common precursor, they finally either differ in the signals they receive or – more likely – in their capability to respond to incoming signals. Type B ESNs share similarities with ESNs described before that did not show NMDAR-mediated synaptic transmission. A functional contribution to the circuitry can be doubted. Type A ESNs show many features of intrinsic neurons. However, in a subpopulation of type A ESNs some aspects of neuronal maturation might not have been completed. Some were aspiny (see below), others were extremely complex with up to seven basal dendrites and a round cell body, and some DG ESNs had fairly thin dendrites. To functionally undermine the distinction between type A and type B ESNs it will be crucial to test whether type A ESNs are capable of NMDAR-mediated synaptic transmission.

Since the main aim of this study was to analyze the integration of ESNs, I next looked into how their development toward type A cells could be promoted. Because of the assumed relation to (lack of) plasticity, it was reasonable to add growth factors which are known to enhance cellular answers to synaptic input (e.g. neurotrophins, McAllister et al., 1999). First, transplanted slice cultures were cultivated in the presence of conditioned cell culture medium which was obtained from primary cortical cultures. It was assumed that primary neurons and glial cells secrete substances which could have a growth- and differentiation-promoting effect on ESNPs. Preliminary data show that survival and complexity of type B ESNs could be increased over a period of 7 DIV (M. Kühnemund). In the next experiments, it will be crucial to assess after longer time periods whether the proportion of type A ESNs can be increased. Since cortical neurons were reported to secrete BDNF, thereby promoting dendritic growth (Horch and Katz, 2002), it seemed likely that BDNF could be one of the factors responsible for the increased dendritic complexity observed in the preliminary experiment. While the

conditioned medium represents a mixture of unknown composition, it will be interesting to directly apply BDNF to find out whether a higher percentage of type A neurons can be achieved.

5.3 Maturation of ESNs

Dendritic morphology of type A ESNs

In the present study I could show that a fraction of ESNPs transplanted into hippocampal slice cultures morphologically matured into pyramidal-like and granule-like cells, respectively. ESNs resembling pyramidal neurons were found in the CA regions while ESNs reproducing granule cell morphology were found in the DG. A major difference between these two ESN groups was that while granule ESNs fully reproduced the dendritic complexity of intrinsic DG cells, pyramidal ESNs were less complex than their resident hippocampal counterparts. A possible explanation is that maturation depends on external signals. The extremely plastic neurogenic niche in the DG has already been discussed in terms of survival and maturation-promoting signals. Transplanted ESNPs might face a competitive situation in the presence of intrinsic neuronal precursors (as described above), but as soon as they enter the loop of supporting signals, they might be provided with all support they need to completely mature and integrate. In contrast, all intrinsic pyramidal neurons are generated before birth, between E10 and E18. It is known that the functional features of pyramidal cells are almost completely preserved in organotypic cultures (Muller et al., 1993; Stoppini et al., 1991). Nevertheless, one cannot exclude that the hippocampus at p10 is devoid of factors or signals needed to complete pyramidal cell maturation. An alternative explanation for pyramidal ESNs being less complex than intrinsic pyramidal neurons is that the amount of EGFP protein was not sufficient to fill their rather thin higher-order dendrites.

Furthermore, activity could be required for ESN maturation. CA1 pyramidal ESNs showed major differences compared to intrinsic neurons in their distal apical compartment, the apical tuft. This is the region, where CA1 cells are typically innervated by the perforant path and other extra-hippocampal fibers. It has been described that the dendritic tree of pyramidal cells growing in slice cultures is less complex than *in vivo*, due to the transsection of these afferents, and concomitantly the lacking input (Gahwiler et al., 1997). This could equally apply to developing ESNs. In CA3 ESNs the differences were most prominent, in the apical and basal dendritic tree. This could also be caused by lacking input and resulting rearrangements of axonal projections. Besides the mossy fiber input, CA3 neurons are innervated by CA3 collaterals from the contra-lateral hippocampus, a projection which is equally missing in slice cultures. In this context it has to be mentioned that the heterogeneity between ESNs was especially high in this hippocampal subdivision (reflected in the tracing

examples in Fig. 15A). CA3 was the region where many cells matched some but not all criteria for type A ESNs, and accordingly had to be excluded from the morphological analysis. These findings support the idea that ESN maturation could be dependent on synaptic input.

In one case, the development of a CA3 pyramidal ESN could be followed using live microscopy (Fig. 18). Remarkably, within four days the complex dendritic tree of a pyramidal neuron was generated. The extension of an axon at 2 DIV and the existence of a clearly separated apical and basal compartment as early as 3 days after transplantation indicate that the ESN followed the maturation time scale of embryonic pyramidal neurons in primary hippocampal cultures (Dotti et al., 1988). By contrast, adult generated neurons in the DG need much longer to reach a comparable stage (for a review see Zhao et al., 2008).

Integration of type A ESNs

I could show that a fraction of type A ESNs in the different hippocampal subdivisions carried synapses located on dendritic spines (Fig. 19; Fig. S1). Spiny dendrites represent a major hallmark of hippocampal pyramidal and granule neurons. Most excitatory synapses are located on spines, which are thought to play an important role in long-term synaptic plasticity (Segal, 2005). Therefore, an integration of the spiny group of ESNs into the hippocampal circuitry can be suggested. Unfortunately, only a minor part of type A ESNs could be examined for the presence of spines, and I could not quantify spine density. The main problem was the insufficient EGFP fluorescence in small structures, due to the cytoplasmic distribution of EGFP. In an attempt to better visualize dendritic spines, I tried to generate an ES cell line expressing a membrane-bound form of EGFP also under the control of the *tau* promoter (in cooperation with I. Lahmann and Prof. Dr. H.-H. Arnold). The approach has so far been unsuccessful. To increase the EGFP signal, immunohistochemistry against EGFP was performed on a routine basis. Antibody staining, however, was restricted to the more superficial dendrites, due to limited penetration. However, low fluorescence intensity did not account for all cases in which aspiny dendrites were seen. Some rather bright and complex neurons appeared not to carry dendritic spines, even at 32 DIV (see Fig. S1C). A similar finding was described by another group who investigated the integration of ESNPs, generated with two different protocols, into the neocortex *in vivo* (Ideguchi et al., 2010). Whereas ESNPs produced with a stromal cell approach were able to reproduce layer 5 pyramidal morphology, projection and spine density, ESNPs generated with our method failed to do so. The resulting ESNs were less complex and devoid of dendritic spines.

In the end, the final proof for synaptic integration of type A ESNs has to occur via electrophysiological experiments, in which these cells can be depolarized and stimulated via

a stimulation electrode positioned close by. This is the only way to find out whether ESNs receive synaptic input and whether they are able to fire action potentials.

In the preceding transplantation studies of Benninger et al. (2003) and Wernig et al. (2004), electrophysiological recordings were performed. Both found that their ESNP progeny (that mostly resembled type B ESNs shown in this study) received excitatory and inhibitory input. The ESNs fired action potentials and their electrophysiological properties (such as capacitance, input resistance and resting membrane potential) matured over time, resembling those of mature granule neurons after 3 weeks in culture. On the other hand, no NMDAR-dependent EPSPs could be detected and no clear correlation between region-specific morphology and marker expression was found. Although these studies examined function to a certain extent, they could not conclude about integration. The morphology of ESNs has never been analyzed in detail. If I could combine the morphological analysis of pyramidal and granule ESNs on a single cell-level with an approach to test their functionality, this would complete the picture of ES cell-derived pyramidal and granule cells integrated into the hippocampus.

Type B ESNs

Although morphologically differing from the hippocampal-like type A ESNs in missing potential prerequisites for a meaningful integration, type B ESNs also showed signs of maturation. They survived, and followed a specific maturation pattern over the course of four weeks (Fig. 22A and B). A significant increase in total dendritic complexity was found during the first week within the culture. While at the beginning dendritic growth mainly occurred in the proximity of the cell body, during the third week, longer dendrites were found. In the end, at four weeks of age, dendritic length and complexity decreased again. At the same time, the standard error was reduced over the complexity curve, suggesting that growth and retraction reached a dynamic equilibrium. However, to be sure that the dendrites do not shrink during subsequent weeks, dendritic complexity also needs to be analyzed at later time points. Immunohistochemical stainings showed that type B ESNs receive glutamatergic and GABAergic synaptic input (Fig. 22C and D). This is in line with previous electrophysiological and ultra-structural findings that ESNs after two to three weeks in culture show (mainly inhibitory) postsynaptic potentials and carry active synapses (Annaheim, 2008).

5.4 ESNP fate

In the present study, different cell types were found in ESN cultures growing on cover slips. Besides non-neuronal cells such as glia (see below) the cell population consisted of glutamatergic (major fraction) as well as GABAergic neurons (they were not quantified since vGAT only stains presynaptic terminals). I could clearly see vGAT-positive presynapses

innervating ESNs (Fig. S2F). Glutamatergic neurons had been the expected progeny of the differentiated precursor population (Bibel et al., 2004). These expectations were based on immunohistochemical and electrophysiological analyses, and western blots of ESN monolayer cultures. The authors showed that Pax6 was expressed in 84% of the precursors and was rapidly down-regulated during the first days after plating. The transcription factor Pax6 is known to be expressed *in vivo* by the high portion of RG acting as neuronal precursors in the developing telencephalon, therefore mediating a neuronal fate (Heins et al., 2002). When RG progeny was mapped expressing LacZ from the hGFAP promoter, the entire dorsal telencephalon was labeled. The ventral region, however, the origin of GABAergic interneurons, was negative (Malatesta et al., 2003). Thus *in vivo*, interneurons do not derive from RG. *In vitro*, however, using Pax6 knockout ES cells for the neuronal differentiation protocol, led to the generation of a GABAergic neuron population (Nikoletopoulou et al., 2007). Upon transplantation of wild type and Pax6 mutant ESNPs into chick embryos, wild type neurons were restricted to dorsal fates, while Pax6 mutant neurons acquired ventral characteristics such as projection and GABA release. Therefore, Pax6 expression may act as switch between a glutamatergic and a GABAergic transmitter phenotype of ES cell-derived RG. The fact that only 84% of the precursor population in Bibel et al. expressed Pax6 accordingly implies that besides glutamate also other transmitter types can be found in ESN cultures, as seen in the present study. Furthermore the precursor population was reported to express markers for pyramidal neurons in a homogenous and highly synchronized manner as shown via western blot (Bibel et al., 2004). This might apply to an entire cell population, however it was found to be difficult to be confirmed at the single cell level (Fig. 23). In a recent review the physiological potential of neural stem cell systems was discussed. The authors stated that stem cell cultures in general deviate from the *in vivo* situation and cells cannot be expected to behave according to the corresponding *in vivo* stage (Conti and Cattaneo, 2010). This might especially apply to ESNPs which are exclusively generated by the influence of artificial cues and have never been in contact to a physiological stem cell niche. On the other hand I was able to show that a fraction of ESNs develops characteristics of hippocampal cells, indicating that *in vivo* and *in vitro* neuronal precursors must share important qualities.

Neurons versus glia

After ESNP transplantation into slice cultures, glial cells were recognized based on their EGFP fluorescence (Fig. 24A). When ESNPs were plated on cover slips, GFAP-positive glial progeny was frequently found (Fig. 24B). The presence of glia as RG progeny is not surprising, since *in vivo* RG in the ventral developing telencephalon give rise to glial cells such as astrocytes (whereas in the dorsal telencephalon they generate cortical neurons, as reviewed by Pinto and Gotz, 2007). However, in my cultures the glial fraction was higher than

the reported 1% of Bibel et al., which could be due to the fact that I did not use “complete medium” (but instead Neurobasal medium supplemented with GlutaMAX and B27 supplement) for the monolayer cultures. Nevertheless, the presence of EGFP-positive glial cells in the slice culture caught my attention because the EGFP transgene of the used cell lines was driven by the *tau* promoter to restrict fluorescence to neuronal progeny. EGFP-positive glia could either represent astrocytes or microglia. Microglia belong to a macrophage lineage and are responsible for phagocytosis of dying cells in the brain under pathological conditions (Hanisch and Kettenmann, 2007). Like other bone marrow-derived cells, microglia have been reported to be able to fuse to neurons upon activation (Alvarez-Dolado et al., 2003; Ackman et al., 2006). Therefore I carefully addressed the question what might be the origin of EGFP-positive glia in slice cultures.

The most likely option is that EGFP-positive glia represent astrocytes generated from transplanted ESNPs and thus are of donor origin. In this case they would themselves express EGFP under the control of the *tau* promoter. A weak EGFP signal had also been detected in astrocytes in monolayer cultures (Fig. 24B). To find out whether the *tau* promoter is indeed active in glial cells I performed immunohistochemical stainings of primary hippocampal cultures against tau in combination with GFAP. Although glial cells were mostly overlapping with neuronal processes which were strongly labeled, some single astrocytes were found that were clearly tau-positive (Fig. 24E) in line with previous reports that astrocytes contain *tau* mRNA (Couchie et al., 1988). Other astrocytes however, which displayed the typical condensed GFAP fibers, appeared to be negative (Fig. S3E-G). Indeed, two different stages of astrocytes might occur, one weakly expressing tau, the other not. It has been described that following injury, reactive astrocytes express tau protein whereas normal astrocytes are tau-negative (Ridet et al., 1997). This explains why labeled glia appeared under special conditions, e.g. when atypically shaped and potentially dying neurons were found (Fig. S3B). Quiescent unlabelled astrocytes may reside in the tissue and upon activation by pathological conditions upregulate tau and thus EGFP protein expression. Glial cells found in the hippocampal cultures (Fig. 11; Fig. 12G; Fig. 24A; Fig. S3A+B) closely resemble astrocytes imaged by others before (Bushong et al., 2002). Furthermore, RG are gliogenic, and even *in vivo* there is a small population of bipotent RG, capable of generating neurons and glia (Pinto and Gotz, 2007). RG can undergo asymmetric division thereby generating a neuron and another RG (Huttner and Kosodo, 2005), and it cannot be excluded that *in vitro* the newly formed RG develops into a mature astrocyte. Interestingly, it could be shown by Janßen (2010) that a complex pyramidal cell developed within 3 days after transplantation (Fig. 18). From the same precursor, or at least from the same region within the culture (possibly the injection site) arose a small diffusely stained structure, possibly a glial cell. One day later, the presumptive glial cell had left, or lost its EGFP fluorescence.

These images suggest a simultaneous development of neurons and glia from the same precursor or precursor-pool. Altogether, these observations support a donor-derived astrocytic identity of EGFP-positive glia.

Another potential scenario is that resident microglia might phagocytose dying ESNs thereby taking over their EGFP protein. The observations that microglia were present in my hippocampal cultures (Fig. 24F and G), and that in a few cases EGFP-positive glia were located close to neurons that appeared to be degenerating (Fig. S3B), support this idea.

The two other possibilities that EGFP-positive glial cells might either represent ESNP-derived microglia or host-derived astrocytes are extremely unlikely. First, microglia do not belong to the neural lineage, but derive from the bone marrow (Cuadros and Navascues, 1998; Chan et al., 2007) and second, astrocytes are much less involved in phagocytosis than microglia (al-Ali and al-Hussain, 1996).

In an attempt to show that EGFP-positive glia are astrocytes and no microglia, I stained a transplanted slice culture containing glia with IB4. Close to the EGFP-positive glia, IB4-positive cells were located, which were clearly EGFP-negative (Fig. S3A). Altogether, it can be suggested that EGFP-positive glia-like cells represent astrocytes derived from ESNPs transplanted into the slice cultures that upon reactive gliosis express EGFP from the *tau* promoter.

5.5 Significance of associated cells

The phenomenon of associated cells which I observed has not been reported before. But in 2006, the discovery was made that microglia virally transduced with GFP can fuse to the apical dendrite of intrinsic neurons and thus transmit the fluorescent protein to the host cell (Ackman et al., 2006). Since then, studies focusing on differentiation and integration of stem cell-derived neuronal precursors based on viral transduction (e.g. Englund et al., 2002) are considered ambiguous, because false positive differentiated ESNs could be obtained. This possibility could also question my experiment. However, it would require some steps that have never been reported, such as microglia adsorbing EGFP, and in a next step transmitting it to an intrinsic cell. The conditions, under which fusion occurred, strongly differed from mine, since I did not use viral transduction which involves the expression of fusogenic proteins. Ackman et al. further found pyramidal neurons that did not show an associated cell body but instead a heterokaryon within the primary soma (Ackman et al., 2006). Therefore the presence of a second nucleus has been taken as a sign for cell fusion (Ideguchi et al., 2010). My results, however, also permit another explanation of secondary cell origin. Taken together, there are two possible scenarios: Either cell fusion has occurred

(between two ESNs or one hippocampal neuron and one ESN) or a precursor has undergone an unfinished cell division (pros and cons are listed in table 2). Associated secondary cells do not resemble microglia. Instead, they have the morphology of simple neurons (type B ESNs). Although fusion events occur among neural stem cells *in vitro* (Raff, 2003), they have never been reported for neurons. Furthermore, connections were not only found between type A and immature neurons, but also among type B neurons and in earlier stages. Often, more than two cells appeared to be associated to one another. Syncytia were mostly seen when an ESN matched some but not all criteria of type A ESNs, e.g. the dendritic tree was more complex than the one of intrinsic cells (when more than one nucleus was found in a soma, the cell was excluded). The DAPI stained ESN examples that unambiguously showed pyramidal structure only had a single nucleus in their soma. A clear phenotype was seen for the $p75^{NTR-/-}$ ESNs which can only be explained by a donor identity of the pyramidal cells. The most telling argument against cell fusion is that we were able to follow the generation of a pyramidal ESN within the first days after transplantation (Fig. 18). Fluorescence intensity increased over time concomitantly with a neighboring cell, ruling out that in this case the EGFP signal was transferred from one cell to the other.

Cell fusion	Unfinished cell division
44.5% of cells show a cytoplasmic connection (Fig. 20C)	Cell connections also found in type B ESNs and earlier stages (Fig. 21B)
Additional swellings represent secondary somas carrying nuclei (Fig. 21A)	
Some ESNs contain two nuclei within one soma (Fig. S1)	Those ESNs match some, but not all criteria for type A (Fig. 21C)
Low fluorescence intensity of type A ESNs (Fig. 10C)	In dissociated culture mature ESNs that are EGFP-negative (Fig. 23C; Fig. S2)
Cell fusion between microglia and pyramidal neurons reported (Ackman et al., 2006)	Secondary cell is neuronal, fusion between neurons is not known
	Lack of $p75^{NTR}$ leads to significant phenotype (Fig. 25B,C)
	Often more than two ESNs connected (Fig. 20D)
	Development of a type A ESN at DIV1-4 was followed (Fig. 18A)

Table 2 | Arguments supporting cell fusion *versus* unfinished cell division.

Altogether, I suggest the following model (Fig. 28): A population of precursors is transplanted into the hippocampal slice. A fraction of precursors undergoes mitosis (Fig. 28 A and C), generating a second nucleus within the soma. The second nucleus either remains in the cell body as the neuron structurally matures (Fig. 28C), or it migrates toward a potentially more favorable environment, e.g. a pyramidal cell layer (Fig. 28A). In this case, the cell bodies could either complete cytokinesis and detach from one another, or remain cytoplasmically connected. Subsequently, the cell body growing within the intrinsic cell body layer receives signals for maturation and integration, whereas the other cell body does not. The result is a type A neuron connected to a type B neuron.

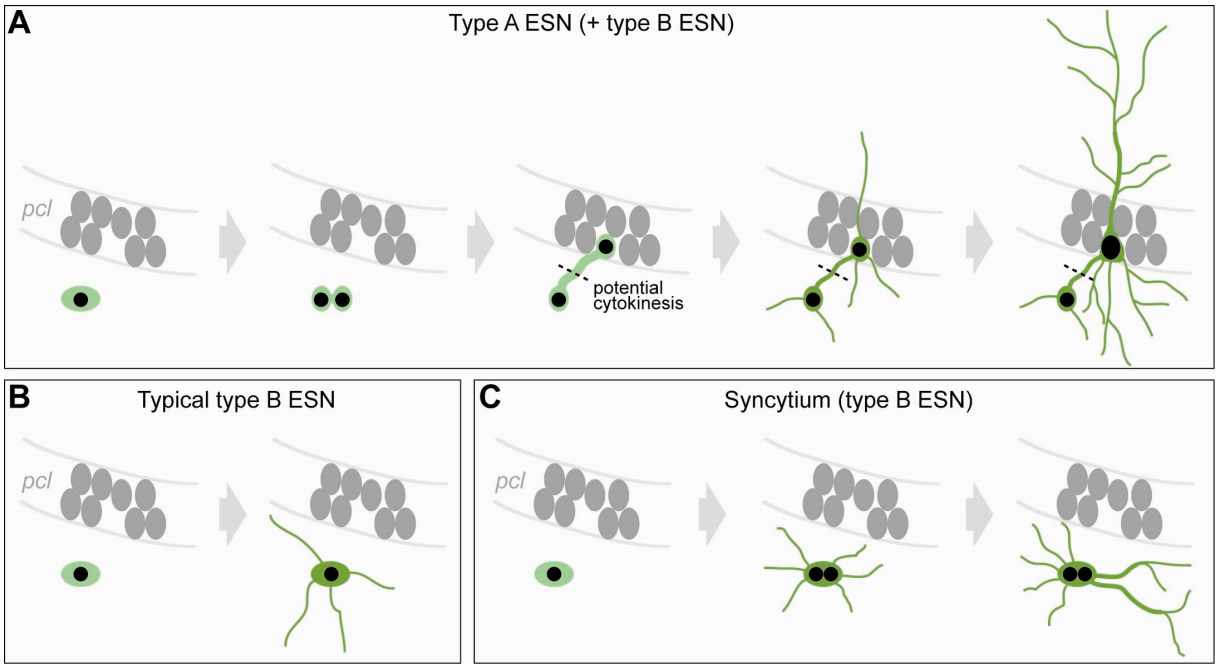

Figure 28 | Potential processes leading to associated ESNs and syncytia. A | If a precursor undergoes mitosis close to an intrinsic cell body layer, one of the newly formed cell bodies might translocate toward this layer (*pcl* – pyramidal cell layer). Either the connection between both daughter somas remains, or cytokinesis is completed. The cell body within the intrinsic layer might develop into a type A ESN. **B,C** | Generation of type B ESNs. Either no cell division takes place (**B**) or mitosis might lead to the formation of a syncytium, resulting in an aberrant orientation and dendritic morphology (**C**).

Interestingly, the presented model of a cell division event preceding a region-specific ESN maturation is supported by earlier publications. It has been suggested by Brüstle et al. that cell division of transplanted precursors within the host environment might be a prerequisite for a successful integration (Brustle et al., 1995). Others stated that precursors might acquire new instructions as they undergo mitosis in a new environment (Chenn et al., 1997). A correlation between cell birthday and laminar fate was found in transplantation studies of young cortical precursors into older tissues, suggesting an influence of the cell cycle stage on neuronal subtype determination (McConnell and Kaznowski, 1991). In the present study, mitosis might therefore be required for ESNPs to respond to regionalizing cues. Furthermore,

somal translocation which could underlie the generation of type A ESNs (Fig. 28), was described to occur upon neurogenic cell division of RG during cortical development (Nadarajah et al., 2001). The neuronal daughter cell inherits the RG process and translocates toward the pial surface. Similarly, it is conceivable that in the present study a transplanted ESNP extends a RG process toward the cell layer, followed by mitosis and somal translocation.

In the end, it has to be proven that type A ESNs are of donor origin. To this aim, I have tried different approaches. The first was to transplant the precursors into female cultures and to detect the y-chromosome of ESNs via DNA *in situ* hybridization. Second, RNA *in situ* hybridizations against EGFP mRNA were performed and third, 5-bromo-2-deoxyuridine (BrdU) pre-labeled ESNPs were transplanted and processed via immunohistochemistry. Unfortunately, so far none of the approaches has been successful. Furthermore, it remains to be investigated whether the cells are indeed cytoplasmically connected or if gap junctions are the reason. It could be observed in the case of mature hippocampal CA1 neurons in acute slices that two or more cells in vicinity were stained, although only one of the neurons had been injected with a fluorescent dye (Church and Baimbridge, 1991).

5.6 The role of $p75^{NTR}$ during maturation of ESNs

$P75^{NTR}$ is known to be involved in multiple processes during neuronal life, reaching from survival to functional and structural plasticity to apoptosis. The neurotrophin receptor is highly expressed in early neuronal development and subsequently down-regulated. In the adult, it is still present in neurons involved in synaptic plasticity processes, e.g. in hippocampal pyramidal neurons. There it was found that $p75^{NTR}$ negatively modulates dendritic structure (Zagrebelsky et al., 2005). Correspondingly, LTD, the long-lasting reduction of synaptic transmission on CA1 synapses, was impaired in the absence of $p75^{NTR}$, as well (Rosch et al., 2005; Woo et al., 2005). These loss-of-function experiments, however, were done in the complete knockout system. Therefore, the effects seen might be influenced by the surrounding tissue and compensatory mechanisms, potentially occurring during the development of the knockout animals. To avoid these possible side effects and to analyze the role of $p75^{NTR}$ during maturation on a single-cell level, in the current study $p75^{NTR-/-}$ ESNPs were transplanted into wild type hippocampal slice cultures. As a result, the same neuronal types A and B were generated as described for the wild type ESNPs above. Thus, neuronal fate commitment was not markedly restricted by the lack of $p75^{NTR}$, although others had suggested that $p75^{NTR}$ might be required for the neuronal differentiation of precursors (Hosomi et al., 2003). They reported that in fetal forebrain-derived neurospheres from exonIII

$p75^{NTR-/-}$ mice BDNF-induced neuronal differentiation was impaired compared to wild type neurospheres.

The morphological analysis was performed separately for type A and type B ESNs, respectively. Comparison of type B ESNs with different genetic backgrounds revealed significant differences between wild type and $p75^{NTR}$ knockout type B ESNs, allowing conclusions about the role of $p75^{NTR}$ in these cells (Fig. 26). Therefore, they can be useful to unravel the function of a protein of interest during maturation of ESNs.

Type A ESNs

I could show that type A ESNs lacking $p75^{NTR}$ are significantly more complex than wild type ESNs after 32 DIV in a wild type environment (Fig. 25), corresponding to a role of $p75^{NTR}$ in negatively influencing dendritic branching. This result is in line with the previous study which revealed that there is a significant complexity increase in the distal apical and the basal compartment of mature pyramidal $p75^{NTR-/-}$ neurons (Zagrebelsky et al., 2005). In the opposing $p75^{NTR}$ overexpression approach, single mature neurons were transfected and analyzed. In this case, complexity was significantly reduced in the proximal apical part of the dendritic tree (Zagrebelsky et al., 2005). Interestingly, I found the increase of complexity in $p75^{NTR-/-}$ CA3 ESNs to be located exactly within the same dendritic region. The dendritic compartment affected might therefore be due to a cell-autonomous effect of $p75^{NTR}$. Accordingly, it was reported *in vivo* that at the age of four weeks $p75^{NTR}$ and its ligand proBDNF were mainly expressed in the *stratum lucidum* of the CA3 region and in granule neurons (Yang et al., 2009). In my experiment, the DG type A ESNs lacking $p75^{NTR}$ were also significantly more complex than their intrinsic counterparts, equally matching the expression pattern of the receptor at four weeks of age. Another group examined the effect of BDNF/TrkB signaling on dendritic arborization in adult-born neurons *in vivo*. Mice expressing the inducible form of Cre recombinase under control of a glial promoter were crossed with $TrkB^{lox/lox}$ animals. Upon Cre induction, the second exon of the TrkB gene was selectively excised in adult-born granule cell precursors (and mature astrocytes). Four weeks after tamoxifen induction, the resulting TrkB-deficient granule neurons showed a significantly reduced complexity compared to control cells (Bergami et al., 2008). This is consistent with the increased dendritic complexity of $p75^{NTR-/-}$ granule ESNs presented in the current study, and undermines the antagonizing effects of $p75^{NTR}$ and TrkB on dendritic complexity during the development of granule neurons. At this point it can be said that the results obtained for type A ESNs are in line with the proposed functions of $p75^{NTR}$ which were derived from studies in transgenic animals. The approach succeeded in analyzing the role of $p75^{NTR}$ during morphological development on a single cell level, for the first time including granule neurons.

Type B ESNs

Strikingly, the effect seen in type B ESNs was the opposite. While time lapse imaging during the first weeks *in vitro* did not reveal a difference in total dendritic length between $p75^{NTR-/-}$ ESNs and the wild type, significant differences were seen after four weeks *in vitro*. ESNs lacking $p75^{NTR}$ showed a significantly decreased total dendritic length and a significantly decreased dendritic complexity. However, the change was found in the higher order dendrites in the proximal region, whereas the primary dendrites appeared to be maintained over the examined time period. This finding led me to ask why the lack of $p75^{NTR}$ in type B ESNs leads to such profound differences compared to type A ESNs. Although the involvement of $p75^{NTR}$ in various pathways is being unraveled more and more, many aspects remain enigmatic. Developmental status, the availability of neurotrophins, and the presence of Trk receptors are known to play a role in the sensitive equilibrium between survival and apoptosis, process elongation and retraction, and other plastic processes mediated by $p75^{NTR}$ (reviewed by Blochl and Blochl, 2007). Its role in process outgrowth has been found in developing mice lacking $p75^{NTR}$ which showed a retarded axonal outgrowth (Yamashita et al., 1999). In the present study, however, it was the maintenance of processes, rather than the outgrowth, which was affected.

A potential explanation for the differing phenotype in type A and type B ESNs could be the well-described effect of $p75^{NTR}$ in regulating cytoskeleton dynamics via the Rho and Ras downstream signaling pathways. It has been shown that $p75^{NTR}$ binds to Rho-GDI, the Rho-GDP dissociation inhibitor (Yamashita and Tohyama, 2003). During early development, the presence of neurotrophins and their binding to $p75^{NTR}$ determines the equilibrium between RhoA-mediated inhibition (Yamashita et al., 1999; Gehler et al., 2004) and Ras-mediated promotion of neurite outgrowth and elongation (Blochl et al., 2004). At this stage, $p75^{NTR}$ thus is involved in both positive and negative effects and a lack of $p75^{NTR}$ might not lead to an obvious phenotype, in type A and type B ESNs. This could be the reason why the phenotype was only detected in later stages (in type B ESNs; Fig. 26). In the mature system, however, the positive and negative pathways get separated and controlled by different receptor systems. $P75^{NTR}$ is expressed at lower levels and negatively modulates complexity via RhoA, whereas the Trk receptors are highly expressed and exert their positive influence on dendritic outgrowth via the Ras pathway (reviewed by Chao, 2003; Reichardt, 2006). In ESNs, TrkB was also shown to be expressed (Bibel et al., 2007). Therefore in the mature neuron (and most likely the mature ESN), the equilibrium between inhibition and promotion of dendritic outgrowth appears to be reflected in equilibrium between $p75^{NTR}$ and TrkB activation. In the absence of $p75^{NTR}$ at this stage, the negative influence would be missing, leading to an increased plasticity, in both type A and type B ESNs. TrkB activation via BDNF would prevail. As discussed above (5.2), type A and type B ESNs most likely differ in their responsiveness

to external signals. This might include neurotrophin signaling in a way that type A ESNs are capable of responding whereas type B ESNs are not. Type A ESNs would respond to BDNF increasing their dendritic outgrowth. In type B ESNs, on the other hand, TrkB signaling might fail to induce dendritic outgrowth. It is conceivable that lack of the stabilizing $p75^{NTR}$ could lead to the process retraction we observed in type B ESNs.

5.7 Conclusions and outlook

In the present study I could show that ESNPs transplanted into hippocampal slice cultures survive and mature, and partly morphologically integrate into the pre-existing neuronal circuit. Although homogeneously pre-differentiated into RG expressing Pax6 (accoring to Bibel et al., 2004), precursors were responsive to local cues, and adopted region-specific morphologies resembling hippocampal neurons. Integration was determined according to cell morphology and orientation in relation to the hippocampal architecture. Most importantly, a subset of ESNs carried dendritic spines co-localizing with presynaptic markers. This finding strongly suggests that ESNs growing in the organotypic culture receive synaptic input and are functionally integrated. So far, functional integration has been shown by others in the hilar region of hippocampal slice cultures, although the examined cells were not characterized morphologically (Benninger et al., 2003). Interestingly, NMDAR-mediated post synaptic currents were missing. Future work on my project will have to focus on the electrophysiological analysis of type A ESNs in order to find out, whether their morphological maturation is accompanied by functionally mature characteristics. Measuring synaptic currents in the presence and absence of AP5, an NMDAR antagonist, and low Mg^{2+} conditions, will reveal if type A ESNs possess functional NMDARs. Responsiveness to synaptic activation can also be tested by immunohistochemical staining for immediate early gene (IEG) expression (Jessberger and Kempermann, 2003; Snyder et al., 2009; Tashiro et al., 2007). IEG upregulation can be induced by kainic acid (KA) application, which leads to a general increase in activity. In a first attempt to address type A *versus* type B ESN ability to respond to strong synaptic activation, we already started to apply KA and subsequently detect IEG expression in a fraction of ESNs growing in the slice.

ESNs lacking $p75^{NTR}$ revealed a significant phenotype in line with the current concept of $p75^{NTR}$ function in negatively modulating dendritic complexity. Importantly, cell-autonomous effects of $p75^{NTR}$ were detected. As a consequence, the transplantation protocol can be used as a model system to examine the role of other plasticity-related proteins during maturation and integration. Since the current concept of structural plasticity in hippocampal pyramidal neurons implicates antagonizing effects of $p75^{NTR}$ and the TrkB receptor, it will be of special interest whether TrkB-deficient ESNs show the opposite phenotype. Once the system is

established in a way that opposing effects can be detected, it can be used for a broader range of knockout ESNs. The precise roles of many interesting molecules involved in synaptic plasticity cannot be investigated in a conventional knockout approach because of lethality and/or compensatory mechanisms. These problems apply to double and triple knockout mutants of the Amyloid Precursor Protein (APP) and its homologous proteins APLP1 and APLP2. The physiological function of APP is not well understood, and stem cell-based approaches are now being used to elucidate its role in synaptic regulation (Schrenk-Siemens et al., 2008). Thus, my system which allows the analysis of a single affected neuron in a mature wild type environment could be helpful.

It has to be kept in mind, however, that some prerequisites have to be dealt with prior to proceeding with new candidate molecules. Primarily, only ES cells carrying a fluorescent marker can be used for transplantation. Since fluorescence intensity of small structures turned out to be critical, the introduction of membrane-bound fluorophores will be carried on. Furthermore it has to be considered that, depending on the molecule of interest, homozygous ES cells might be required for the analysis. It will be important to find conditions increasing the percentage of type A ESNs compared to the undirected growing type B ESNs. To this aim, stimulation of transplanted ESNPs with growth-promoting substances should be addressed. This has already been started using conditioned medium and will be extended to the addition of neurotrophic factors such as BDNF. Furthermore, it was shown recently that in the rat hippocampus, more adult-born granule neurons survive and mature in comparison to mice (Snyder et al., 2009). Transplanting into rat hippocampal slices could therefore also be an option.

Finally, the donor identity of EGFP-labeled hippocampal-like neurons needs to be proven. Potential strategies include *in situ* hybridization against EGFP mRNA and transplantation of BrdU pre-labeled precursors to distinguish between somas and nuclei of donor and host origin, respectively.

6 REFERENCES

Ackman JB, Siddiqi F, Walikonis RS, LoTurco JJ (2006) Fusion of microglia with pyramidal neurons after retroviral infection. J Neurosci 26:11413-11422.

al-Ali SY, al-Hussain SM (1996) An ultrastructural study of the phagocytic activity of astrocytes in adult rat brain. J Anat 188 (Pt 2):257-262.

Altman J, Bayer SA (1990) Prolonged sojourn of developing pyramidal cells in the intermediate zone of the hippocampus and their settling in the stratum pyramidale. J Comp Neurol 301:343-364.

Altman J, Das GD (1965) Autoradiographic and histological evidence of postnatal hippocampal neurogenesis in rats. J Comp Neurol 124:319-335.

Alvarez P, Zola-Morgan S, Squire LR (1994) The animal model of human amnesia: long-term memory impaired and short-term memory intact. Proc Natl Acad Sci U S A 91:5637-5641.

Alvarez-Buylla A, Lim DA (2004) For the long run: maintaining germinal niches in the adult brain. Neuron 41:683-686.

Alvarez-Dolado M, Pardal R, Garcia-Verdugo JM, Fike JR, Lee HO, Pfeffer K, Lois C, Morrison SJ, Alvarez-Buylla A (2003) Fusion of bone-marrow-derived cells with Purkinje neurons, cardiomyocytes and hepatocytes. Nature 425:968-973.

Amaral DG, Ishizuka N, Claiborne B (1990) Neurons, numbers and the hippocampal network. Prog Brain Res 83:1-11.

Andersen P, Morris R, Amaral D, Bliss T, O'Keefe J (2007) The Hippocampus Book. New York: Oxford Univ. Press.

Andersen SS, Bi GQ (2000) Axon formation: a molecular model for the generation of neuronal polarity. Bioessays 22:172-179.

Andreadis A (2005) Tau gene alternative splicing: expression patterns, regulation and modulation of function in normal brain and neurodegenerative diseases. Biochim Biophys Acta 1739:91-103.

Angevine JB, Jr. (1965) Time of neuron origin in the hippocampal region. An autoradiographic study in the mouse. Exp Neurol SupplSuppl-70.

Annaheim C (2008) Untersuchungen über die funktionelle Rolle des Neurotrophinrezeptors p75 basierend auf embryonalen Stammzellen der Maus

Arimura N, Kaibuchi K (2007) Neuronal polarity: from extracellular signals to intracellular mechanisms. Nat Rev Neurosci 8:194-205.

Arlotta P, Molyneaux BJ, Chen J, Inoue J, Kominami R, Macklis JD (2005) Neuronal subtype-specific genes that control corticospinal motor neuron development in vivo. Neuron 45:207-221.

Barde YA, Edgar D, Thoenen H (1982) Purification of a new neurotrophic factor from mammalian brain. EMBO J 1:549-553.

Barria A, Malinow R (2005) NMDA receptor subunit composition controls synaptic plasticity by regulating binding to CaMKII. Neuron 48:289-301.

Bayer KU, Lohler J, Schulman H, Harbers K (1999) Developmental expression of the CaM kinase II isoforms: ubiquitous gamma- and delta-CaM kinase II are the early isoforms and most abundant in the developing nervous system. Brain Res Mol Brain Res 70:147-154.

Benninger F, Beck H, Wernig M, Tucker KL, Brustle O, Scheffler B (2003) Functional integration of embryonic stem cell-derived neurons in hippocampal slice cultures. J Neurosci 23:7075-7083.

Bergami M, Rimondini R, Santi S, Blum R, Gotz M, Canossa M (2008) Deletion of TrkB in adult progenitors alters newborn neuron integration into hippocampal circuits and increases anxiety-like behavior. Proc Natl Acad Sci U S A 105:15570-15575.

Bibel M, Richter J, Lacroix E, Barde YA (2007) Generation of a defined and uniform population of CNS progenitors and neurons from mouse embryonic stem cells. Nat Protoc 2:1034-1043.

Bibel M, Richter J, Schrenk K, Tucker KL, Staiger V, Korte M, Goetz M, Barde YA (2004) Differentiation of mouse embryonic stem cells into a defined neuronal lineage. Nat Neurosci 7:1003-1009.

Bischofberger J (2007) Young and excitable: new neurons in memory networks. Nat Neurosci 10:273-275.

Bjorklund LM, Sanchez-Pernaute R, Chung S, Andersson T, Chen IY, McNaught KS, Brownell AL, Jenkins BG, Wahlestedt C, Kim KS, Isacson O (2002) Embryonic stem cells develop into functional dopaminergic neurons after transplantation in a Parkinson rat model. Proc Natl Acad Sci U S A 99:2344-2349.

Bliss TV, Collingridge GL (1993) A synaptic model of memory: long-term potentiation in the hippocampus. Nature 361:31-39.

Bliss TV, Lomo T (1973) Long-lasting potentiation of synaptic transmission in the dentate area of the anaesthetized rabbit following stimulation of the perforant path. J Physiol 232:331-356.

Blochl A, Blochl R (2007) A cell-biological model of p75NTR signaling. J Neurochem 102:289-305.

Blochl A, Blumenstein L, Ahmadian MR (2004) Inactivation and activation of Ras by the neurotrophin receptor p75. Eur J Neurosci 20:2321-2335.

Bon CL, Garthwaite J (2003) On the role of nitric oxide in hippocampal long-term potentiation. J Neurosci 23:1941-1948.

Bonhoeffer T (1996) Neurotrophins and activity-dependent development of the neocortex. Curr Opin Neurobiol 6:119-126.

Borrelli E, Nestler EJ, Allis CD, Sassone-Corsi P (2008) Decoding the epigenetic language of neuronal plasticity. Neuron 60:961-974.

Bothwell M (1995) Functional interactions of neurotrophins and neurotrophin receptors. Annu Rev Neurosci 18:223-253.

Bruel-Jungerman E, Laroche S, Rampon C (2005) New neurons in the dentate gyrus are involved in the expression of enhanced long-term memory following environmental enrichment. Eur J Neurosci 21:513-521.

Brustle O, Maskos U, McKay RD (1995) Host-guided migration allows targeted introduction of neurons into the embryonic brain. Neuron 15:1275-1285.

Bui NT, Konig HG, Culmsee C, Bauerbach E, Poppe M, Krieglstein J, Prehn JH (2002) p75 neurotrophin receptor is required for constitutive and NGF-induced survival signalling in PC12 cells and rat hippocampal neurones. J Neurochem 81:594-605.

Bushong EA, Martone ME, Jones YZ, Ellisman MH (2002) Protoplasmic astrocytes in CA1 stratum radiatum occupy separate anatomical domains. J Neurosci 22:183-192.

Cameron HA, Woolley CS, McEwen BS, Gould E (1993) Differentiation of newly born neurons and glia in the dentate gyrus of the adult rat. Neuroscience 56:337-344.

Carlone RL, Ganagarajah M, Rathbone MP (1981) Bovine pituitary fibroblast growth factor has neurotrophic activity on newt limb regenerates and skeletal muscles in vitro. Exp Cell Res 132:15-21.

Carpentino JE, Hartman NW, Grabel LB, Naegele JR (2008) Region-specific differentiation of embryonic stem cell-derived neural progenitor transplants into the adult mouse hippocampus following seizures. J Neurosci Res 86:512-524.

Chan WY, Kohsaka S, Rezaie P (2007) The origin and cell lineage of microglia: new concepts. Brain Res Rev 53:344-354.

Chao MV (2003) Neurotrophins and their receptors: a convergence point for many signalling pathways. Nat Rev Neurosci 4:299-309.

Chenn A, Brainsted JE, McConnell SK, O'Leary DDM (1997) Development of the cerebral cortex: Mechanisms controlling cell fate, laminar and areal patterning, and axonal connectivity. In: WM Cowan, TM Jessell, SL Zipursky. Molecular and cellular Approaches to Neural Development, pp. 440-473. New York: Oxford Univ. Press.

Church J, Baimbridge KG (1991) Exposure to high-pH medium increases the incidence and extent of dye coupling between rat hippocampal CA1 pyramidal neurons in vitro. J Neurosci 11:3289-3295.

Cingolani LA, Goda Y (2008) Actin in action: the interplay between the actin cytoskeleton and synaptic efficacy. Nat Rev Neurosci 9:344-356.

Citri A, Malenka RC (2008) Synaptic plasticity: multiple forms, functions, and mechanisms. Neuropsychopharmacology 33:18-41.

Claiborne BJ, Amaral DG, Cowan WM (1990) Quantitative, three-dimensional analysis of granule cell dendrites in the rat dentate gyrus. J Comp Neurol 302:206-219.

Cleaver O, Melton DA (2003) Endothelial signaling during development. Nat Med 9:661-668.

Cohen S, Levi-Montalcini R, Hamburger V (1954) A nerve growth-stimulating factor isolated from sarcomas 37 and 180. Proc Natl Acad Sci U S A 1014-1018

Conti L, Cattaneo E (2010) Neural stem cell systems: physiological players or in vitro entities? Nat Rev Neurosci.

Couchie D, Charriere-Bertrand C, Nunez J (1988) Expression of the mRNA for tau proteins during brain development and in cultured neurons and astroglial cells. J Neurochem 50:1894-1899.

Cuadros MA, Navascues J (1998) The origin and differentiation of microglial cells during development. Prog Neurobiol 56:173-189.

Culmsee C, Gerling N, Lehmann M, Nikolova-Karakashian M, Prehn JH, Mattson MP, Krieglstein J (2002) Nerve growth factor survival signaling in cultured hippocampal neurons is mediated through TrkA and requires the common neurotrophin receptor P75. Neuroscience 115:1089-1108.

Dechant G, Barde YA (2002) The neurotrophin receptor p75(NTR): novel functions and implications for diseases of the nervous system. Nat Neurosci 5:1131-1136.

Deng W, Aimone JB, Gage FH (2010) New neurons and new memories: how does adult hippocampal neurogenesis affect learning and memory? Nat Rev Neurosci.

Dotti CG, Sullivan CA, Banker GA (1988) The establishment of polarity by hippocampal neurons in culture. J Neurosci 8:1454-1468.

Dougherty KD, Milner TA (1999) p75NTR immunoreactivity in the rat dentate gyrus is mostly within presynaptic profiles but is also found in some astrocytic and postsynaptic profiles. J Comp Neurol 407:77-91.

Dudek SM, Bear MF (1992) Homosynaptic long-term depression in area CA1 of hippocampus and effects of N-methyl-D-aspartate receptor blockade. Proc Natl Acad Sci U S A 89:4363-4367.

Engert F, Bonhoeffer T (1999) Dendritic spine changes associated with hippocampal long-term synaptic plasticity. Nature 399:66-70.

Englund U, Bjorklund A, Wictorin K, Lindvall O, Kokaia M (2002) Grafted neural stem cells develop into functional pyramidal neurons and integrate into host cortical circuitry. Proc Natl Acad Sci U S A 99:17089-17094.

Ericson J, Muhr J, Placzek M, Lints T, Jessell TM, Edlund T (1995) Sonic hedgehog induces the differentiation of ventral forebrain neurons: a common signal for ventral patterning within the neural tube. Cell 81:747-756.

Eriksson PS, Perfilieva E, Bjork-Eriksson T, Alborn AM, Nordborg C, Peterson DA, Gage FH (1998) Neurogenesis in the adult human hippocampus. Nat Med 4:1313-1317.

Evans MJ, Kaufman MH (1981) Establishment in culture of pluripotential cells from mouse embryos. Nature 292:154-156.

Felsenfeld G, Groudine M (2003) Controlling the double helix. Nature 421:448-453.

Fink CC, Bayer KU, Myers JW, Ferrell JE, Jr., Schulman H, Meyer T (2003) Selective regulation of neurite extension and synapse formation by the beta but not the alpha isoform of CaMKII. Neuron 39:283-297.

Finley MF, Kulkarni N, Huettner JE (1996) Synapse formation and establishment of neuronal polarity by P19 embryonic carcinoma cells and embryonic stem cells. J Neurosci 16:1056-1065.

Fitch JM, Juraska JM, Washington LW (1989) The dendritic morphology of pyramidal neurons in the rat hippocampal CA3 area. I. Cell types. Brain Res 479:105-114.

Gage FH (2000) Mammalian neural stem cells. Science 287:1433-1438.

Gage FH (2002) Neurogenesis in the adult brain. J Neurosci 22:612-613.

Gahwiler BH (1981) Organotypic monolayer cultures of nervous tissue. J Neurosci Methods 4:329-342.

Gahwiler BH, Capogna M, Debanne D, McKinney RA, Thompson SM (1997) Organotypic slice cultures: a technique has come of age. Trends Neurosci 20:471-477.

Gaillard A, Prestoz L, Dumartin B, Cantereau A, Morel F, Roger M, Jaber M (2007) Reestablishment of damaged adult motor pathways by grafted embryonic cortical neurons. Nat Neurosci 10:1294-1299.

Ge S, Goh EL, Sailor KA, Kitabatake Y, Ming GL, Song H (2006) GABA regulates synaptic integration of newly generated neurons in the adult brain. Nature 439:589-593.

Gehler S, Gallo G, Veien E, Letourneau PC (2004) p75 neurotrophin receptor signaling regulates growth cone filopodial dynamics through modulating RhoA activity. J Neurosci 24:4363-4372.

Glaser T, Brustle O (2005) Retinoic acid induction of ES-cell-derived neurons: the radial glia connection. Trends Neurosci 28:397-400.

Glass DJ, Nye SH, Hantzopoulos P, Macchi MJ, Squinto SP, Goldfarb M, Yancopoulos GD (1991) TrkB mediates BDNF/NT-3-dependent survival and proliferation in fibroblasts lacking the low affinity NGF receptor. Cell 66:405-413.

Gogolla N, Galimberti I, DePaola V, Caroni P (2006a) Long-term live imaging of neuronal circuits in organotypic hippocampal slice cultures. Nat Protoc 1:1223-1226.

Gogolla N, Galimberti I, DePaola V, Caroni P (2006b) Preparation of organotypic hippocampal slice cultures for long-term live imaging. Nat Protoc 1:1165-1171.

Golgi C (1886) Sulla fina anatomia degliorgani centrali del sistema nervosa. Milan: Hoepli.

Gonschior C (2009) Analyse von Neuronen aus $p75^{NTR}$-defizienten ES-Zellen nach Integration in hippocampale Schnittkulturen

Gospodarowicz D, Jones KL, Sato G (1974) Purification of a growth factor for ovarian cells from bovine pituitary glands. Proc Natl Acad Sci U S A 71:2295-2299.

Gotz M, Huttner WB (2005) The cell biology of neurogenesis. Nat Rev Mol Cell Biol 6:777-788.

Gould E, Beylin A, Tanapat P, Reeves A, Shors TJ (1999) Learning enhances adult neurogenesis in the hippocampal formation. Nat Neurosci 2:260-265.

Hanisch UK, Kettenmann H (2007) Microglia: active sensor and versatile effector cells in the normal and pathologic brain. Nat Neurosci 10:1387-1394.

Hatanaka Y, Mukai H, Mitsuhashi K, Hojo Y, Murakami G, Komatsuzaki Y, Sato R, Kawato S (2009) Androgen rapidly increases dendritic thorns of CA3 neurons in male rat hippocampus. Biochem Biophys Res Commun 381:728-732.

Heins N, Malatesta P, Cecconi F, Nakafuku M, Tucker KL, Hack MA, Chapouton P, Barde YA, Gotz M (2002) Glial cells generate neurons: the role of the transcription factor Pax6. Nat Neurosci 5:308-315.

Hering H, Sheng M (2001) Dendritic spines: structure, dynamics and regulation. Nat Rev Neurosci 2:880-888.

Hirota H, Kiyama H, Kishimoto T, Taga T (1996) Accelerated Nerve Regeneration in Mice by upregulated expression of interleukin (IL) 6 and IL-6 receptor after trauma. J Exp Med 183:2627-2634.

Holtmaat A, Svoboda K (2009) Experience-dependent structural synaptic plasticity in the mammalian brain. Nat Rev Neurosci 10:647-658.

Horch HW, Katz LC (2002) BDNF release from single cells elicits local dendritic growth in nearby neurons. Nat Neurosci 5:1177-1184.

Hosomi S, Yamashita T, Aoki M, Tohyama M (2003) The p75 receptor is required for BDNF-induced differentiation of neural precursor cells. Biochem Biophys Res Commun 301:1011-1015.

Huang EJ, Reichardt LF (2001) Neurotrophins: roles in neuronal development and function. Annu Rev Neurosci 24:677-736.

Husseini L, Schmandt T, Scheffler B, Schroder W, Seifert G, Brustle O, Steinhauser C (2008) Functional analysis of embryonic stem cell-derived glial cells after integration into hippocampal slice cultures. Stem Cells Dev 17:1141-1152.

Huttner WB, Kosodo Y (2005) Symmetric versus asymmetric cell division during neurogenesis in the developing vertebrate central nervous system. Curr Opin Cell Biol 17:648-657.

Ideguchi M, Palmer TD, Recht LD, Weimann JM (2010) Murine embryonic stem cell-derived pyramidal neurons integrate into the cerebral cortex and appropriately project axons to subcortical targets. J Neurosci 30:894-904.

Janßen S (2010) Maturation of $p75^{NTR}$ KO ES cell-derived neuronal precursors within organotypic hippocampal slices

Jessberger S, Kempermann G (2003) Adult-born hippocampal neurons mature into activity-dependent responsiveness. Eur J Neurosci 18:2707-2712.

Jones SP, Rahimi O, O'Boyle MP, Diaz DL, Claiborne BJ (2003) Maturation of granule cell dendrites after mossy fiber arrival in hippocampal field CA3. Hippocampus 13:413-427.

Kamada M, Li RY, Hashimoto M, Kakuda M, Okada H, Koyanagi Y, Ishizuka T, Yawo H (2004) Intrinsic and spontaneous neurogenesis in the postnatal slice culture of rat hippocampus. Eur J Neurosci 20:2499-2508.

Kandel ER, Schwartz JC, Jessel TM (2000) Principles of neural science. McGraw-Hill Companies.

Kee N, Teixeira CM, Wang AH, Frankland PW (2007) Preferential incorporation of adult-generated granule cells into spatial memory networks in the dentate gyrus. Nat Neurosci 10:355-362.

Kempermann G (2002) Why new neurons? Possible functions for adult hippocampal neurogenesis. J Neurosci 22:635-638.

Kempermann G, Kuhn HG, Gage FH (1997) More hippocampal neurons in adult mice living in an enriched environment. Nature 386:493-495.

Kempermann G, Wiskott L, Gage FH (2004) Functional significance of adult neurogenesis. Curr Opin Neurobiol 14:186-191.

Kernie SG, Erwin TM, Parada LF (2001) Brain remodeling due to neuronal and astrocytic proliferation after controlled cortical injury in mice. J Neurosci Res 66:317-326.

Kornack DR, Rakic P (1999) Continuation of neurogenesis in the hippocampus of the adult macaque monkey. Proc Natl Acad Sci U S A 96:5768-5773.

Korte M, Carroll P, Wolf E, Brem G, Thoenen H, Bonhoeffer T (1995) Hippocampal long-term potentiation is impaired in mice lacking brain-derived neurotrophic factor. Proc Natl Acad Sci U S A 92:8856-8860.

Korte M, Griesbeck O, Gravel C, Carroll P, Staiger V, Thoenen H, Bonhoeffer T (1996) Virus-mediated gene transfer into hippocampal CA1 region restores long-term potentiation in brain-derived neurotrophic factor mutant mice. Proc Natl Acad Sci U S A 93:12547-12552.

Kosik KS, Orecchio LD, Bakalis S, Neve RL (1989) Developmentally regulated expression of specific tau sequences. Neuron 2:1389-1397.

Kuhn HG, Dickinson-Anson H, Gage FH (1996) Neurogenesis in the dentate gyrus of the adult rat: age-related decrease of neuronal progenitor proliferation. J Neurosci 16:2027-2033.

Lamprecht R, LeDoux J (2004) Structural plasticity and memory. Nat Rev Neurosci 5:45-54.

Lavado A, Oliver G (2007) Prox1 expression patterns in the developing and adult murine brain. Dev Dyn 236:518-524.

Lee FS, Kim AH, Khursigara G, Chao MV (2001a) The uniqueness of being a neurotrophin receptor. Curr Opin Neurobiol 11:281-286.

Lee J, Duan W, Mattson MP (2002) Evidence that brain-derived neurotrophic factor is required for basal neurogenesis and mediates, in part, the enhancement of neurogenesis by dietary restriction in the hippocampus of adult mice. J Neurochem 82:1367-1375.

Lee R, Kermani P, Teng KK, Hempstead BL (2001b) Regulation of cell survival by secreted proneurotrophins. Science 294:1945-1948.

Leibrock J, Lottspeich F, Hohn A, Hofer M, Hengerer B, Masiakowski P, Thoenen H, Barde YA (1989) Molecular cloning and expression of brain-derived neurotrophic factor. Nature 341:149-152.

Leid M, Ishmael JE, Avram D, Shepherd D, Fraulob V, Dolle P (2004) CTIP1 and CTIP2 are differentially expressed during mouse embryogenesis. Gene Expr Patterns 4:733-739.

Lemaire V, Koehl M, Le MM, Abrous DN (2000) Prenatal stress produces learning deficits associated with an inhibition of neurogenesis in the hippocampus. Proc Natl Acad Sci U S A 97:11032-11037.

Lendvai B, Stern EA, Chen B, Svoboda K (2000) Experience-dependent plasticity of dendritic spines in the developing rat barrel cortex in vivo. Nature 404:876-881.

Lisman J, Schulman H, Cline H (2002) The molecular basis of CaMKII function in synaptic and behavioural memory. Nat Rev Neurosci 3:175-190.

Lledo PM, Alonso M, Grubb MS (2006) Adult neurogenesis and functional plasticity in neuronal circuits. Nat Rev Neurosci 7:179-193.

Lorente de Nó R (1934) Studies on the structure of the cerebral cortex. II. Continuation of the study of the ammonic system. J Psychol Neurol (Leipz) 46:113–177

Lu B, Pang PT, Woo NH (2005) The yin and yang of neurotrophin action. Nat Rev Neurosci 6:603-614.

Malatesta P, Hack MA, Hartfuss E, Kettenmann H, Klinkert W, Kirchhoff F, Gotz M (2003) Neuronal or glial progeny: regional differences in radial glia fate. Neuron 37:751-764.

Malatesta P, Hartfuss E, Gotz M (2000) Isolation of radial glial cells by fluorescent-activated cell sorting reveals a neuronal lineage. Development 127:5253-5263.

Malenka RC, Bear MF (2004) LTP and LTD: an embarrassment of riches. Neuron 44:5-21.

Maletic-Savatic M, Malinow R, Svoboda K (1999) Rapid dendritic morphogenesis in CA1 hippocampal dendrites induced by synaptic activity. Science 283:1923-1927.

Matsumoto T, Rauskolb S, Polack M, Klose J, Kolbeck R, Korte M, Barde YA (2008) Biosynthesis and processing of endogenous BDNF: CNS neurons store and secrete BDNF, not pro-BDNF. Nat Neurosci 11:131-133.

Matsuzaki M, Ellis-Davies GC, Nemoto T, Miyashita Y, Iino M, Kasai H (2001) Dendritic spine geometry is critical for AMPA receptor expression in hippocampal CA1 pyramidal neurons. Nat Neurosci 4:1086-1092.

McAllister AK, Katz LC, Lo DC (1999) Neurotrophins and synaptic plasticity. Annu Rev Neurosci 22:295-318.

McConnell SK, Kaznowski CE (1991) Cell cycle dependence of laminar determination in developing neocortex. Science 254:282-285.

Ming GL, Song H (2005) Adult neurogenesis in the mammalian central nervous system. Annu Rev Neurosci 28:223-250.

Minichiello L, Calella AM, Medina DL, Bonhoeffer T, Klein R, Korte M (2002) Mechanism of TrkB-mediated hippocampal long-term potentiation. Neuron 36:121-137.

Monyer H, Burnashev N, Laurie DJ, Sakmann B, Seeburg PH (1994) Developmental and regional expression in the rat brain and functional properties of four NMDA receptors. Neuron 12:529-540.

Muller D, Buchs PA, Stoppini L (1993) Time course of synaptic development in hippocampal organotypic cultures. Brain Res Dev Brain Res 71:93-100.

Nacher J, Varea E, Blasco-Ibanez JM, Castillo-Gomez E, Crespo C, Martinez-Guijarro FJ, McEwen BS (2005) Expression of the transcription factor Pax 6 in the adult rat dentate gyrus. J Neurosci Res 81:753-761.

Nadarajah B, Brunstrom JE, Grutzendler J, Wong RO, Pearlman AL (2001) Two modes of radial migration in early development of the cerebral cortex. Nat Neurosci 4:143-150.

Nagerl UV, Eberhorn N, Cambridge SB, Bonhoeffer T (2004) Bidirectional activity-dependent morphological plasticity in hippocampal neurons. Neuron 44:759-767.

Nikoletopoulou V, Plachta N, Allen ND, Pinto L, Gotz M, Barde YA (2007) Neurotrophin receptor-mediated death of misspecified neurons generated from embryonic stem cells lacking Pax6. Cell Stem Cell 1:529-540.

Nikonenko I, Jourdain P, Muller D (2003) Presynaptic remodeling contributes to activity-dependent synaptogenesis. J Neurosci 23:8498-8505.

Okamoto K, Narayanan R, Lee SH, Murata K, Hayashi Y (2007) The role of CaMKII as an F-actin-bundling protein crucial for maintenance of dendritic spine structure. Proc Natl Acad Sci U S A 104:6418-6423.

Otmakhov N, Griffith LC, Lisman JE (1997) Postsynaptic inhibitors of calcium/calmodulin-dependent protein kinase type II block induction but not maintenance of pairing-induced long-term potentiation. J Neurosci 17:5357-5365.

Overstreet-Wadiche LS, Bensen AL, Westbrook GL (2006) Delayed development of adult-generated granule cells in dentate gyrus. J Neurosci 26:2326-2334.

Parent JM (2007) Adult neurogenesis in the intact and epileptic dentate gyrus. Prog Brain Res 163:529-540.

Parent JM, Yu TW, Leibowitz RT, Geschwind DH, Sloviter RS, Lowenstein DH (1997) Dentate granule cell neurogenesis is increased by seizures and contributes to aberrant network reorganization in the adult rat hippocampus. J Neurosci 17:3727-3738.

Patterson SL, Abel T, Deuel TA, Martin KC, Rose JC, Kandel ER (1996) Recombinant BDNF rescues deficits in basal synaptic transmission and hippocampal LTP in BDNF knockout mice. Neuron 16:1137-1145.

Pinto L, Gotz M (2007) Radial glial cell heterogeneity--the source of diverse progeny in the CNS. Prog Neurobiol 83:2-23.

Plachta N, Annaheim C, Bissiere S, Lin S, Ruegg M, Hoving S, Muller D, Poirier F, Bibel M, Barde YA (2007) Identification of a lectin causing the degeneration of neuronal processes using engineered embryonic stem cells. Nat Neurosci.

Plachta N, Bibel M, Tucker KL, Barde YA (2004) Developmental potential of defined neural progenitors derived from mouse embryonic stem cells. Development 131:5449-5456.

Poo MM (2001) Neurotrophins as synaptic modulators. Nat Rev Neurosci 2:24-32.

Qian X, Shen Q, Goderie SK, He W, Capela A, Davis AA, Temple S (2000) Timing of CNS cell generation: a programmed sequence of neuron and glial cell production from isolated murine cortical stem cells. Neuron 28:69-80.

Raff M (2003) Adult stem cell plasticity: fact or artifact? Annu Rev Cell Dev Biol 19:1-22.

Raineteau O, Rietschin L, Gradwohl G, Guillemot F, Gahwiler BH (2004) Neurogenesis in hippocampal slice cultures. Mol Cell Neurosci 26:241-250.

Ramón y Cajal S (1911) Histologie du système nerveux de l'homme et des vertébrés. Paris: A. Maloine.

Redmond L, Kashani AH, Ghosh A (2002) Calcium regulation of dendritic growth via CaM kinase IV and CREB-mediated transcription. Neuron 34:999-1010.

Reichardt LF (2006) Neurotrophin-regulated signalling pathways. Philos Trans R Soc Lond B Biol Sci 361:1545-1564.

Riddle RD, Johnson RL, Laufer E, Tabin C (1993) Sonic hedgehog mediates the polarizing activity of the ZPA. Cell 75:1401-1416.

Ridet JL, Malhotra SK, Privat A, Gage FH (1997) Reactive astrocytes: cellular and molecular cues to biological function. Trends Neurosci 20:570-577.

Rohwedel J, Guan K, Wobus AM (1999) Induction of cellular differentiation by retinoic acid in vitro. Cells Tissues Organs 165:190-202.

Rosch H, Schweigreiter R, Bonhoeffer T, Barde YA, Korte M (2005) The neurotrophin receptor p75NTR modulates long-term depression and regulates the expression of AMPA receptor subunits in the hippocampus. Proc Natl Acad Sci U S A 102:7362-7367.

Rossi C, Angelucci A, Costantin L, Braschi C, Mazzantini M, Babbini F, Fabbri ME, Tessarollo L, Maffei L, Berardi N, Caleo M (2006) Brain-derived neurotrophic factor (BDNF) is required for the enhancement of hippocampal neurogenesis following environmental enrichment. Eur J Neurosci 24:1850-1856.

Schmidt-Hieber C, Jonas P, Bischofberger J (2004) Enhanced synaptic plasticity in newly generated granule cells of the adult hippocampus. Nature 429:184-187.

Schrenk-Siemens K, Perez-Alcala S, Richter J, Lacroix E, Rahuel J, Korte M, Muller U, Barde YA, Bibel M (2008) Embryonic stem cell-derived neurons as a cellular system to study gene function: lack of amyloid precursor proteins APP and APLP2 leads to defective synaptic transmission. Stem Cells 26:2153-2163.

Scoville WB, Milner B (1957) Loss of recent memory after bilateral hippocampal lesions. J Neurol Neurosurg Psychiatry 20:11-21.

Segal M (2005) Dendritic spines and long-term plasticity. Nat Rev Neurosci 6:277-284.

Seidah NG, Benjannet S, Pareek S, Chretien M, Murphy RA (1996) Cellular processing of the neurotrophin precursors of NT3 and BDNF by the mammalian proprotein convertases. FEBS Lett 379:247-250.

Seri B, Garcia-Verdugo JM, McEwen BS, Alvarez-Buylla A (2001) Astrocytes give rise to new neurons in the adult mammalian hippocampus. J Neurosci 21:7153-7160.

Shen K, Meyer T (1999) Dynamic control of CaMKII translocation and localization in hippocampal neurons by NMDA receptor stimulation. Science 284:162-166.

Sin WC, Haas K, Ruthazer ES, Cline HT (2002) Dendrite growth increased by visual activity requires NMDA receptor and Rho GTPases. Nature 419:475-480.

Skrede KK, Westgaard RH (1971) The transverse hippocampal slice: a well-defined cortical structure maintained in vitro. Brain Res 35:589-593.

Snyder JS, Choe JS, Clifford MA, Jeurling SI, Hurley P, Brown A, Kamhi JF, Cameron HA (2009) Adult-born hippocampal neurons are more numerous, faster maturing, and more involved in behavior in rats than in mice. J Neurosci 29:14484-14495.

Song H, Stevens CF, Gage FH (2002) Astroglia induce neurogenesis from adult neural stem cells. Nature 417:39-44.

Spruston N (2008) Pyramidal neurons: dendritic structure and synaptic integration. Nat Rev Neurosci 9:206-221.

Stanton PK, Sejnowski TJ (1989) Associative long-term depression in the hippocampus induced by hebbian covariance. Nature 339:215-218.

Stoppini L, Buchs PA, Muller D (1991) A simple method for organotypic cultures of nervous tissue. J Neurosci Methods 37:173-182.

Tashiro A, Makino H, Gage FH (2007) Experience-specific functional modification of the dentate gyrus through adult neurogenesis: a critical period during an immature stage. J Neurosci 27:3252-3259.

Tashiro A, Sandler VM, Toni N, Zhao C, Gage FH (2006) NMDA-receptor-mediated, cell-specific integration of new neurons in adult dentate gyrus. Nature 442:929-933.

Tessier-Lavigne M, Goodman CS (1996) The molecular biology of axon guidance. Science 274:1123-1133.

Thoenen H (1995) Neurotrophins and neuronal plasticity. Science 270:593-598.

Toni N, Buchs PA, Nikonenko I, Bron CR, Muller D (1999) LTP promotes formation of multiple spine synapses between a single axon terminal and a dendrite. Nature 402:421-425.

Toni N, Laplagne DA, Zhao C, Lombardi G, Ribak CE, Gage FH, Schinder AF (2008) Neurons born in the adult dentate gyrus form functional synapses with target cells. Nat Neurosci 11:901-907.

Toni N, Teng EM, Bushong EA, Aimone JB, Zhao C, Consiglio A, van Praag H, Martone ME, Ellisman MH, Gage FH (2007) Synapse formation on neurons born in the adult hippocampus. Nat Neurosci 10:727-734.

Trachtenberg JT, Chen BE, Knott GW, Feng G, Sanes JR, Welker E, Svoboda K (2002) Long-term in vivo imaging of experience-dependent synaptic plasticity in adult cortex. Nature 420:788-794.

Urrea C, Castellanos DA, Sagen J, Tsoulfas P, Bramlett HM, Dietrich WD (2007) Widespread cellular proliferation and focal neurogenesis after traumatic brain injury in the rat. Restor Neurol Neurosci 25:65-76.

Vaillant AR, Zanassi P, Walsh GS, Aumont A, Alonso A, Miller FD (2002) Signaling mechanisms underlying reversible, activity-dependent dendrite formation. Neuron 34:985-998.

van Praag, H, Kempermann G, Gage FH (1999) Running increases cell proliferation and neurogenesis in the adult mouse dentate gyrus. Nat Neurosci 2:266-270.

van Praag, H, Schinder AF, Christie BR, Toni N, Palmer TD, Gage FH (2002) Functional neurogenesis in the adult hippocampus. Nature 415:1030-1034.

Wernig M, Benninger F, Schmandt T, Rade M, Tucker KL, Bussow H, Beck H, Brustle O (2004) Functional integration of embryonic stem cell-derived neurons in vivo. J Neurosci 24:5258-5268.

Wong RO, Ghosh A (2002) Activity-dependent regulation of dendritic growth and patterning. Nat Rev Neurosci 3:803-812.

Woo NH, Teng HK, Siao CJ, Chiaruttini C, Pang PT, Milner TA, Hempstead BL, Lu B (2005) Activation of p75NTR by proBDNF facilitates hippocampal long-term depression. Nat Neurosci 8:1069-1077.

Woolley CS, Weiland NG, McEwen BS, Schwartzkroin PA (1997) Estradiol increases the sensitivity of hippocampal CA1 pyramidal cells to NMDA receptor-mediated synaptic input: correlation with dendritic spine density. J Neurosci 17:1848-1859.

Yamasaki N, et al. (2008) Alpha-CaMKII deficiency causes immature dentate gyrus, a novel candidate endophenotype of psychiatric disorders. Mol Brain 1:6.

Yamashita T, Tohyama M (2003) The p75 receptor acts as a displacement factor that releases Rho from Rho-GDI. Nat Neurosci 6:461-467.

Yamashita T, Tucker KL, Barde YA (1999) Neurotrophin binding to the p75 receptor modulates Rho activity and axonal outgrowth. Neuron 24:585-593.

Yan Q, Radeke MJ, Matheson CR, Talvenheimo J, Welcher AA, Feinstein SC (1997) Immunocytochemical localization of TrkB in the central nervous system of the adult rat. J Comp Neurol 378:135-157.

Yang J, Siao CJ, Nagappan G, Marinic T, Jing D, McGrath K, Chen ZY, Mark W, Tessarollo L, Lee FS, Lu B, Hempstead BL (2009) Neuronal release of proBDNF. Nat Neurosci 12:113-115.

Yasuda H, Barth AL, Stellwagen D, Malenka RC (2003) A developmental switch in the signaling cascades for LTP induction. Nat Neurosci 6:15-16.

Yuste R, Bonhoeffer T (2001) Morphological changes in dendritic spines associated with long-term synaptic plasticity. Annu Rev Neurosci 24:1071-1089.

Yuste R, Majewska A, Holthoff K (2000) From form to function: calcium compartmentalization in dendritic spines. Nat Neurosci 3:653-659.

Zagrebelsky M, Holz A, Dechant G, Barde YA, Bonhoeffer T, Korte M (2005) The p75 neurotrophin receptor negatively modulates dendrite complexity and spine density in hippocampal neurons. J Neurosci 25:9989-9999.

Zhao C, Deng W, Gage FH (2008) Mechanisms and functional implications of adult neurogenesis. Cell 132:645-660.

Zhao C, Teng EM, Summers RG, Jr., Ming GL, Gage FH (2006) Distinct morphological stages of dentate granule neuron maturation in the adult mouse hippocampus. J Neurosci 26:3-11.

Zhou Q, Homma KJ, Poo MM (2004) Shrinkage of dendritic spines associated with long-term depression of hippocampal synapses. Neuron 44:749-757.

7 APPENDICES

7.1 Supplementary Figures

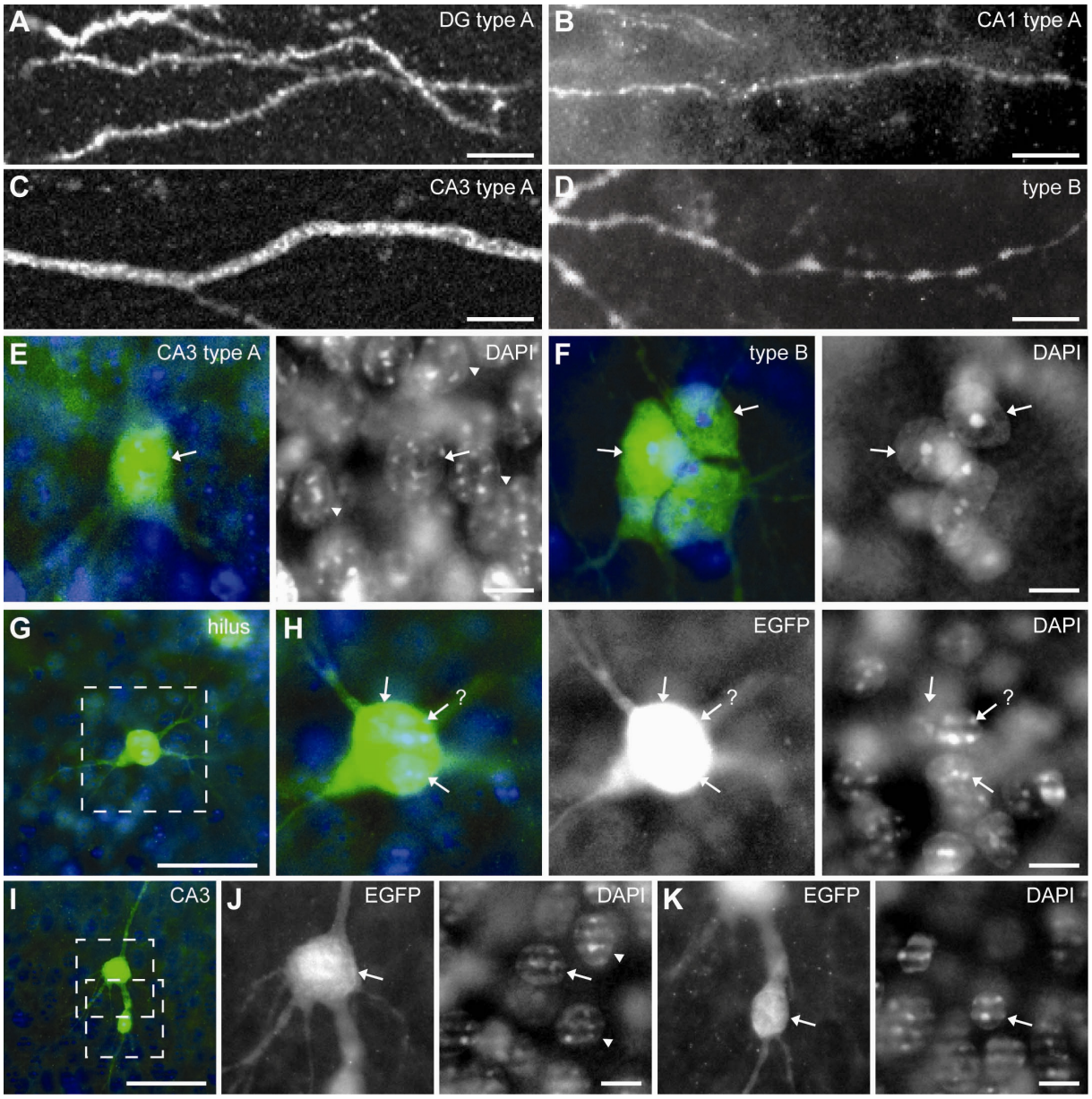

Figure S1 | Dendrites and nuclei of type A *versus* type B ESNs. A | Example of a spiny type A ESN dendrite from the DG region at 28 DIV. **B** | Thin and faint dendrite of a highly complex CA1 type A ESN. **C** | Aspiny dendrite of a highly complex CA3 type A ESN. **D** | Example of a spineless and bubbly type B ESN dendrite. **E** | CA3 type A ESN. Its nucleus (arrow) closely resembles the CA3 nuclei of the surrounding cell layer (arrowheads): It carries multiple small DAPI-positive dots. **F** | Three associated type B ESNs; the nuclei of two of them show the typical type B structure (arrows): one bright chromatin accumulation in the middle. **G** | Complex ESN in the hilar region of the DG. **H** | Higher magnification view of boxed region in G; the ESN contains 2-3 nuclei (arrows). **I-K** | Two connected CA3 ESNs. One of the ESNs (**J**) shows pyramidal-like structure and a nucleus (arrow) resembling the surrounding nuclei (arrowheads), the other ESN (**K**) shows immature morphology and nucleus shape (arrow). Except for **A**, all slices were fixed at 32 DIV. Scale bars in **A, B, C, D, E, F, H, J** and **K** 10 µm; in **G** and **I** 50 µm.

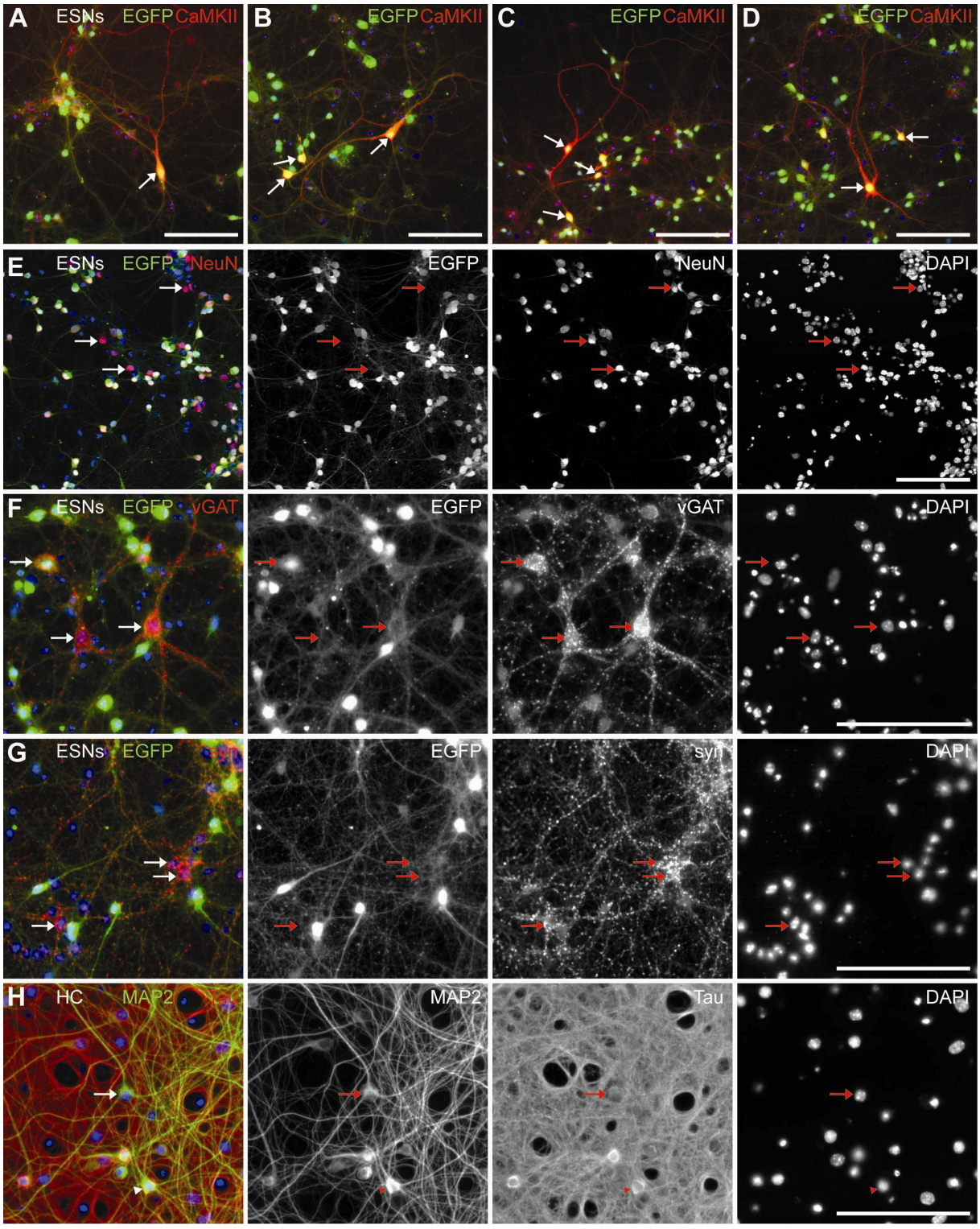

Figure S2 | Heterogeneity of dissociated ESN cultures. A-D | CaMKII stainings of ESNs cultured for 21 DIV (**C,D**) and 28 DIV (**A,B**), respectively. Only a minor fraction of ESNs is CaMKII-positive (arrows). The more complex ESNs display a weak EGFP signal, and partly show pyramidal-like morphology (**A,B**). **E** | ESN culture at 14 DIV stained against the neuronal antigen N (NeuN) specific for mature neurons. Many ESNs show a NeuN signal, some of them are devoid of EGFP fluorescence (arrows). **F** | ESN culture at 28 DIV stained against vGAT. Three ESNs are highly innervated by vGAT-positive nerve terminals (arrows); two of them are EGFP-negative and appear to show pyramidal-like morphology. **G** | ESN culture at 14 DIV stained with synapsin antibody; three highly innervated cells are EGFP-negative (arrows). **H** | Primary hippocampal culture (HC) at 28 DIV, stained against MAP2 and tau. Some neurons are clearly tau-positive (arrowhead); others appear to be tau-negative (arrow). Scale bars 100 µm.

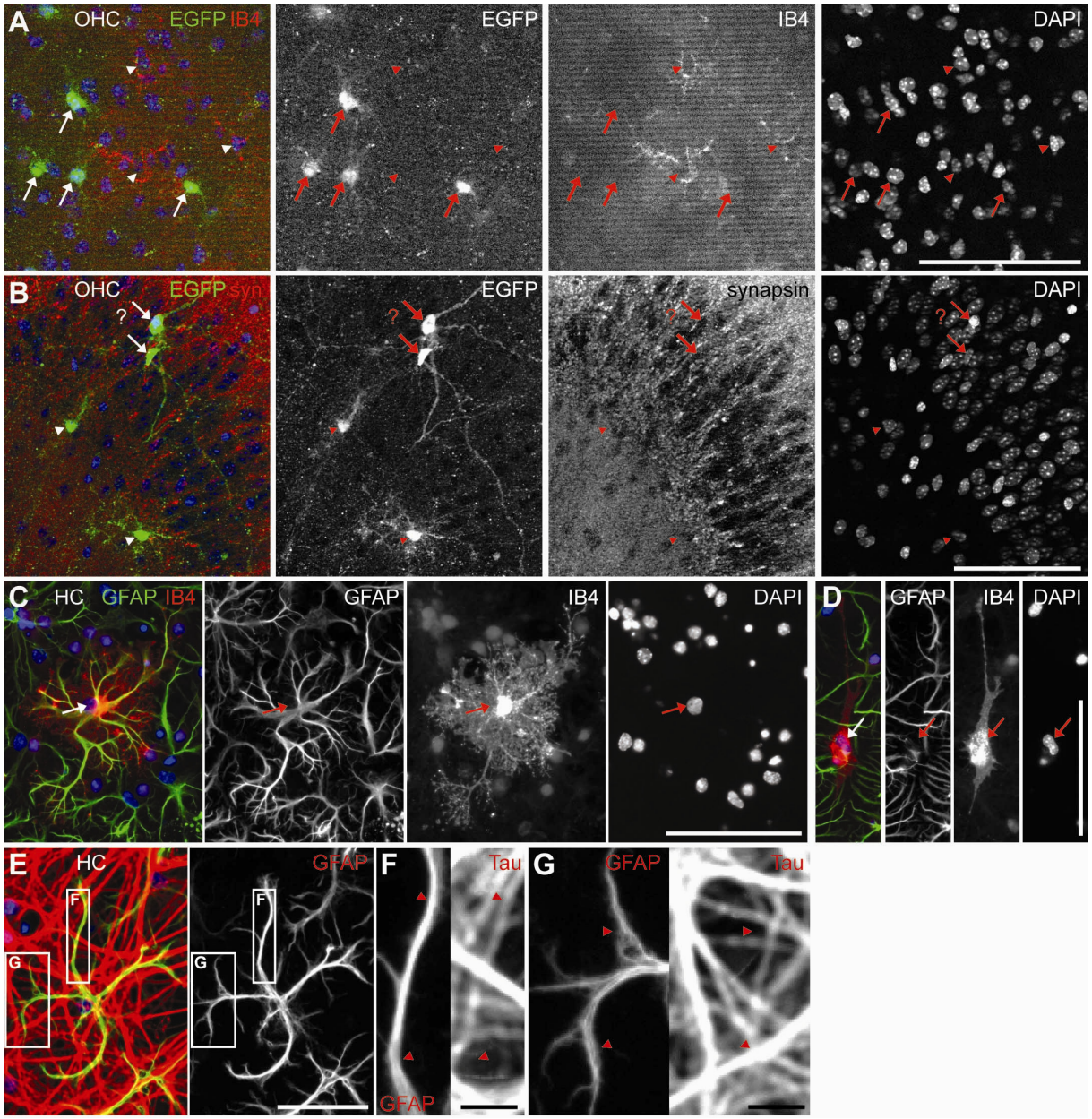

Figure S3 | Glial cells. A | EGFP-positive glia in organotypic cultures (OHC; arrows) are IB4-negative, intrinsic microglia (arrowheads) do not express EGFP. **B** | EGFP-positive glial cells (arrowheads) in the CA3 region of a slice culture fixed at 29 DIV and stained against EGFP, synapsin and DAPI (single section). Arrows point to atypically shaped neurons. **C** | Microglial cell in primary hippocampal culture (HC) at 21 DIV expressing GFAP. **D** | Microglial cell in primary hippocampal culture at 21 DIV that does not express GFAP and appears to be dividing. **E-G** | GFAP-positive glial cell which is tau-negative (arrowheads). **F** and **G** are higher magnification views of boxed regions in **E**. Scale bars in **A-C** 100 µm; in **E** 50 µm, and in **F** and **G** 10 µm.

7.2 Table of Figures

Figure 1	A maturing neuron traverses 5 characteristic stages	10
Figure 2	Overview over the hippocampal pathway	15
Figure 3	The hippocampus displays a unique cytoarchitecture	17
Figure 4	Functional and structural plasticity are linked to one another	19
Figure 5	Depending on the receptor system, neurotrophins trigger partly antagonizing cellular answers	22
Figure 6	ES cell culture and differentiation into neuronal precursors	34
Figure 7	Transplantation setup and procedure	38
Figure 8	Analysis of neuronal morphology	41
Figure 9	Transplantation efficiency and survival of ESNs	44
Figure 10	ESNs adopting pyramidal structure are found deep within the slice	46
Figure 11	Overview over morphologies of ES cell-derived fluorescent cells	48
Figure 12	DAPI staining of morphologically different ESN types show their spatial relationship to intrinsic nuclei	49
Figure 13	Categorization into type A and type B ESNs	50
Figure 14	Morphological analysis of CA1 ESNs compared to intrinsic hippocampal neurons	52
Figure 15	Morphological analysis of CA3 ESNs compared to intrinsic hippocampal neurons	53
Figure 16	CA1 ESNs are significantly less complex than CA3 ESNs	54
Figure 17	ESNs in the dentate gyrus depict granule cell-like morphology	55
Figure 18	Maturation into a pyramidal-like cell occurs within 4 days	56
Figure 19	ESNs carry spines co-localizing with presynaptic markers	57
Figure 20	A high percentage of type A ESNs appears to be connected to other cells	59
Figure 21	Associated soma-like structures contain nuclei	60
Figure 22	Type B ESNs morphologically develop and receive excitatory as well as inhibitory synaptic input	62
Figure 23	ESNs partially adopt the immunohistochemical identity of resident hippocampal neurons	64
Figure 24	Glia-like ESNP-derived cells resemble astrocytes	66
Figure 25	$p75^{NTR-/-}$ ESNs are more complex than the wild type	69
Figure 26	With time, $p75^{NTR-/-}$ type B ESNs become less complex	71
Figure 27	Presumptive generation of type A and type B ESNs	80
Figure 28	Potential processes leading to associated ESNs and syncytia	90

7.3 Frequently used abbreviations

AMPA(R)	α-amino-3-hydroxy-5-methyl-4-isoxazole propionic acid (receptor)
BDNF	brain-derived neurotrophic factor
CA	cornu ammonis
CaMKII	Ca^{2+}/calmodulin-dependent kinase II
CNS	central nervous system
CREB	cyclic AMP response element binding protein
DAPI	4',6-diamidino-2-phenylindole
DIV	days *in vitro* (post transplantation)
DG	dentate gyrus
EBs	embryoid bodies
EC	entorhinal cortex
EGFP	enhanced green fluorescent protein
EPSP	excitatory postsynaptic potential
ES	embryonic stem (cells)
ESN	embryonic stem cell-derived neuron
ESNP	embryonic stem cell-derived neuronal precursor
GABA	gamma-aminobutyric acid
GFAP	glial fibrillary acidic protein
IB4	isolectin B4
LIF	leukemia inhibitory factor
LTD	long-term depression
LTP	long-term potentiation
MAP2	microtubule-associated protein 2
MEFs	mouse embryonic fibroblasts
NMDA(R)	N-methyl-D-aspartic acid (receptor)
PP	perforant path
PSD	postsynaptic density
$P75^{NTR}$	pan neurotrophin receptor p75
RG	radial glia
SEM	standard error of the mean
SGZ	sub-granular zone
SVZ	sub-ventricular zone
TrkB	tropomyosin-related kinase receptor B
vGAT	vesicular GABA transporter
vGLUT1	vesicular glutamate transporter 1

Acknowledgements

Mein größter Dank gilt meinem Mentor Prof. Dr. Martin Korte für die Möglichkeit, an diesem interessanten und breit gefächerten Projekt arbeiten zu dürfen. Ich bin ihm dankbar für die Unterstützung und tolle persönliche Betreuung. Gleichzeitig forderte er mich immer wieder neu heraus und half mir, eine eigenständige Arbeitsweise zu entwickeln.

Ich danke Herrn Prof. Dr. Hans-Henning Arnold für die freundliche Übernahme des Ko-Referates und die nette Kooperation und Herrn Prof. Dr. Ralf-Rainer Mendel dafür, dass er sich bereit erklärt hat, den Vorsitz der Promotionskommission zu übernehmen.

Meine Arbeit ist in Kooperation mit der Arbeitsgruppe von Prof. Dr. Yves-Alain Barde in Basel entstanden. Ich danke ihm für die Bereitstellung der Zelllinien und des weiteren Materials und für die nette Zeit, die ich in Basel verbringen durfte. Vielen Dank außerdem an Dr. Christine Annaheim für die Anregungen und vor allem an Valérie Crotet für den ES-Zell-Differenzierungskurs sowie unzählige E-Mails und Telefonate, in denen sie mir mit Rat und Tat zur Seite stand.

Ein ganz großer Dank geht an Dr. Marta Zagrebelsky-Holz, die mich vor allem in der letzten Phase unglaublich unterstützt hat. Die anregenden Diskussionen mit ihr, ihre konstruktiv kritischen Fragen und gleichzeitig die nette Atmosphäre in unserem Büro haben dazu geführt, dass ich sehr viel gelernt habe und mir die Freude am Arbeiten bis zum Schluss gelieben ist. Ich bin sehr dankbar für die tolle Zeit, die ich mit Dr. Kristin Michaelsen und Dr. Susanne Kilian verbringen durfte. Beide haben mich – nicht nur wissenschaftlich – begleitet und unterstützt.

Martin Polack hat mich so einige Male vor der Verzweiflung an meinem PC gerettet und ist auch sonst ein absoluter Fachmann in allen möglichen Software-, Server- und Druck-Belangen. Von Ines Lahmann (AG Arnold) habe ich viel über ES-Zellen gelernt. Ich möchte mich herzlich für die freundschaftliche Zusammenarbeit bedanken! Tolle fachmännische Unterstützung bekam ich von Eva Saxinger, Diane Mundil, Reinhard Huwe und Angela Traudt. Außerdem hat Dr. Martin Rothkegel mir molekularbiologische Fragen beantwortet, und Prof. Dr. Robert Hänsch hatte immer Zeit, mir am konfokalen LSM weiterzuhelfen.

Die Zusammenarbeit mit meinen Master-, Diplom- und Bachelorstudenten hat mir besonders viel Spaß gemacht. Vielen Dank an Stefanie Janßen, Christine Gonschior, Malte Kühnemund und Melanie Rohde! Insgesamt habe ich mich in der Arbeitsgruppe sehr gut aufgehoben gefühlt. Dazu haben besonders meine Doktoranden-Kolleginnen Andrea Delekate, Anita Dreznjak, Janina Berndt-Huch und Melissa O'Brien beigetragen. Gleichzeitig geht mein Dank natürlich auch an alle anderen Mitglieder dieser netten und bunt gemischten Arbeitsgruppe.

Ich bedanke mich beim Land Niedersachsen für das Georg-Lichtenberg-Stipendium und damit die finanzielle Unterstützung meiner Arbeit, sowie bei Dr. Manuela Schüngel und den Kollegen vom internationalen Graduiertenkolleg für die schöne gemeinsame Zeit.

Ein besonderer Dank geht an meine Eltern und Geschwister, die mich in den letzten Jahren leider nur sehr selten zu Gesicht bekommen haben. Dennoch haben sie meine Arbeit aus der Ferne immer unterstützt.

Mein Mann Michael hat in den letzten Jahren am meisten unter meinem Zeitmangel gelitten. Vielen Dank, dass du mich dennoch unterstützt hast, und dass du meinen Blick auch mal wieder gerade gerückt hast, wenn es nötig war. Dein Rückhalt hat mich getragen.